Chapter – 1

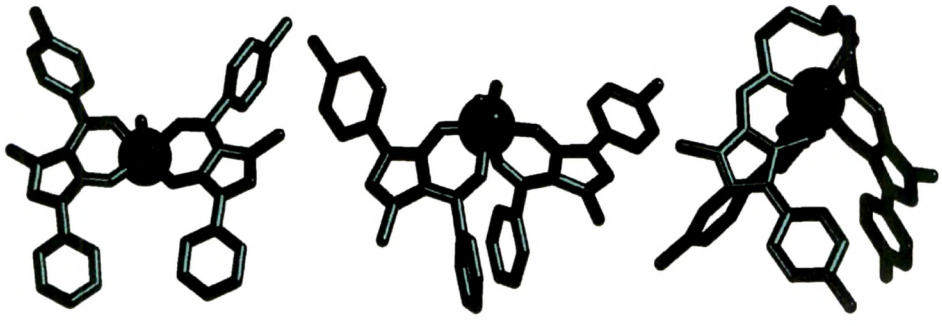

Synthesis, characterization and catalytic activities of vanadium complexes of acylpyrazolones & their structural analogues

1. Introduction

1.1 Introduction and brief history of pyrazolone

The first pyrazolone synthesis was reported in 1883 by Knorr [1, 2], who suggested the structure (I). The correct structure (II) was proposed three years later by the same author [3].

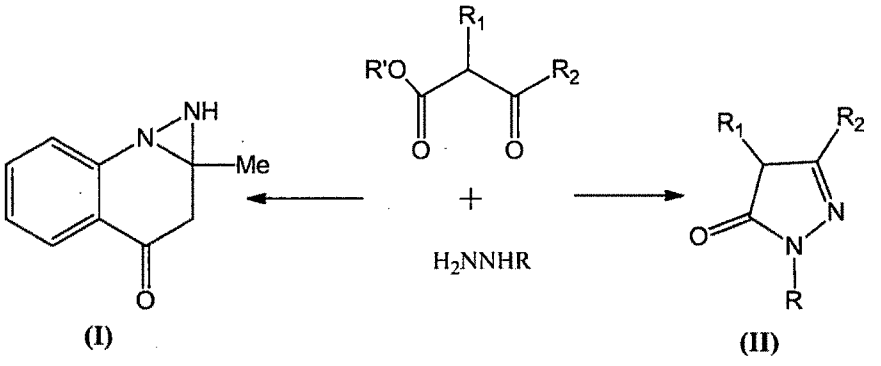

Scheme 1. First synthesis of pyrazolone by Knorr.

In 1892 Ruhemann and Morell provided further confirmation of the structure (II). A compound with the structure (II) was one of the first analgesic and antipyretic drugs to be marketed [4]. But, the use of these compounds in the treatment of humans declined significantly after their toxicity for bone marrow was discovered. A new advance in this field occurred in 1949 when H. Stenzl [5] synthesized phenylbutazone, a product for the treatment of rheumatoid arthritis. Once again, the high toxicity of these compounds in human beings has restricted their use, which is currently limited to the veterinary field. Outside pharmaceutical field pyrazolone are widely used for solvent extractions of metal ions [6], for analytical purpose [7], laser working materials [8], as ligands in complexes with catalytic activities [9] and in the synthesis of rare earth metal complexes with interesting photophysical properties [10]. Pyrazolone compound exist in a keto-enol tautomeric equilibrium (*see* Figure 1).

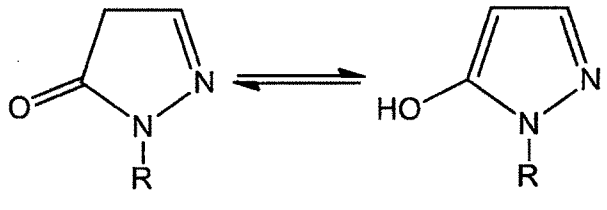

Figure 1. Keto-enol tautomerism in pyrazolone.

There are four possible pyrazol-3-one structures I-IV (*see* Figure 2). We are currently interested in carried out our studies on the structure II.

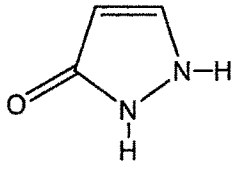

1,2-dihydro-3H-pyrazol-3-one

(I)

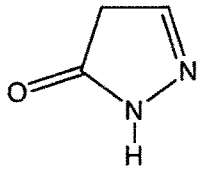

2,4-dihydro-3H-pyrazol-3-one

(II)

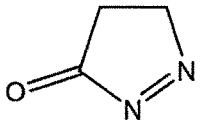

4,5-dihydro-3H-pyrazol-3-one

(III)

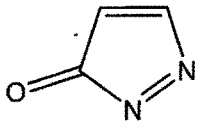

3H-pyrazol-3-one

(IV)

Figure 2. Possible pyrazol-3-one structures.

4-acyl and 4-formyl derivatives of pyrazolone are an important class of β-diketones. The first synthesis of 4-acyl pyrazolone was appeared in 1897 by F. Stoltz [11]. An advantageous synthesis of 1-phenyl-3-methyl-4-acylpyrazol-5-ones was presented by B. S. Jensen in 1959 [12]. The 4-formyl derivatives of 2-pyrazolind-ones have been known for some time. The first reference to a compound of this type appeared in *Monatschefte fur Chemie* in 1910. The synthesis involved the hydrolysis of the reaction product of 3-methyl-l-phenyl-2-pyrazolin-5-one and 2-phenyliminopseudoindoxyl. In 1937, Passerini and Cassini reported a synthesis which involved hydrolysis of the reaction product of the pyrazolinone and phenyl isocyanide. In 1940, Losco obtained a 12% yield of the 3-methyl-5-oxo-1-phenyl-2-pyrazoline-4-carboxaldehyde by treating the pyrazolinone with chloroform. The synthesis of 1-phenyl-3-methyl-5-oxo-2-pyrazoline-4-carbaldehyde in a high yield was reported by D. J. Wallace and J. M. Straley in 1961 [13]. 4-acyl and 4-formyl derivatives of pyrazolone are widely used in the formation of coordination complexes with various metal ions. Due to the presence of two oxygen donor atoms and facile keto–enol tautomerism, they easily coordinate with metal ions after deprotonation of the enolic hydrogen and provide stable metal complexes with six-membered chelate

rings. In addition, 4-acyl and 4-formyl derivatives can form a variety of Schiff bases and are reported to be superior reagents in biological, clinical and analytical applications [14]. Pyrazolones are used in analytical chemistry for the determination and isolation of almost all metal ions due to their high extracting ability, intense color of the complex extracts and low solubility of the complex in some solvents [15].

1.2 Vanadium (Introduction and Background)

In 1802, Andres Manuel del Rio (1764-1849) a mineralogist believed that he discovered a new metal similar to chromium and uranium in a brown lead mineral from Mexico [16]. He first named it *panchromium*, because of the diverse colors of its salts, but changed the name afterward in *erythronium* ('red') as a reference to the red color of its salts when treated with acids [16b]. However, shortly he withdrew his discovery, since a French chemist incorrectly declared that this new element was only impure chromium. In 1831, vanadium was rediscovered by the Swedish chemist Nils Gabriel Sefström (1787-1845) in the remnants of iron ore quarried at the Taberg in Småland [17]. Sefström named the element *vanadin*, after the goddess of beauty, youth and love, Vanadis, referring to the beautiful multicoloured compounds [18]. Vanadis is a common name for Freyja according to the Northern Germanic tribes (*see* Figure 3). After Sefström announced the discovery of vanadium, the brown lead ore from Mexico was reanalysed and it was shown that it really contained vanadium instead of chromium.

Figure 3. The Nordic goddess Vanadis, alias Freya [20].

Vanadium is a widely dispersed element that is found in about 65 minerals and generally occurs in low concentrations. In the Earth's crust, vanadium is 22nd in abundance (0.014% w/w) and thus more abundant than copper and zinc [19]. Natural vanadium is a mixture of two isotopes, ^{51}V (99.76%) and ^{50}V (0.24%), the latter being slightly radioactive with a half-life of > 3.9×10^{17} years. More than 120 vanadium-based minerals are known, containing the element in cationic and anionic form, and in the oxidation states III, IV and V [20].

In sea water, commonly considered the cradle of life on our planet, the average concentration of vanadium, which is present mainly in the form of ion pairs $Na^{+}H_2VO_4^{-}$, is around 30 nm. Vanadium is thus the second most abundant transition element in marine environments, outmatched only by molybdenum [ca 100 nm molybdate(VI)]. Vanadium is supplied by riverine input; scavenging by vent-derived iron oxides helps to control the concentration and cycling of vanadium in the oceans [21]. The vanadium content of human blood plasma is around 200 nm; this ca 10-fold increase with respect to sea water points to its possible biological function. The vanadium level in tissue is even higher, averaging 0.3 mg kg^{-1} (ca 6 μm). Vanadium accumulates in bones, liver and kidneys.

In 1983, a naturally occurring vanadium-containing enzyme, vanadium bromoperoxidase (V-BrPO), was discovered in the marine brown alga *Ascophyllum nodosum* [22]. Since then, several vanadium haloperoxidases (*vide infra*) have been isolated and studied [23, 24]. Many of these enzymes have been detected in brown and red seaweeds [25]. However, the accumulation of vanadium is not restricted to marine organisms, since vanadium containing haloperoxidases have also been isolated from terrestrial fungi [26] and a vanadium compound of low molecular weight (amavadin) has been isolated from the toadstool *Amanita muscaria* [27].

Vanadium can exist in eight oxidation states ranging from –3 to +5, with the exception of -2 [28]. Under ordinary conditions, the most stable oxidation states are +4 and +5. The coordination chemistry of vanadium is strongly influenced by the oxidizing/reducing properties of the metallic centre and the chemistry of vanadium ions in aqueous solution are limited to +2, +3, +4 and +5 oxidation states. Although many vanadium(III) complexes are unstable towards air, there are very less

compounds in this oxidation state, most with octahedral geometry. However some seven coordinated compounds were also characterized.

The +4 oxidation state of vanadium is the most stable under ordinary conditions and majority of vanadium(IV) compounds contain the VO^{2+} unit (vanadyl ion). Vanadium(IV) complexes typically have square pyramidal or bipyramidal geometry with axial vanadyl oxygen. Due to the d^1 configuration of V^{+4} ions, vanadium(IV) species are easily identified by EPR spectroscopy. Typical eight line pattern are observed due to hyperfine interaction of the ^{51}V nucleus (I = 7/2).

The coordination chemistry of vanadium(V) compounds is dominated by oxo complexes, containing the VO^{3+} or the VO^{2+} moiety. The oxidizing properties of vanadium(V) compounds are useful for many reactions, especially for the catalysis of oxidations. Vanadium(V) is EPR silent due to its d^0 state. Vanadium(V) complexes are therefore diamagnetic, which makes them appropriate for NMR analyses. Especially, ^{51}V NMR is a useful tool in the characterization of vanadium(V) complexes.

1.3 Vanadium complexes of pyrazolone

In 1976 first report on vanadium(IV) complex of acylpyrazolone derivatives was appeared. Oxovanadium(IV) complex was synthesized by the reaction between $VOSO_4{\cdot}5H_2O$ and 4-acyl pyrazolone in presence of sodium acetate and ethanol. The synthesized complex was characterized spectroscopically and magnetically [29]. In 1991 Uzoukwu synthesized a series of dioxovanadium(V) complexes from the interaction between an ethanolic solution of 4-acyl pyrazolone and aqueous solution of NH_4VO_3 acidified with HCl (*see* Figure 4). The acylpyrazolone ligands coordinated in both anionic and neutral keto-enol monodentate forms. IR studies shows that O=V=O system is likely bent in trigonal bipyramidal environment [30].

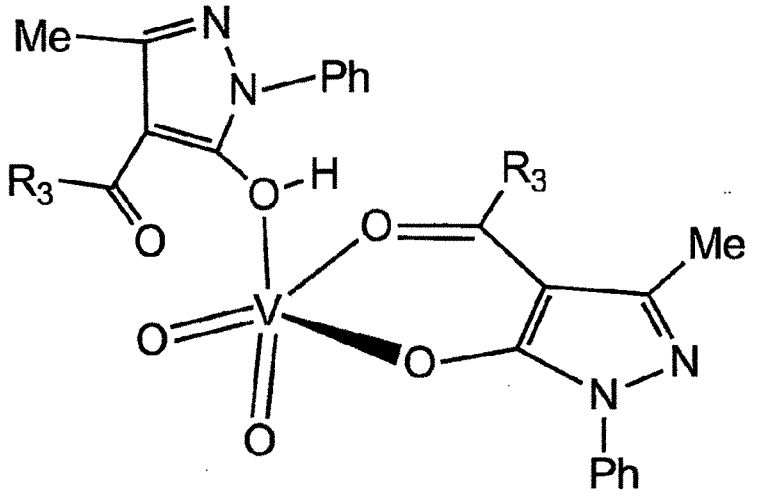

R_3 = Ph, Me, Et, Pr, Bu, Hp, CF_3, CCl_3

Figure 4. Structure of the derivatives $[VO_2(L)(HL)]$.

Oxovanadium(IV) complexes having square pyramidal geometry were synthesized by mixing an ethanolic solution of 4-acyl pyrazolone with ethanolic/aqueous solution of V_2O_5 acidified with HCl (*see* Figure 5) [31].

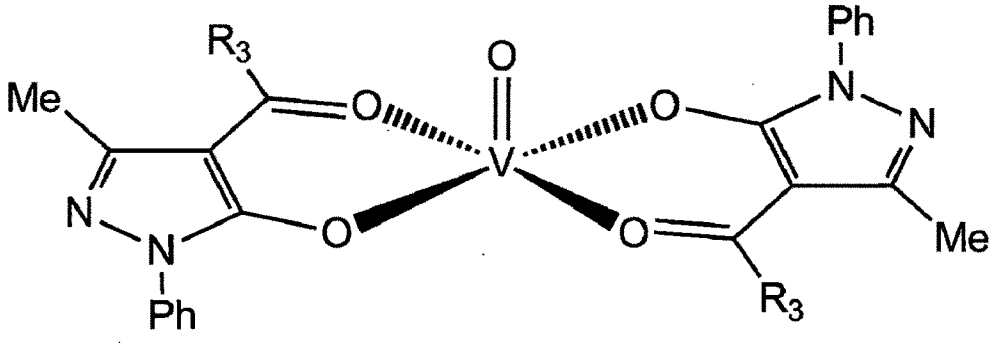

R_3 = Ph, Me, Et, Pr, Bu, Hp, CF_3, CCl_3

Figure 5. Structure of the derivatives $[VO(L)_2]$.

Mixed ligand complexes having the general formula $[VO(L)(Q)(H_2O)]$ were synthesized by the interaction of $VOSO_4 \cdot 5H_2O$ with HL and HQ in aqueous-ethanol medium [32]. The three dimensional modelling and spectroscopic studies on some of these complexes indicates an octahedral geometry around vanadium metal with an $O{=}V\text{-}OH_2$ moiety (*see* Figure 6).

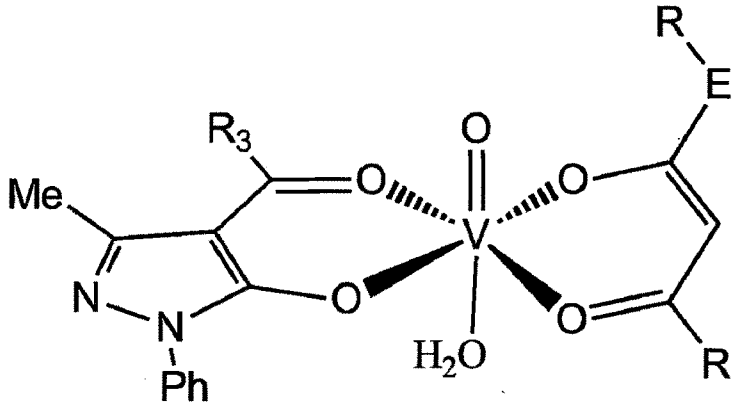

R_3 = Ph, Pr; E = O, NH; R = Me, Et, Ph, PhOMe

Figure 6. Structure of the derivatives $[VO(Q)(L)(H_2O)]$.

Similar type of mixed ligand complexes $[VO(L)(sm)(H_2O)]$ were synthesized and characterized by magnetic measurements, ESR, UV-Vis and IR spectroscopic studies, indicating octahedral geometries of these complexes (*see* Figure 7) [33].

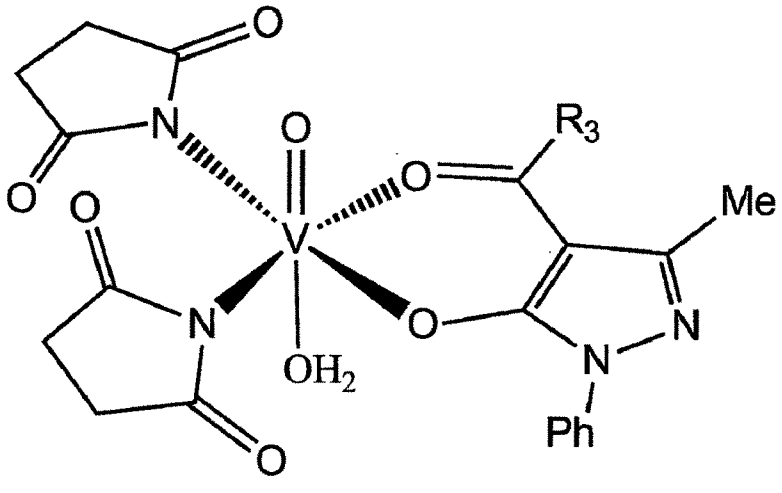

R_3 = Me, Pr

Figure 7. Structure of the derivatives $[VO(L)(sm)(H_2O)]$.

Oxovanadium complexes, containing the bis(acylpyrazolone) ligands in monoanionic form and acting as η^3-tridentate O donors, have been reported and characterized by Uzoukwu *et al* [34]. IR spectra of these complexes show that O=V=O species exist in the *cis* form.

Oxovanadium complex of 4-acylpyrazolone ligand having square pyramidal geometry was synthesized by Reddy *et al* by the reduction of ammonium monovanadate from V(V) to V(IV). The geometry of the synthesized oxovanadium(IV) complex was also optimized at the B3LYP/6-31G* level of density functional theory (DFT) method [35] (*see* Figure 8).

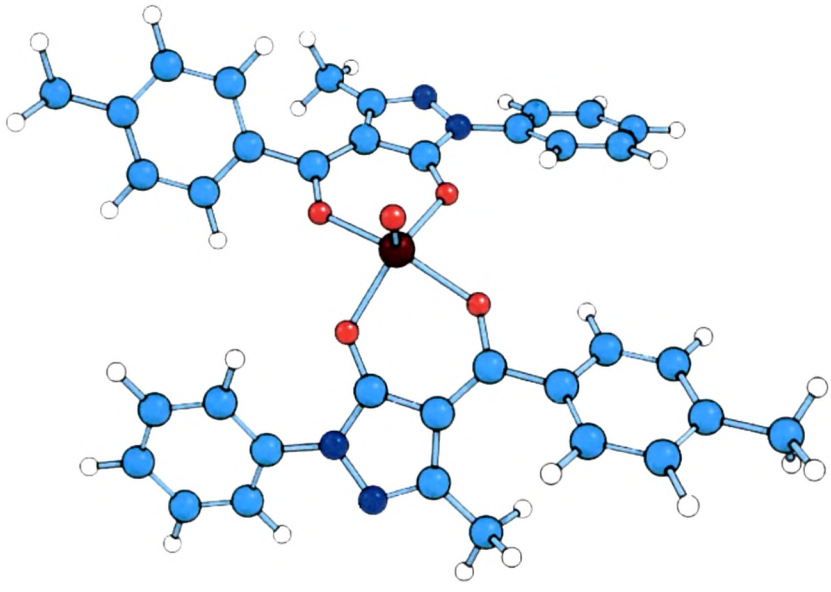

Figure 8. The optimized geometry of a distorted square pyramidal oxovanadium(IV) complex [35].

Mixed ligand oxovanadium(IV) complexes with 4-fomyl pyrazolone derivatives and 2,2'-bipyridyl were also reported by some researchers [37] (*see* Figure 9).

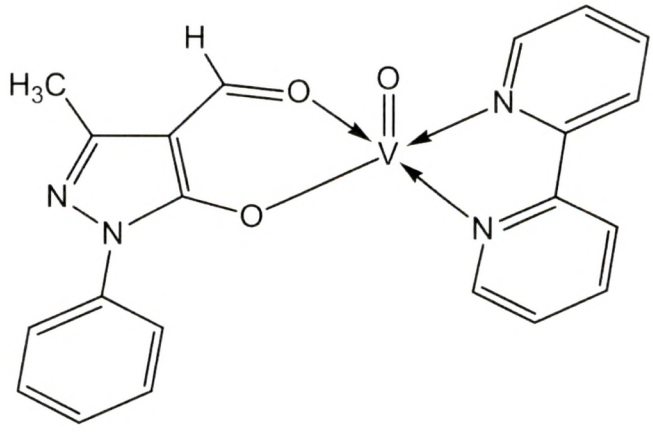

Figure 9. Structure of the derivative $[VO(L)(bipy)](ClO_4)$.

Oxovanadium(IV) complexes of 4-acylpyrazolones having octahedral and square pyramidal geometries [36] were synthesized by (Fabio *et al*) mixing an aqueous solution of $VOSO_4 \cdot 5H_2O$ with an methanol solution of ligand HL and of sodium methoxide as a base, in a 1:2:2 molar ratio (*see* Figure 10).

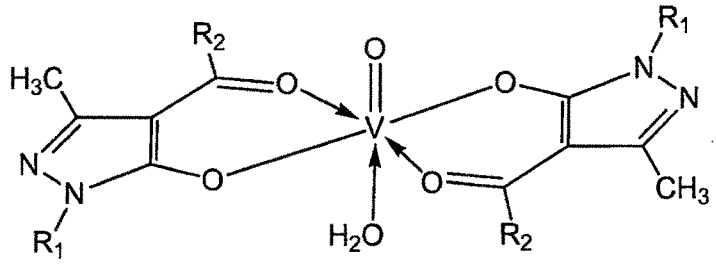

R^1= Ph, Me, R^2 = neopentyl, Me, 1-naphthyl

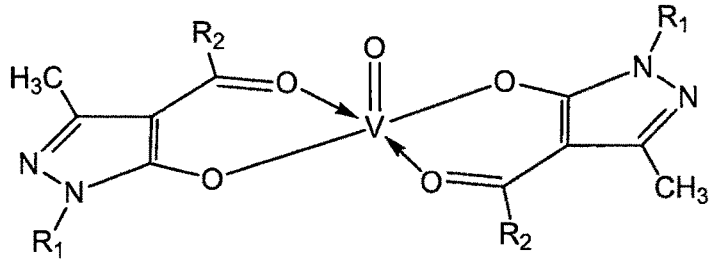

R_1= Ph, R_2 = Ph, CF3

Figure 10. General structure of the derivatives $[VO(L_2)(H_2O)]$ and $[VO(L_2)]$.

Crucianelli *et al* synthesized the octahedral oxovanadium(IV) complexes of 4-acylpyrazolones by mixing an aqueous solution of $VOSO_4 \cdot 5H_2O$ with an methanol solution of ligand and of sodium methoxide as a base [38] (*see* Figure 11).

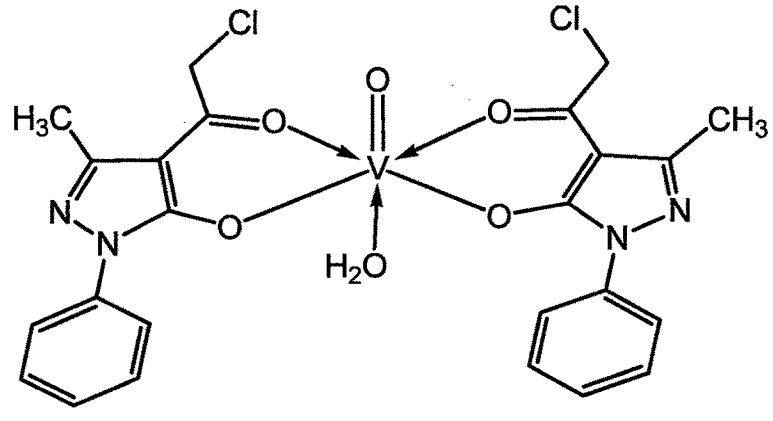

Figure 11. Structure of the oxovanadium(IV) complex.

2. Objective and methodology of the present work

The interest in the coordination chemistry of oxovanadium(IV) complexes of acylpyrazolones and their structural analogues is continuously progressing after the synthesis of first oxovanadium(IV) complex of acylpyrazolone in 1976 [29]. Since then many oxovanadium(IV) complexes of 4-acylpyrazolones and their structural analogues have been synthesized by various research groups. But almost no attention was given to the single crystal X-ray analysis of the synthesized complexes. This is might be due to the difficulty in getting good crystals of X-ray diffraction quality. We are interested in synthesizing the oxovanadium(IV) complexes of 4-acylpyrazolones and their structural analogues and study their geometry using single crystal XRD technique along with the other spectroscopic and analytical techniques. It was also found that there are only a few reports available on the use of oxovanadium(IV) complexes as a catalyst in the organic transformations [36-38]. This chapter is devoted to the synthesis, characterization and catalytic activities of oxovanadium(IV)/ vanadium(III) complexes and their structural analogues. The chapter is divided into three parts:

1. Homogeneous catalysis using oxovanadium(IV) complexes.
2. Heterogeneous catalysis using oxovanadium(IV) complexes.
3. Homogeneous catalysis using vanadium(III) complexes of tripodal ligands.

First part of the chapter **1** contain the synthesis, characterization and crystal structure of oxovanadium(IV) complexes of 4-acylpyrazolones and their catalytic activity towards the oxidation of various derivatives of benzylic alcohols. The complexes were used as homogeneous catalysts and H_2O_2 was used as an oxidant.

Second part of the chapter **1** include immobilization of oxovanadium(IV) complex of 4-acylpyrazolone onto a solid support to use it as a heterogeneous catalyst for the oxidation of styrene to benzaldehyde. Supported heterogeneous catalyst was characterized by various physiochemical techniques and successfully used for the solvent free oxidation of styrene.

Third part of the chapter **1** contain the synthesis and characterization of vanadium(III) complexes with tripodal ligands derived from 4-formylpyrazolones. The synthesized tripodal ligands and their vanadium(III) complexes were

characterized by various spectroscopic and analytical techniques along with the single crystal X-ray analysis. The synthesized vanadium(III) complexes were used as homogeneous catalysts for the oxidation of benzyl alcohol to benzaldehyde.

3. References

[1] L. Knorr, *Chem. Ber.*, **1883**,*16*, 2597-2599.

[2] L. Knorr, *Chem. Ber.*, **1884**,*17*, 546-552.

[3] L. Knorr, *Lieigs Ann. Chem.*, **1887**, *238*, 137-219.

[4] S. Ruhemann, P. Morell, *J. Chem. Soc.*, **1892**, *61*, 791-800.

[5] H. R. Wiley, P. Wiley, *Pyrazolones, Pyrazolidones and Derivatives*, Interscience Publishers, **1964**.

[6] R. Bose, D.S.R. Murty, G. Chakrapani, *J. Radioanal. Nucl. Chem.*, **2005**, *265*, 115-122.

[7] T. Ito, C. Goto, K. Noguchi, *Anal. Chim. Acta.*, **2001**, *443*, 41-51.

[8] A. Whitaker, *J. Soc. Dyers Colour*, **1995**, *111*, 66-72.

[9] F. Bao, X. Lu, B. Kang, Q. Wu, *Eur. Polym. J.*, **2006**, *42*, 928-934.

[10] M. Shi, F. Li, T. Yi, D. Zhang, H. Hu, C. Huang, *Inorg. Chem.*, **2005**, *44*, 8929-8936.

[11] F. Stoltz, *J. Prakt. Chem.*, **1897**, *55*, 145-171.

[12] B. S. Jensen, *Acta Chem. Scand.*, **1959**, *13*, 1668-1670.

[13] D. J. Wallace, J. M. Straley, *J. Org. Chem.*, **1961**, *26*, 3825-3826 and references cited therein.

[14] R. N. Jadeja, K. M. Vyas, V. K. Gupta, R. G. Joshi, C. Ratna Prabha, *Polyhedron*, **2012**, *31*, 767–778.

[15] P. N. Remya, R. Pavithran, M. L. P. Reddy, *Solvent Extr. Ion Exch.*, **2005**, *24*, 501–518.

[16] (*a*) D. Rehder, Coord. *Chem. Rev.*, **1999**, *182*, 297-322; (*b*) J. O. Nriagu, *Vanadium in the Environment Part One: Chemistry and Biochemistry*, J. O. Nriagu, Ed. John Wiley & Sons, New York, **1998**, Chapter 1; (*c*) A. G. J. Ligtenbarg, *Vandium and Iron Complexes for Catalytic Oxidation*, Ph. D. Thesis, **1974**.

[17] (*a*) N. G. Sefström, *Kgl. Vetenkapsacad. Handl.*, **1830**, 255–261; (*b*) N. G. Sefström, *Ann. Phys. Chem.*, **1831**, *21*, 43–49.

[18] *Handbook of Chemistry and Physics*, D. R. Lide, Ed. 72nd Edition, **1991-1992**.

[19] D. Rehder, *Angew. Chem. Int. Ed.*, **1991**, *30*, 148-167.

[20] D. Rehder, *Bioinorganic Vanadium Chemistry*, John Wiley & Sons, Chichester, **2008.**

[21] J. H. Trefrey, S. Metz, *Nature,* **1989**, *342*, 531–533.

[22] H. Vilter, *Phytochemistry*, **1984**, *23*, 1387-1390.

[23] H. Vilter, *Met. Ions Biol. Syst.*, **1995**, *31*, 325-362.

[24] (*a*) M. Căsný, D. Rehder, H. Schmidt, H. Vilter, V. Conte, *J. Inorg. Biochem.*, **2000**, *80*, 157-160; (*b*) Rao, A.V.S.; Ravishankar, H.N.; Ramasarma, T. *Arch. Biochem. Biophys.*, **1996**, *334*, 121-134; (*c*) M. Weyand, H. -J. Hecht, H. Vilter, D. Schomburg, *Acta Cryst.*, **1996**, *D52*, 864-865; (*d*) H. S. Soedjak, J. V. Walker, A. Butler, *Biochem.*, **1995**, *34*, 12689-12696; (*e*) R. A. Tschirret-Guth, , A. Butler, *J. Am. Chem. Soc.*, **1994**, *116*, 411-412; (*f*) P. Coughlin, S. Roberts, C. Rush, A. Willetts, *Biotechnol. Lett.*, **1993**, *15*, 907-912; (*g*) J. W. P. M. Van Schijndel, E. G. M. Vollenbroek, R. Wever, *Biochim. Biophys. Acta,* **1993**, *1161*, 249-256; (*h*) H. S. Soedjak, A. Butler, *Biochem.*, **1990**, *29*, 7974-7981; (*i*) R. R. Everett, H. S. Soedjak, A. Butler, *J. Biol. Chem.*, **1990**, *265*, 15671-15679; (*j*) R. R. Everett, J. R. Kanofsky, A. Butler, *J. Biol. Chem.*, **1990**, *265*, 4908-4914; (*k*) B. E. Krenn, M. G. M. Tromp, R. Wever, *J. Biol. Chem.*, **1989**, *264*, 19287-19292; (*l*) H. Plat, B. E. Krenn, R. Wever, *Biochem.* J., **1987**, *248*, 277-279; (*m*) E. De Boer, H. Plat, M. G. M. Tromp, R. Wever, M. C. R. Franssen, H. C. Van der Plas, E. M. Meijer, H. E. Schoemaker, *Biotechnol. Bioeng.*, **1987**, *30*, 607-610.

[25] (*a*) A. Butler, *Bioinorganic Catalysis*, J. Reedijk, , Ed., Marcel Dekker, New York, **1993**, Chapter 13; (*b*) R. Wever, W. Hemrika, *Vanadium in the Environment, Part One: Chemistry and Biochemistry*, J. O. Nriagu, , Ed., John Wiley & Sons, New York, **1998**, Chapter 12.

[26] J. W. P. M. Van Schijndel, E. G. M. Vollenbroek, R. Wever, *Biochim. Biophys. Acta.*, **1993**, *1161*, 249-256.

[27] H. Kneifel, E. Bayer, *Angew. Chem. Int. Ed.*, **1973**, *12*, 508-509.

[28] L. F. V. Boas, J. C. Pessoa, *Comprehensive Coordination Chemistry: The Synthesis, Reaction, Properties & Applications of Coordination Compounds* (Eds: G. Wilkinson, R. D. Gillard, J. A. McCleverty) Pergamon: Oxford, **1987**, Vol. *3*, 454.

[29] E. R. Menzel, D. R. Lorenz, J. R. Wasson, K. R. Radigan, B. J. Mc-Cormik, *J. Inorg. Nucl. Chem.*, **1976**, *38*, 993-996.

[30] B. A. Uzoukwu, *Synth. React. Inorg. Met. Org. Chem.*, **1991**, *21*, 881-896.

[31] B. A. Uzoukwu, *Synth. React. Inorg. Met. Org. Chem.*, **1992**, *22*, 185-194.

[32] (*a*) R. C. Maurya, S. Rajput, *J. Mol. Struct.*, **2004**, *687*, 35-44; (*b*) R. C. Maurya, H. Singh, *Synth. React. Inorg. Met. Org. Chem.*, **2004**, *34*, 269-290.

[33] R. C. Maurya, S. Rajput, *Synth. React. Inorg. Met. Org. Chem.*, **2003**, *33*, 1877-1894.

[34] B. A. Uzoukwu, K. Gloe, P. U. Adiukwu, *Synth. React. Inorg. Met. Org. Chem.*, **2000**, *30*, 433-443.

[35] P. N. Remya, C. H. Suresh, M. L. P. Reddy, *Polyhedron*, **2007**, *26*, 5016-5022.

[36] F. Marchetti, C. Pettinari, C. D. Nicola, R. Pettinari, A. Crispini, M. Crucianelli, A. D. Giuseppe, *Appl. Catal. A*, **2010**, *378*, 211-233.

[37] B. T. Thaker, K. R. Surati, C. K. Modi, *Russ. J. Coord. Chem.*, **2008**, *34*, 25-33.

[38] A. D. Giuseppe, C. D. Nicola, R. Pettinari, I. Ferino, D. Meloni, M. Passacantando, M. Crucianelli, *Catal. Sci. Technol.*, **2013**, *3*, 1972—1984.

Chapter – 1

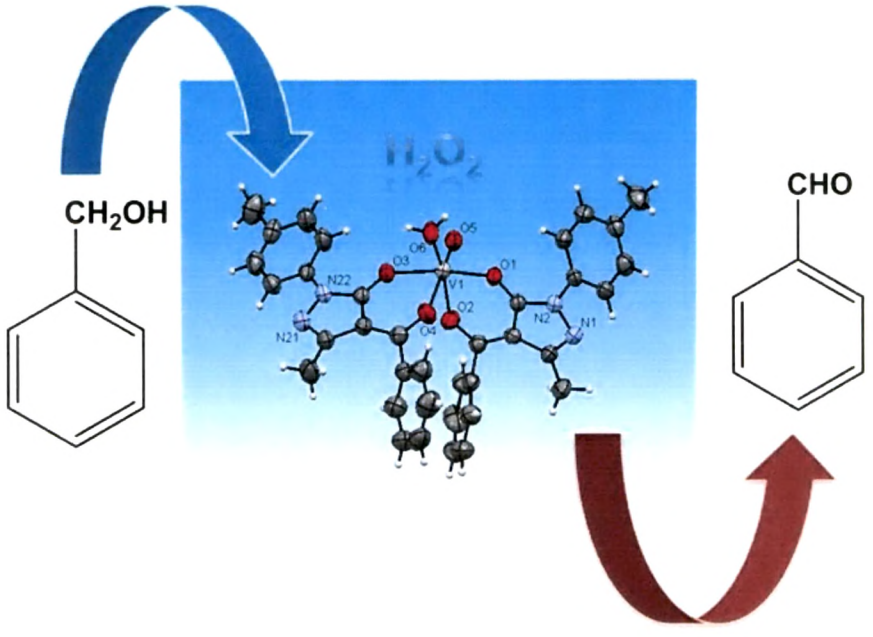

Part 1

Homogeneous catalysis using oxovanadium(IV) complexes

1.1.1. Introduction

The term catalysis was used by Berzelius over 150 years ago when he had noticed changes in substances when they were brought in contact with small amounts of certain species called "ferments". Many years later in 1895 Ostwald came up with the definition that we use until today: *A catalyst is a substance that changes the rate of a chemical reaction without itself appearing into the products.* This means that according to Ostwald a catalyst can also slow down a reaction! The definition used today reads as follows: *A catalyst is a substance which increases the rate at which a chemical reaction approaches equilibrium without becoming itself permanently involved* [1]. Catalysis deals with changes on the route to equilibrium. It is about reaction kinetics, not thermodynamics.

Today it is estimated that some 90% of the chemicals used have, at some stage in their manufacture, come into contact with a catalyst. Virtually all major bulk chemical and refining processes employ catalysts. The number of fine, specialty and pharmaceutical processes currently using catalysts is still relatively small by comparison, but a combination of economic and environmental factors is focusing much research on this area. The great economic benefit of catalysts lies with their incredible activity, sometimes converting tens of millions times their own weight of chemicals. This result in a catalyst market worth less than 1% of the value of the products they create. Because the catalyst is not consumed in the process, each catalyst molecule can participate in many consecutive cycles, so we need only a small amount of catalyst relative to the substrate. There are three important parameters [2] that impact on both the commercial viability and the inherent greenness of a particular catalyst:

1. **Selectivity** - the amount of substrate converted to the desired product as a percentage of total consumed substrate (a catalyst will be of limited benefit if it also enhances the rate of by-product formation).
2. **Turnover frequency** - the number of moles of product produced per mole of catalyst per second (low turnover frequency will mean large amount of catalyst are required, resulting in high cost and potentially more waste).
3. **Turnover number** - the amount of product per mole of catalyst (this is related to catalyst life time and hence to cost and waste).

Catalysts are commonly divided into two basic types, heterogeneous and homogeneous, depending on their state relative to the reaction medium.

Heterogeneous catalysts, sometimes referred to as surface catalysts or contact catalysts owing to their mode of action, are in a different phase to the reaction medium. Heterogeneous catalysts are widely used industrially. In most cases the catalyst is a solid and the actual reaction takes place on the surface of the catalyst, which may be the external surface or, more effectively, a surface within internal pores of the solid.

In homogeneous catalysis, the catalyst is in the same phase as the reactants and products and is uniformly distributed. In almost all cases the reaction takes place within the liquid phase, the catalyst being dissolved in the reaction medium. Homogeneous catalysis using transition metal complexes is an area of research that has grown enormously in recent years. Many amazing catalytic discoveries have been reported by researchers both in industry and in academia. The number of homogeneously catalyzed processes has been steadily growing in the eighties and nineties. For fine chemicals variety of sophisticated homogeneous catalysts are being used. In the laboratories a wide range of catalytic reactions has become necessary.

Vanadium compounds have attracted much attention because of their involvement in various biological processes [3] and for their use as homogeneous and heterogeneous catalysts in various reactions and in industrial processes [4]. Vanadium based oxidants are effectively used for various oxidation reactions such as the epoxidation of alkenes [4*j*, 4*l*, 5], the oxidation of sulfides [6], hydro and oxidative amination [7] and the oxidation of alcohols [8] to aldehydes and ketones, thus showing their influence on the yield and selectivity in chemical transformations. Oxo and peroxo derivatives of vanadium complexes play an important role in such catalytic oxidations, acting as oxo-transfer agents [9]. Aqueous hydrogen peroxide is a highly attractive oxidant because it is a cheap, mild and environmentally benign reagent with a high content of 'active' oxygen, and water is the only by-product. Thus, many catalytic systems were studied for selective-oxidation of alcohols with H_2O_2 [10]. The catalytic species resulting from the interaction of hydrogen peroxide with suitable transition metal ions are considered among the most active oxidants [11] toward a number of organic and inorganic substrates.

The selective oxidation of alcohols to carbonyl compounds is one of the most important organic transformations, with recognized importance to fundamental organic synthesis, but also to the fine chemical industry [12]. Selective oxidation of benzyl alcohol to benzaldehyde is a practically important reaction for the production of chlorine-free benzaldehyde, required in the perfumery and pharmaceutical industries [13]. Benzaldehyde is an attractive target because it is an important intermediate in the production of derivatives for perfumery, pharmaceutical, dyestuff and agrochemical industries.

As per literature search, only one report on the use of oxovanadium complexes with 4-acylpyrazolone ligand as homogeneous catalysts [14] is available and no report is existing in the literatures for the selective oxidation of alcohols with the oxovanadium(IV) complexes of 4-acylpyrazolone ligands as catalysts. The objective of the present study is to emphasis the geometry of oxovanadium(IV) complexes of 4-acylpyrazolone ligands and to establish the viability of the newly synthesized oxovanadium(IV) complexes in oxidation reactions. The catalytic properties of the new mononuclear complexes have been thoroughly studied, in the hydrogen peroxide promoted oxidation of benzylic alcohols, under homogeneous reaction conditions. To investigate the effectiveness of the synthesized complexes in oxidation reactions, benzyl alcohol was chosen as a model substrate. The oxidation of benzyl alcohol was studied in more detail to optimize the reaction variables such as the amount of catalyst, alcohol/oxidant molar ratio, length of reaction time and solvent. To evaluate the scope and limitations of the current procedure, oxidation reactions with a wide array of electronically diverse benzylic alcohols were examined using oxovanadium(IV) complex of 1-toluoyl-3-methyl-4-Phenyl-5-pyrazolone ligand.

1.1.2. Experimental Section

1.1.2.1. Materials and Physical measurments

All reagents and solvents were purchased from commercial sources and were further purified by the standard methods, if necessary [15]. Pyrazolone derivatives were obtained from Nutan Dye Chem. Sachin, Surat. Vanadyl sulfate, acetonitrile, benzyl alcohol, hexane and 30% aqueous H_2O_2 were purchased from Merck and used as received. 2-methoxy benzyl alcohol, 3-methoxy benzyl alcohol, 4-methoxy benzyl

alcohol, 2-chloro benzyl alcohol, 3-chloro benzyl alcohol, 4-methyl benzyl alcohol, and 4-nitro benzyl alcohol were purchased from Sigma-Aldrich.

The synthesized ligands and their oxovanadium(IV) complexes were characterized by ^{1}H & ^{13}C NMR, ESI-MS, Single crystal XRD, FT-IR, EPR and ESI-Mass. ^{1}H and ^{13}C NMR spectra of ligands were recorded with Avance-III 400 MHz Bruker FT-NMR instrument. Elemental analyses of C, H, and N were determined using a Perkin Elmer series-II 2400 elemental analyzer. GC-MS analysis was carried out using gas chromatograph mass spectrometer (Agilent 5975 GC/MSD with 7890A GC system) having HP-5 capillary column of 60 m length and 250 μm diameter with a programmed oven temperature from 50 to 280 °C, at 1 mL min^{-1} flow rate of He as a carrier gas and ion source at 230 °C. X-ray intensity data were collected on Bruker CCD area-detector diffractometer equipped with graphite monochromated MoKα radiation (λ = 0.71073 Å). FT-IR spectra of ligands and complexes were recorded as the KBr pellet on the Perkin Elmer Fourier transform (FT-IR) spectrum RX 1 spectrometer. Electronic spectra were recorded on a Perkin Elmer Lambda 35 UV-Vis spectrometer. EPR spectrum was recorded on X-band instrument in EPR laboratory, SAIF, IIT, Bombay, at liquid nitrogen temperature. Electro spray ionization mass spectrometry (ESI-MS) spectra were recorded on a Waters Q-ToF micromass at SAIF, Panjab University, Chandigarh.

1.1.2.2. Synthesis of 4-acylpyrazolone ligands

Synthesis of 1-phenyl-3-methyl-4-toluoyl-5-pyrazolone (L^1): 1-phenyl-3-methyl-5-pyrazolone (17.4 g, 0.1 mol) and 80 ml of 1,4-dioxane were placed in a three necked 250 ml round bottom flask equipped with a stirrer, an addition funnel and a reflux condenser. The reaction mass was heated at 70 °C for 10 min. To the resulting yellow solution was added in small portions calcium hydroxide (14.82 g, 0.2 mol) and then toluoyl chloride (15.5 g, 0.1 mol) was added dropwise. During this addition, the whole mass was converted into a thick paste. After the complete addition, the reaction mixture was heated to reflux for 2 h. The yellowish mixture was cooled to room temperature and poured into a 250 ml solution of ice-cold hydrochloric acid (2 mol L^{-1}) under stirring. The yellow precipitate was filtered, washed with water and dried in a vacuum. After drying a pale-yellow solid was obtained and recrystallized from an acidified methanol-water mixture. (Yield 22.79 gm, 78%) Mp: 120 °C. ^{1}H NMR (400

MHz, $CDCl_3$, TMS): δ 2.16 (*s*, 3H), 2.47 (*s*, 3H), 7.32-7.34 (*t*, 3H), 7.46-7.5 (*t*, J = 7.6 & 8.4 Hz, 2H), 7.57-7.59 (*d*, J = 8.4 Hz, 2H), 7.88-7.9 (*d*, J = 8 Hz, 2H). ^{13}C NMR ($CDCl_3$): δ 191.6, 161.77, 147.93, 142.72, 137.28, 134.63, 129.14, 129.1, 128.21, 126.62, 120.72, 103.56, 21.70, 16.04. Elem. anal. calcd. for $C_{18}H_{16}N_2O_2$: C, 73.95; H, 5.52; N, 9.58. Found: C, 74.24; H, 5.58; N, 9.57. ESI-MS: *m/z* 292.07 (calcd: *m/z* 292.33).

Synthesis of 1-toluoyl-3-methyl-4-phenyl-5-pyrazolone (L^2): The ligand L^2 was synthesized by similar procedure to L^1 using 1-toluoyl-3-methyl-5-pyrazolone (18.8 g, 0.1 mol) and benzoyl chloride (14.0 g, 0.1 mol). (Yield 23.9 gm, 81%) ^1H NMR (400 MHz, $CDCl_3$, TMS): δ 2.12 (*s*, 3H), 2.41 (*s*, 3H), 7.30 (*d*, 2H), 7.51-7.56 (*m*, 2H), 7.58-7.6 (*m*, 1H), 7.66-7.67 (*m*, 2H), 7.74-7.76 (*m*, 2H). ^{13}C NMR ($CDCl_3$): δ 192.26, 161.01, 147.76, 137.80, 136.57, 134.80, 131.83, 129.68, 128.41, 127.90, 120.76, 103.48, 21.08, 15.86. ESI-MS: *m/z* 292.23 (calcd: *m/z* 292.33).

Synthesis of 1-toluoyl-3-methyl-4-toluoyl-5-pyrazolone (L^3): The ligand L^3 was synthesized by similar procedure to L^1 using 1-toluoyl-3-methyl-5-pyrazolone (18.8 g, 0.1 mol) and toluoyl chloride (15.5 g, 0.1 mol). (Yield 23.3 gm, 76%) ^1H NMR (400 MHz, $CDCl_3$, TMS): δ 2.15 (*s*, 3H), 2.41 (*s*, 3H), 2.47 (*s*, 3H), 7.27-7.29 (*d*, J = 8 Hz, 2H), 7.32-7.34 (*d*, J = 8 Hz, 2H), 7.57-7.59 (*d*, J = 8 Hz, 2H), 7.74-7.76 (*d*, J = 8.4 Hz, 2H), 10.33(*s*, 1H). ^{13}C NMR ($CDCl_3$): δ 191.96, 161.24, 147.73, 142.59,136.93, 134.89, 134.83, 129.67, 129.07, 128.16, 120.77, 103.43, 21.68, 21.08, 15.99. ESI-MS: *m/z* 306.09 (calcd: *m/z* 306.14).

Synthesis of 1-(3,4-dichlorophenyl)-3-methyl-4-toluoyl-5-pyrazolone (L^4): The ligand L^5 was synthesized by similar procedure to L^1 using 1-(3,4-dichlorophenyl)-3-methyl-5-pyrazolone (24.2 g, 0.1 mol) and toluoyl chloride (15.5 g, 0.1 mol). (21.6 gm, 60%) ^1H NMR (400 MHz, $CDCl_3$, TMS): δ 2.15 (*s*, 3H), 2.48 (*s*, 3H), 7.34-7.36 (*d*, J = 8 Hz, 2H), 7.52-7.54 (*d*, J = 8.8 Hz, 1H), 7.57-7.59 (*d*, J = 8 Hz, 2H), 7.86-7.89 (*dd*, J = 2.4 Hz, 1H), 8.13-8.14 (*d*, J = 2.4 Hz, 1H). ^{13}C NMR ($CDCl_3$): δ 189.23, 163.56, 148.38, 143.19, 136.83, 133.24, 133.05, 130.66, 129.60, 129.18, 128.40, 121.54, 118.92, 103.86, 21.73, 16.20. ESI-MS: *m/z* 360.28 (calcd: *m/z* 360.04).

Synthesis of 1-(3,4-dichlorophenyl)-3-methyl-4-phenyl-5-pyrazolone (L^5): The ligand L^6 was synthesized by similar procedure to L^1 using 1-(3,4-dichlorophenyl)-3-methyl-5-pyrazolone (24.2 g, 0.1 mol) and benzoyl chloride (14.0 g, 0.1 mol). (Yield

22.1 gm, 64%) ^{1}H NMR (400 MHz, $CDCl_3$, TMS): δ 2.11 (*s*, 3H), 7.53-7.57 (*m*, 3H), 7.61-7.67 (*m*, 3H), 7.58-7.88 (*dd*, J = 2.4 Hz, 1H), 8.12-8.13 (*d*, J = 2.4 Hz, 1H). ^{13}C NMR ($CDCl_3$): δ 189.98, 163.10, 148.45, 136.72, 136.35, 133.12, 132.27, 130.72, 129.84, 128.53, 128.09, 121.72, 129.05, 103.95, 16.01. ESI-MS: *m/z* 346.28 (calcd: *m/z* 346.03).

Synthesis of 1-toluoyl-3-methyl-4-naphthoyl-5-pyrazolone (L^6): 1-toluoyl-3-methyl-5-pyrazolone (4.7 g, 0.025 mol) and 80 ml of dried 1,4-dioxane were placed in a 100 ml flask with a magnetic stirrer and heated at 70 °C for 10 min. To the resulting yellow solution, calcium hydroxide (3.7 g, 0.05 mol) in small portions was added and then naphthoyl chloride (4.75 g, 0.025 mol) was added drop wise. The resulting mixture was heated to reflux for 24 h. The cloudy yellowish mixture was cooled to room temperature and poured into a 350 ml solution of ice-cold hydrochloric acid (3 mol L^{-1}) under stirring. The yellow precipitate was filtered and recrystallized from acetone and water. (6.07 gm, 71%) ^{1}H NMR (400 MHz, $CDCl_3$, TMS): δ 1.66 (*s*, 3H), 2.42 (*s*, 3H), 7.30-7.32 (*d*, J = 8.4 Hz, 2H), 7.56-7.60 (*m*, 4H), 7.77-7.79 (*d*, J = 8.8 Hz, 2H), 7.94-7.97 (*m*, 1H), 8.01-8.03 (*t*, 2H). ^{13}C NMR ($CDCl_3$): δ 193.22, 160.49, 148.58, 136.75, 135.65, 133.52, 130.94, 129.75, 129.70, 128.52, 127.41, 126.70, 125.38, 124.89, 124.80, 120.86, 105.26, 21.12, 14.6. ESI-MS: *m/z* 342.54 (calcd: *m/z* 342.14).

1.1.2.3. Synthesis of oxovanadium(IV) complexes of 4-acylpyrazolone ligands

Synthesis of complex 1 [$VO(L^1)_2(H_2O)$]: To a well-stirred hot ethanolic solution of ligand L^1 (0.292 g, 0.001 mol), an aqueous solution of $VOSO_4{\cdot}5H_2O$ (0.127 g, 0.005 mol) was added drop wise. The reaction mixture was refluxed with stirring for 6 hours. A green precipitate was formed which was filtered, washed with hot distilled water and then washed from ethanol and dried under vacuum yielding 0.210 g (72%) green solid. The solid product was dissolved in hot CH_3CN and allowed to crystallize at room temperature. Blue crystals of single-crystal XRD quality were obtained in 2-4 days. The obtained material was designated as $VO(L^1)_2$ ESI-MS calcd. for $C_{36}H_{30}N_4O_5V$ $[M]^+$ 649.17; found 650.03 $[M+H]^+$. Elem. anal. calcd. for $C_{36}H_{32}N_4O_6V$ $[VO(L^2)_2{\cdot}H_2O]$ (667.6): C 64.77, H 4.83, N 8.39; found C 64.71, H 4.87, N 8.40.

Synthesis of complex 2 $[VO(L^2)_2(H_2O)]$: The complex was synthesized by the similar procedure to complex 1. The green solid obtained was dissolved in acetonitrile and heated till the solution become clear and then it was allowed to crystallize at RT. Blue crystals of single crystal X-ray diffraction quality were obtained within a week. Yield 0.207g (71%). ESI-MS calcd for $C_{36}H_{30}N_4O_5V$ $[M]^+$ 649.17; found 650.14 $[M+H]^+$. Elem. anal. calcd. for $C_{36}H_{32}N_4O_6V$ $[VO(L^1)_2{\cdot}H_2O]$ (667.6): C 64.77, H 4.83, N 8.39; found C 64.82, H 4.89, N 8.39.

Synthesis of complex 3 $[VO(L^3)_2(H_2O)]$: The complex was synthesized by similar procedure to complex 1. Yield 0.205g (67%). ESI-MS calcd. for $C_{38}H_{34}N_4O_5V$ $[M^+]$ 677.20; found 678.21 $[M+H]^+$. Elem. anal. calcd. for $C_{38}H_{36}N_4O_6V$ $[VO(L^3)_2{\cdot}H_2O]$ (695.21): C 65.61, H 5.22, N 8.05; found C 65.68, H 5.27, N 8.07.

Synthesis of complex 4 $[VO(L^4)_2(H_2O)]$: The complex was synthesized by similar procedure to complex 1. Yield 0.231g (67%). ESI-MS calcd. for $C_{36}H_{26}Cl_4N_4O_5V$ $[M]^+$ 785.01; found 787.92 $[M+2H]^+$. Elem. anal. calcd. for $C_{36}H_{28}Cl_4N_4O_6V$ $[VO(L^4)_2{\cdot}H_2O]$ (803.02): C 53.69, H 3.50, N 6.96; found C 53.72, H 3.56, N 7.02.

Synthesis of complex 5 $[VO(L^5)_2(H_2O)]$: The complex was synthesized by similar procedure to complex 1. Yield 0.245g (68 %). ESI-MS calcd. for $C_{34}H_{22}Cl_4N_4O_5V$ $[M]^+$ 756.98; found 757.91 $[M+H]^+$. Elem. anal. calcd for $C_{34}H_{24}Cl_4N_4O_6V$ $[VO(L^5)_2{\cdot}H_2O]$ (774.99): C 52.53, H 3.11, N 7.21; found C 52.58, H 3.15, N 7.20.

Synthesis of complex 6 $[VO(L^6)_2(H_2O)]$: The complex was synthesized by similar procedure to complex 1. Yield 0.268 (70%). ESI-MS calcd. For $C_{44}H_{34}N_4O_5V$ $[M]^+$ 749.20; found 750.11 $[M+H]^+$. Elem. anal. calcd. for $C_{44}H_{36}N_4O_6V$ $[VO(L^6)_2{\cdot}H_2O]$ (767.21): C 68.84, H 4.73, N 7.30; found C 68.88, H 4.77, N 7.32.

1.1.2.4. Crystallography

The complex $VO(L^1)_2$ was dissolved in acetonitrile and heated till the solution become clear and then it was allowed to crystallize at RT. Blue crystals of single crystal X-ray diffraction quality were obtained within a week. The crystal used for data collection was of dimensions 0.3 × 0.2 × 0.1 mm^3. The cell dimensions were determined by least-square fit of angular settings of 5634 reflections in the θ range 3.32 to 29.07°. The intensities were measured by ø and ω scan mode for θ ranges 3.37 to 26.00°.

Single crystal of the complex $VO(L^2)_2$ was obtained by the slow evaporation of acetonitrile solution of the complex. Blue crystals of single-crystal XRD quality were obtained in 2-4 days. The crystal used for data collection was of dimensions 0.30 × 0.20 × 0.20 mm. The cell dimensions were determined by least-squares fit of angular settings of 5156 reflections in the θ range 3.37 to 28.95 °. The intensities were measured by ø and ω scan mode for θ ranges 3.34 to 24.00°. 3037 reflections were treated as observed ($I > 2\sigma(I)$).

Data were corrected for Lorentz, polarization and absorption factors. The structure was solved by direct methods using *SHELXS97* [16]. All non-hydrogen atoms of the molecule were located in the best E-map. Full-matrix least-squares refinement was carried out using *SHELXL97* [16]. All hydrogen atoms except water hydrogen were included as idealized atoms riding on the respective carbon atoms with C-H bond lengths appropriate to the carbon atom hybridization. Water hydrogen atoms were located from the difference Fourier map and included in the refinement.

For the complexes $VO(L^1)_2$ and $VO(L^2)_2$ final refinement cycles converged to an $R = 0.0768$ & $R_w(F^2) = 0.1795$ and $R = 0.0562$ & $R_w(F^2) = 0.1795$, respectively for the observed data. Residual electron densities ranged from -0. 370 to 0.374 $eÅ^{-3}$ for the complex $VO(L^1)_2$ and from -0.427 to 0.425 $eÅ^{-3}$ for the complex $VO(L^2)_2$. Atomic scattering factors were taken from International Tables for X-ray Crystallography (1992, Vol. C, Tables 4.2.6.8 and 6.1.1.4). The crystallographic data are summarized in Table 1. H atoms are shown as small spheres of arbitrary radii. The geometry of the molecules were calculated using the *WinGX* [17] and *PARST* [18] software.

1.1.2.5. Catalytic reaction

Catalytic oxidation of benzyl alcohol was carried out in a 50 mL round bottom flask fitted with a water circulated condenser using oxovanadium(IV) complexes $[VO(L^{1-6})_2]$ of 4-acylpyrazolone ligands as a catalyst. In a typical reaction, benzyl alcohol, catalyst and 30% H_2O_2 were intensively stirred at the 90 °C temperature for the whole duration of the reaction. After completion of the reaction, reaction mixture was concentrated on rotary evaporator. Hexane was added to the system, and the organic phase was separated. By this simple procedure, isolation of the carbonyl product in the organic phase was achieved.

1.1.3. Results and Discussion

1.1.3.1. Synthesis and characterization of 4-acylpyrazolone ligands (1-6)

The ligands L^1, L^2, L^3, L^4, L^5 and L^6 (Scheme 1.1.1) were synthesized by the reaction between various derivatives of pyrazol-5-one and corresponding acylchloride. Acylation occurs at C-4 position of pyrazole ring in basic (calciumhydroxide) dioxane at reflux. Subsequent treatment with acid aqueous solution affords the ligands in high yield as a solid powder insoluble in water. The ligands were recrystallized by acidic methanol-water mixture (80% methanol + 19% water + 1% HCl). Ligand L^4 was recrystallized by acetone-water mixture. The synthesized ligands were characterized by ^1H & ^{13}C NMR, ESI-Mass spectrometry and elemental analyses. On the basis of spectroscopic and analytical evidences structures of the ligands were proposed.

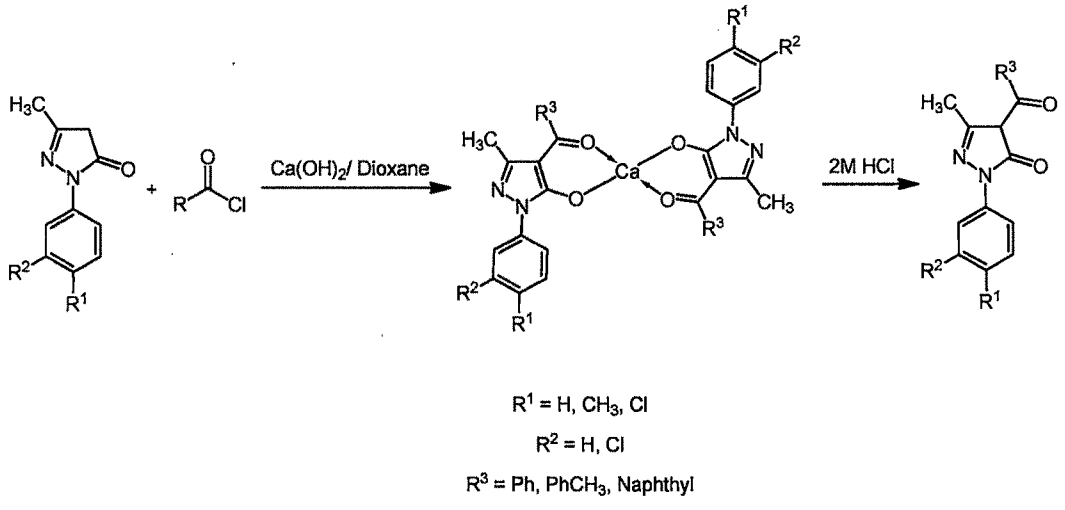

Scheme 1.1.1. Synthetic route for ligands L^1-L^6.

NMR spectral characterization of the ligands L^1-L^6

^1H & ^{13}C NMR spectra of all the ligands were in good agreement with the proposed structures of the ligands. ^1H NMR spectra of the ligand L^1 shows two peaks 2.16 (3H) & 2.47 (3H) δ, which confirm the presence of two methyl groups and also confirm that toluoyl ring has attached to the C4 carbon of pyrazolone. The two doublets appear at 7.46 (2H) and 7.57 (2H) δ also confirm the presence of toluoyl ring at the C4 carbon of pyrazolone. The proton ratio of aliphatic and aromatic region is also equal to the expected proton ratio of the ligand. The ^{13}C NMR spectrum is also in

good agreement with the structure of ligand. ^{1}H NMR spectrum of ligand L^2 shows 2 peaks in the aliphatic region at 2.12 and 2.41 δ, which are corresponds to the two methyl groups present in the ligand. The spectrum of L^2 shows 5 peaks in the aromatic region from 7.51 to 7.76 δ for the 9 aromatic protons of the phenyl and toluoyl rings of the ligand. The proton ratio of aliphatic and aromatic protons also matches with the calculated protons for the ligand. ^{13}C NMR of the ligand L^2 shows 14 peaks in the spectrum, which are corresponds to the presence of 14 carbons of different chemical environment. The spectrum shows two singlet at 15.86 (3H) & 21.08 (3H) δ for the methyl groups. The peaks at 192.26 & 161.01 δ show the presence of the keto and amide carbons in the ligand. The ^{1}H NMR spectrum of the ligand L^3 shows three singlets at 2.15 (3H), 2.41 (3H) & 2.47 (3H) δ, which confirm the presence of three methyl groups in the ligand and also confirm the presence of two toluoyl rings in the ligand. The presence of four doublets at 7.27 (2H), 7.31 (2H), 7.57(2H) & 7.74 (2H) δ also confirm the presence of two toluoyl rings in the ligand. The broad peak at 10.33 (1H) δ confirm the presence of –OH group in the pyrazolone and shows that it has tatuomerized in the enolic form. The ^{13}C NMR spectrum shows three peaks in aliphatic region at 15.99, 21.08 & 21.68 δ, which confirm the presence of three methyl groups in the ligand. ^{1}H NMR spectrum of the ligand L^4 shows two singlets in aliphatic region at 2.15 (3H) & 2.48 (3H) δ, which confirm the presence of two methyl groups. The presence of four doublets at 7.34 (2H), 7.52 (1H), 7.57 (2H) & 8.13 (1H) δ and one double doublet at 7.86-7.89 (1H) δ confirm the presence of a toluoyl ring at C4 position and the presence of dichlorophenyl ring at N1 of pyrazolone ring. ^{13}C NMR also confirms the presence of two methyl groups (16.20 & 21.73 δ). ^{1}H NMR spectrum of the ligand L^5 shows one peak in the aliphatic region at 2.113 δ, which confirm the presence of one methyl group in the ligand. The spectrum shows one doublet at 8.12 (1H) δ, one double doublet at 7.85-7.88 (1H) δ and one doublet which has been overlapped with the other aromatic protons at 7.53 (2H) δ, which confirm the presence of dichorophenyl ring at N1 of pyrazolone ring. The spectrum also shows a peak at 10.89 δ, which confirm the presence of enolic form of the pyrazolone ligand. The ^{13}C NMR spectrum also confirms the presence of one methyl group by the peak at 16.01 δ. ^{1}H NMR spectrum of one of the ligand is illustrated in the Figure 1.1.1.

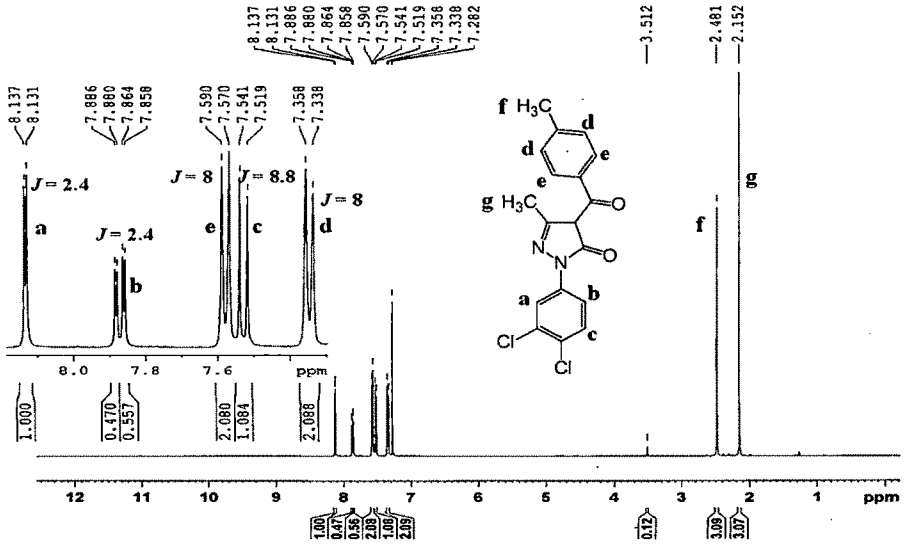

Figure 1.1.1. ^{1}H NMR spectrum of the ligand L^{4}.

^{1}H NMR spectrum of the ligand L^{6} shows two peaks in the aromatic region at 1.66 (3H) & 2.42 δ, which confirm the presence of two methyl groups in the ligand. The aromatic region shows one doublet and five multiplets correspond to the presence of ten aromatic protons. The ^{13}C NMR spectrum of the ligand shows two peaks in the aliphatic region at 14.6 & 21.12 δ, which confirm the presence of two methyl groups in the ligand. The appearance of 19 peaks in the ^{13}C spectrum shows the presence of 19 carbons in the different chemical environment and confirms the proposed structure of the ligand L^{6}. ^{13}C NMR spectrum of one of the ligand is illustrated in the Figure 1.1.2.

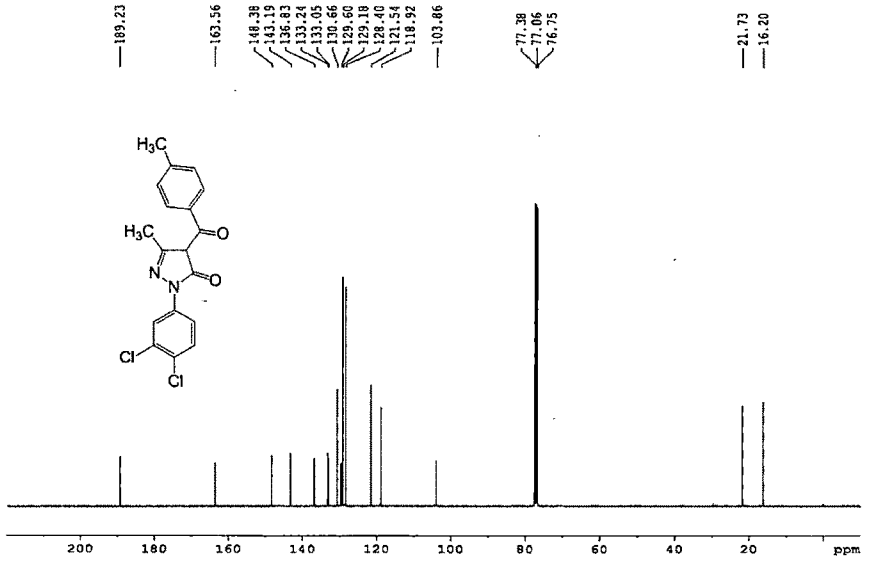

Figure 1.1.2. ^{13}C NMR spectrum of the ligand L^{4}.

Mass spectral analysis of the ligands

ESI-Mass spectral analyses of all the six ligands were carried out and matched with the calculated mass of the proposed structures of the ligands synthesized. Mass spectral values of the ligands are presented in the Table 1.1.1. ESI-MS of one of the ligand is illustrated in the Figure 1.1.3.

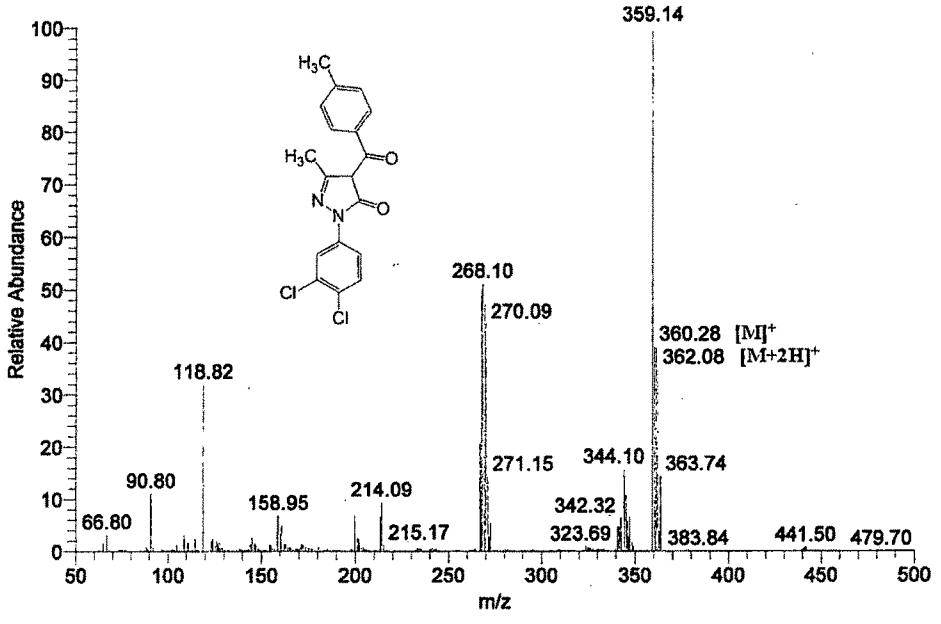

Figure 1.1.3. ESI-MS of ligand L^4.

Table 1.1.1. ESI-Mass spectral values of ligands.

Ligands	Molecular ion peak (calculated mass)
1	*m/z*: 292.23 (292.12)
2	*m/z*: 292.07 (292.12)
3	*m/z*: 306.09 (306.14)
4	*m/z*: 360.28 (360.04)
5	*m/z*: 346.28 (346.03)
6	*m/z*: 342.54 (342.14)

As shown in the Table 1.1.1 mass spectra of the ligands show molecular ion peaks corresponds to the molecular mass of the ligands and matches with the calculated mass of ligands.

1.1.3.2.Syntheses and characterization of oxovanadium(IV) complexes

The oxovanadium(IV) complexes here reported, having the general composition $[VO(L)_2(H_2O)]$. The complexes (**1-6**) were synthesized by a general procedure based on the mixing of an ehanolic solution of ligand with aqueous solution of $VOSO_4 \cdot 5H_2O$ in 2:1 molar ratio (*see* scheme 1.1.2) and isolation of final product by filtration. The complexes were characterized by elemental analyses, FT-IR, TG-DTA, Mass spectrometry, UV-Vis, EPR spectroscopy and single crystal XRD analysis. All the complexes are stable to air and moisture without any kind of decomposition also after several months. The complexes are insoluble in water, hexane and petroleum ether, but soluble in DMF, DMSO, acetonitrile and chlorinated solvents. The obtained complexes were designated as $VO(L^{1\text{-}6})_2$.

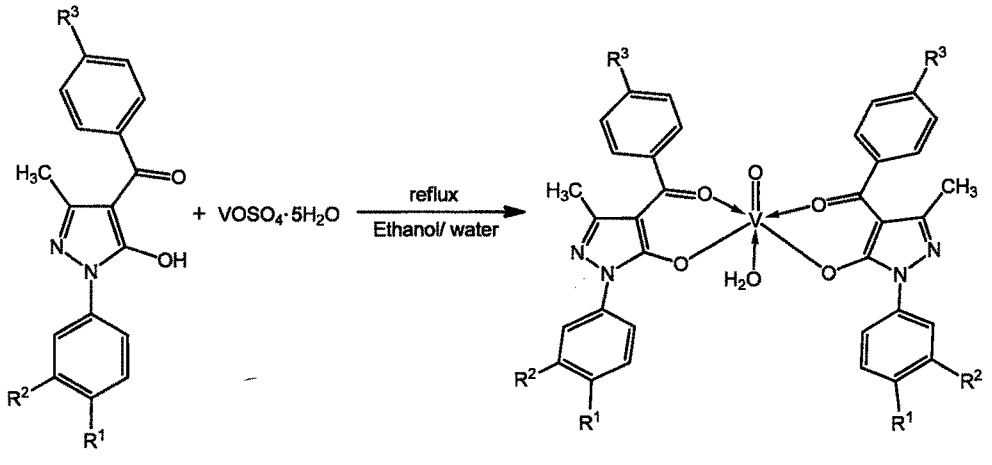

Scheme 1.1.2. Synthetic procedure of oxovanadium(IV) complexes.

Blue block-shaped single crystals of the complex $VO(L^1)_2$, suitable for X-ray diffraction analysis were obtained by slow evaporation of $VO(L^1)_2$ in acetonitrile. The crystal structure of the complex $VO(L^1)_2$ was solved by single-crystal XRD in the space group $P2_1/c$ of the monoclinic system and refined to give formula $[VO(L^1)_2.H_2O]$. The single crystals of the complex $VO(L^2)_2$ were obtained by the slow evaporation of its acetonitrile solution. The crystal was solved by single crystal XRD in the space group $P2_1/c$ of the monoclinic system and refined to give formula $[VO(L^2)_2.H_2O](CH_3CN)$. Data collection parameters and refinement results of the complexes $VO(L^1)_2$ and $VO(L^2)_2$ are summarized in Table 1.1.2.

Table 1.1.2. Crystal structure data and structure refinement details for $VO(L^1)_2$ and $VO(L^2)_2$.

	$[VO(L^1)_2(H_2O)]$	$[VO(L^2)_2(H_2O)]CH_3CN$
Empirical formula	$C_{36}H_{34}N_4O_6V$	$C_{36}H_{32}N_4O_6V_1.C_2H_3N_1$
F_w	669.61	708.65
Wavelength (Å)	0.71073	0.71073
Crystal system	Monoclinic	Monoclinic
Space group	$P2_1/c$	$P2_1/c$
Crystal colour and size (mm^3)	Blue, 0.3 × 0.2 × 0.1	Blue, 0.3 × 0.2 × 0.2
a (Å)	13.6618(12)	17.2079(7)
b (Å)	27.5554(17)	11.4667(5)
c (Å)	9.7253(10)	18.6877(8)
α (°)	90.00	90.00
β (°)	104.747(10)	105.196(4)
γ (°)	90.00	90.00
V ($Å^3$)	3540.6(5)	3558.5(3)
Z	4	4
D_{calcd} (gm/cm^3)	1.256	1.323
F(000)	1396	1476
θ range for data collection	$3.34 < \theta < 24.00°$	$3.37 < \theta < 26.00°$
Index ranges	$-15 \le h \le 15, -31 \le k \le 31, -11 \le l \le 11$	$-14 \le h \le 21, -14 \le k \le 13, -23 \le l \le 17$
Reflections collected/ Unique	34372 / 5527	14753 / 6979
Final R	0.0768	0.0522
Goodness-of-fit on F^2	0.993	1.022
Final residual electron density ($eÅ^{-3}$)	$-0.370 < \Delta\rho < 0.374$	$-0.428 < \Delta\rho < 0.303$
CCDC	817984	859107

As per our knowledge, there is only one crystal structure of the vanadium complex of the acylpyrazolone ligand that has been reported in the literature [14] having acylpyrazolonate ligands in the *anti* configuration to each other. Single-crystal data reveal that the two O,O-chelating acylpyrazolonate ligands occupy the equatorial plane of the oxovanadium(IV) complex in a *syn* configuration to each other, which is in contrast to the structure published elsewhere [14], the distorted octahedral geometry exists through coordination to the vanadium center of a water molecule trans to the oxo group. Thus, the ligands form two six-membered chelate rings with the vanadium metal center. The V-O bond distances of the two chelated acylpyrazolonate ligands are in the range 1.962.02 Å. The average "bite" angles are 88.3(1) and 90.2(1)°. An ORTEP view of the $VO(L^1)_2$ compound with atomic labeling is shown in Figure 1.1.4.

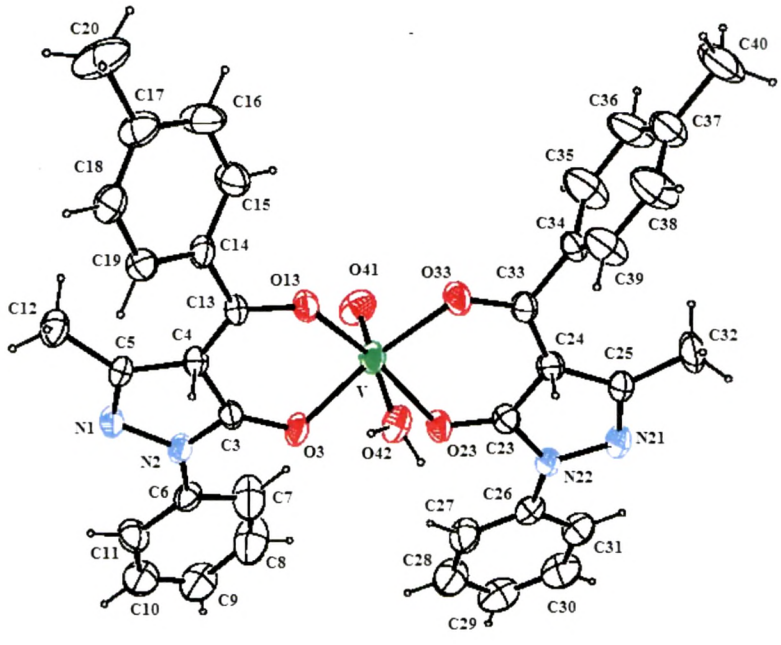

Figure 1.1.4. ORTEP view of the $VO(L^1)_2$ with displacement ellipsoids drawn at 50% probability level.

Selected bond distances and bond angles are listed in Table 1.1.3. H atoms are shown as small spheres of arbitrary radii. Examination of nonbonded contacts reveals O-H···N, C-H···O, and C-H···π intermolecular hydrogen bonds (Table 1.1.4), which are responsible for the stability of the molecules within the unit cell. Hydrogen bonding geometry of the complex $VO(L^1)_2$ is shown in Figure 1.1.5.

Table 1.1.3. Selected bond lengths (Å) and bond angles (°) of $VO(L^1)_2$ (e.s.d.'s are given in parentheses)

V1-O41	1.593(4)	**V1-O3**	1.969(3)
V1-O23	1.978(3)	**V1-O13**	1.999(3)
V1-O33	2.022(3)	**V1-O42**	2.247(4)
O41-V1-O3	99.10(18)	**O41-V1-O23**	100.31(16)
O3-V1-O23	87.49(13)	**O41-V1-O13**	96.91(16)
O3-V1-O13	88.31(13)	**O23-V1-O13**	162.72(14)
O41-V1-O33	95.60(18)	**O3-V1-O33**	165.30(15)
O23-V1-O33	90.24(13)	**O13-V1-O33**	89.58(13)
O41-V1-O42	175.42(19)	**O3-V1-O42**	84.13(15)
O23-V1-O42	83.03(15)	**O13-V1-O42**	79.87(14)
O33-V1-O42	81.18(15)		

Table 1.1.4. C-H...O and C-H...π hydrogen bonding geometry of $VO(L^1)_2$. Cg4 represents the center of gravity of the ring C26-C31.[a]

D-H...A[b]	D-H(Å)	D...A(Å)	H...A(Å)	D-H...A(°)
O42-H421...N1i	0.80(6)	2.851(5)	2.09(6)	159(6)
C30-H30...O41ii	0.93(1)	3.248(8)	2.425(4)	148(4)
O42-H422...N21iii	0.80(4)	2.904(6)	2.16(5)	156(4)
C35-H35...Cg4iii	0.93(1)	3.498(7)	2.639(4)	154(4)

[a]Cg4 represents the center of gravity of the ring C26-C31.

[b]Symmetry Code (i) x,-y+1/2,+z+1/2 (ii) -x,-y,-z+1 (iii) -x,-y,-z+2

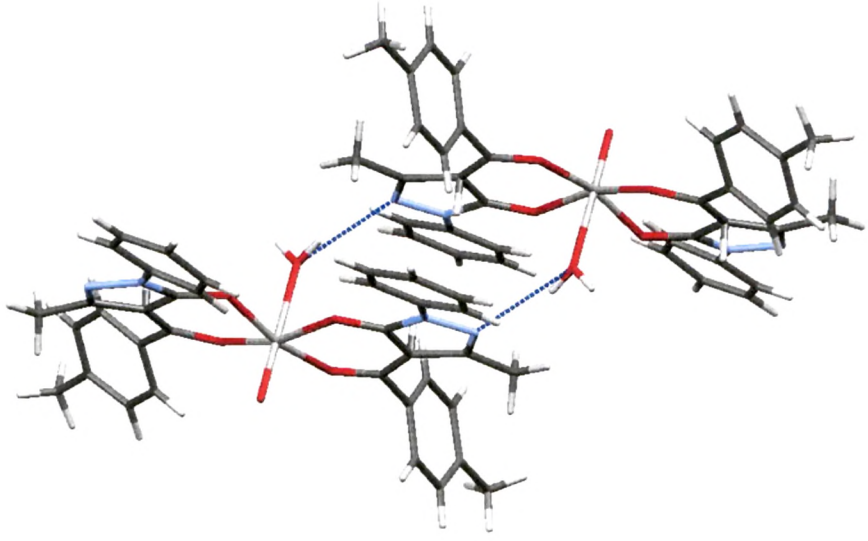

Figure 1.1.5. Intermolecular hydrogen bonds of O_{water}-H···N_{py} type.

The packing of molecules in the unit cell is further stabilized by π-π stacking interactions (Figure 1.1.6). A summary of π-π interactions is given in Table 1.1.5.

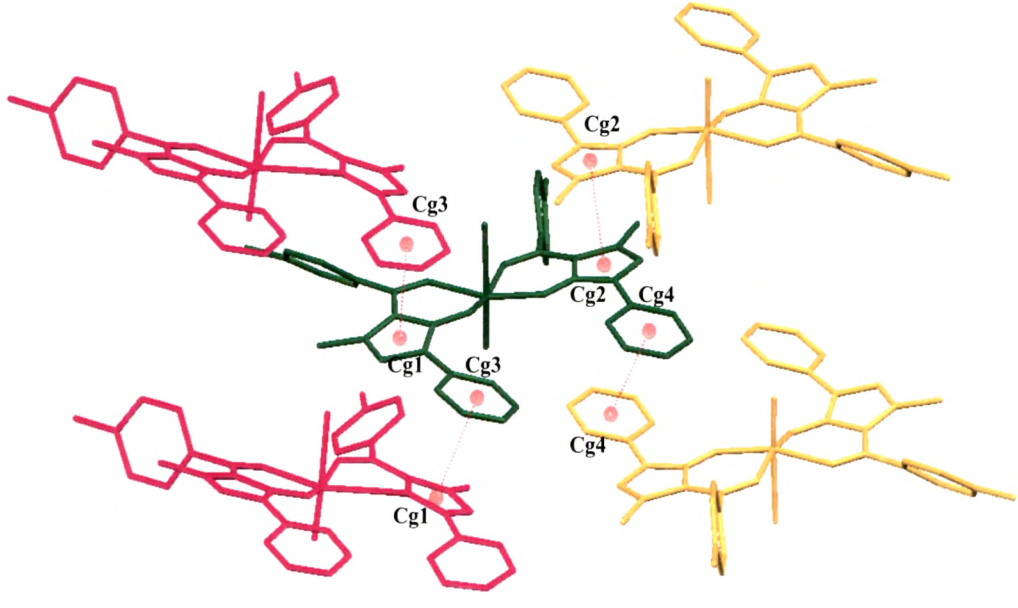

Figure 1.1.6. View of the layers formed by intermolecular π-π stacking interactions of $VO(L^1)_2$. Different colors represent different chains formed by π-π interaction. Cg1, Cg2, Cg3 and Cg4 represents, ring (N1, N2, C3-C5), ring (N21, N22, C23-C25), ring (C6-C11) and ring (C26-C31) respectively. H atoms were omitted for clarity.

Table 1.1.5. Geometry of π-π interactions.[a, b]

CgI CgJ[b]	CgI...CgJ(Å)	CgI...P(Å)	α (°)	β (°)	Δ (Å)
Cg1-Cg3i	3.677(4)	3.645	8.51	12.53	0.48
Cg2-Cg2ii	3.702(3)	3.665	0.00	8.14	0.52
Cg3-Cg1iii	3.677(4)	3.589	8.51	7.55	0.80
Cg4-Cg4iv	3.797(4)	3.631	0.00	17.02	1.11

[a]Cg represents the center of gravity of the following rings : Cg1 ring (N1, N2, C3-C5), Cg2 ring (N21, N22, C23-C25), Cg3 ring (C6-C11) and Cg4 ring (C26-C31). CgI...CgJ represents the distance between the ring centroids; CgI...P, the perpendicular distance of the centroid of one ring from the plane of the other; α is the dihedral angle between the planes of rings I and J; β is the angle between normal to the centroid of ring I and the line joining ring centroids; Δ is the displacement of the centroid of ring J relative to the intersection point of the normal to the centroid of ring I and the least-squares plane of ring J.

[b]**Symmetry Code:** (i) x,1/2-y, 1/2+z (ii) -x, -y, 2-z (iii) x,1/2-y, -1/2+z (iv) -x, -y, 1-z

The crystal structure study of complex $VO(L^1)_2$ unveil that oxovanadium(IV) complexes of 4-acylpyrazolone ligands can also exist in the *syn* conformation and $VO(L^1)_2$ is the first example of this type. In the literatures existence of only *anti* conformations of oxovanadium(IV) complexes of 4-acylpyrazolone ligands were reported and *syn* conformation was not taken in the consideration.

Single crystal data of the complex $VO(L^2)_2$ shows that the two *O,O*-chelating acylpyrazolonate ligands and one water molecule are coordinated to the vanadium centre creating a distorted octahedral geometry. Thus both the ligands form a six membered chelate ring with the vanadium metal center. One acetonitrile molecule has also been trapped in the crystal lattice. An ORTEP view of the $VO(L^2)_2$ with atomic labeling is shown in Figure 1.1.7.

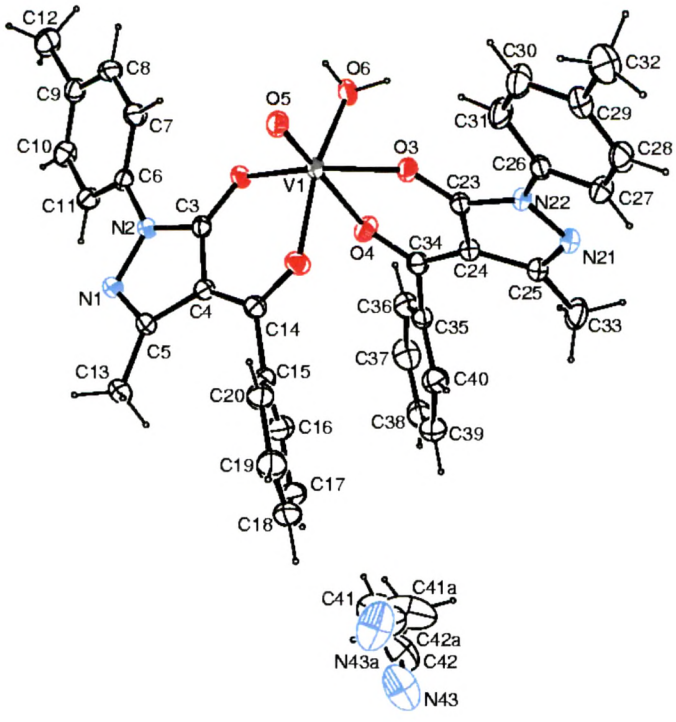

Figure 1.1.7. ORTEP view of the $VO(L^2)_2$ with displacement ellipsoids drawn at 50% probability level.

It is reported from the crystal structure evidence that the oxovanadium(IV) complexes of acylpyrazone ligands exist in octahedral geometry, where the ligands are coordinated in *anti* conformation and the V-$O_{(oxo)}$ group is located *trans* to the coordinated water molecule [14]. However, in the $VO(L^1)_2$ complex, ligands are coordinated in *syn* configuration and the V-$O_{(oxo)}$ group is still located *trans* to the coordinated water molecule. Somewhat surprisingly, in the present complex $VO(L^2)_2$, the coordination mode of ligands with the centre metal were changed, the V–$O_{(oxo)}$ group is located *cis* to the coordinated water molecule and the ligands are in *twisted* geometry.

The V^{IV} has a distorted $\{O_6\}$ octahedral environment with six different V-O bond lengths. The shortest bond length 1.594(2) Å is found for the oxovanadium bond (V1-O5). The longest bond length 2.205(2) Å is found for the oxygen of coordinated acylpyrazolone ligand and metal centre (V1-O4), located *trans* to the V-O(oxo) group. The middle range 1.982(2)-2.022(3) Å is found for the oxygen atoms of coordinated acylpyrazolone ligands (V1-O1, V1-O2 and V1-O3) and coordinated water molecule (V1-O6). The bond length of coordinated water molecule (V1-O6) is

2.022(3) Å, which is in contrast to the previously reported bond lengths in *anti* (2.262 Å) configuration [14] and in *syn* (2.247 Å) configuration. The bond length V1-O4 has been increased from 1.999 (*syn*) and 2.013 (*anti*) to 2.205(2). Bond length V1-O3 has also been increased from 1.969 (*syn*) and 1.989 (*anti*) to 2.018(2). Selected bond lengths and bond angles of $[VO(L^1)_2]$ are listed in Table 1.1.6.

Table 1.1.6. Selected bond lengths (Å) and bond angles (°).

V1-O1	1.982 (2)	**V1-O4**	2.205 (2)
V1-O2	2.021 (2)	**V1-O5**	1.594 (2)
V1-O3	2.018 (2)	**V1-O6**	2.022 (3)
O1-V1-O2	91.06 (9)	**O2-V1-O3**	88.48 (9)
O3-V1-O4	83.19 (8)	**O3-V1-O6**	89.1 (1)
O5-V1-O6	98.8 (1)	**O4-V1-O6**	83.0 (1)
O1-V1-O4	82.22 (8)	**O1-V1-O5**	99.1 (1)
O1-V1-O6	86.8 (1)	**O2-V1-O5**	99.0 (1)
O2-V1-O6	162.1 (1)	**O3-V1-O5**	95.5 (1)
O2-V1-O4	79.13 (9)	**O4-V1-O5**	177.8 (1)
O1-V1-O3	165.23 (9)		

Examination of nonbonded contacts reveals O-H···N and C-H···O intermolecular hydrogen bonds (Table 1.1.7), which are responsible for the stability of the molecules within the unit cell. The H atoms of a coordinated water molecule are creating two hydrogen bonds; one with the N atom of acetonitrile molecule and another one with the N atom of pyrazolone ring of another molecule (*see* Figure 1.1.8). Due to the hydrogen bonding geometry, the molecule has been *twisted* from its usual geometry (*syn* or *anti*).

Table 1.1.7. Hydrogen bonding geometry. [a]

D-H...A	D-H(Å)	D...A(Å)	H...A(Å)	D-H...A(°)
O6-H61...N21 [i]	0.82(1)	2.744(3)	1.94(1)	169(1)
C41-H41C...O2 [ii]	0.96	3.210(7)	2.579(2)	123.4(4)
C38-H38...O5 [ii]	0.93	3.416(5)	2.543(2)	156.5(3)
C41-H41B...O5 [ii]	0.96	3.097(7)	2.427(2)	126.6(4)
O6-H62...N43 [iii]	0.81(2)	2.665(9)	1.87(2)	168(2)

[a]Symmetry code: (i) -x+2,-y,-z+1, (ii) x,+y-1,+z, (iii) x,-y-1/2,+z-1/2.

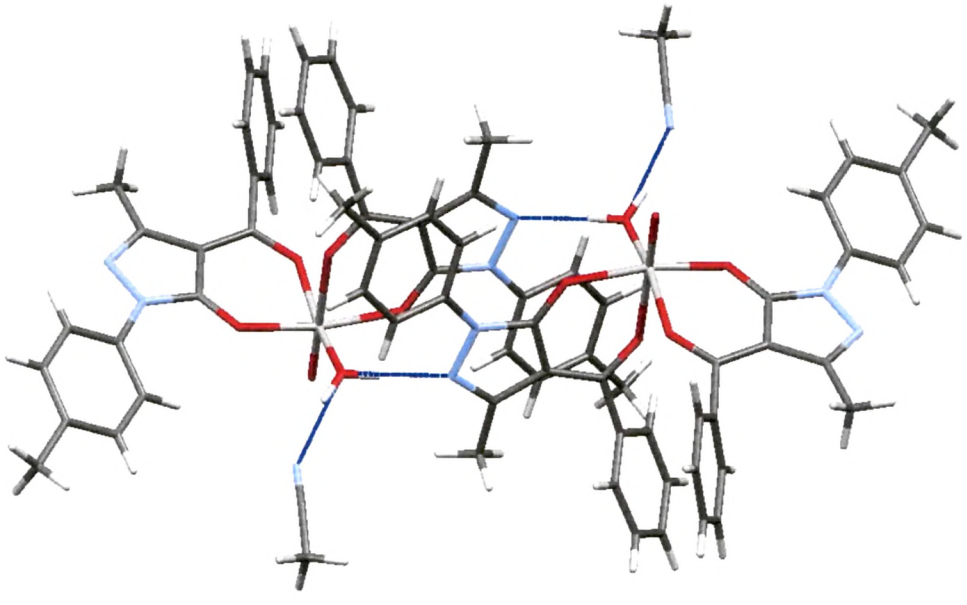

Figure 1.1.8. Intermolecular hydrogen bonds of O_{water}-H···N_{py} type and O_{water}-H···N_{MeCN} type.

A comparison with the published crystal structure data for *anti* configuration of oxovanadium(IV)complex of acylpyrazolone ligands [14] and *syn* configuration $[VO(L^1)_2]$ shows that the O5-V1-O6 angle within the $VO(L^2)_2$ complex has been decreased from 175-179° to 98.8(1)°. The angle O1-V1-O3 has been increased from 87.4-87.9° to 165.23(9)°, while the angle O2-V1-O4 has been decreased from 89.5-89.76° to 79.13(9)°. It is obvious from the crystal structure data that the geometry of the $VO(L^2)_2$ differs from the previous reports. The acylpyrazolone ligands are

coordinated with a vanadium atom in a *twisted* form to create a distorted octahedral geometry, where the two oxygen donors of two acylpyrazolones constitute a six-member ring with the metal atom. The resulting bite angles O1-V1-O2 and O3-V1-O4 are 91.06(9)° and 83.19(8)°, respectively.

The mass spectrum of $VO(L^1)_2$ shows a molecular ion peak ($C_{36}H_{30}N_4O_5V$) at *m/z* = 650.14 $[M+H]^+$ which indicate that it is a mono vanadium species having two 1-phenyl-3-methyl-4-toluoyl-5-pyrazolone ligands (*see* Figure 1.1.9). The peak at m/z = 672.72 is attributed to $[M+Na]^+$. Fragmentation of weakly coordinated water/solvent molecules in ESI mass spectrum is not observed. Mass spectra of complexes $VO(L^2)_2$, $VO(L^3)_2$, $VO(L^4)_2$, $VO(L^5)_2$ and $VO(L^6)_2$ showed molecular ion peaks at m/z = 650.03 $[M+H]^+$, 678.21 $[M+H]^+$, 787.92 $[M+2H]^+$, 757.91 $[M+H]^+$ and 750.1 $[M+H]^+$, respectively, which are in good agreement with the proposed structures. Elemental analyses of C, H and N shows that the complexes are pure and matches with the proposed structures.

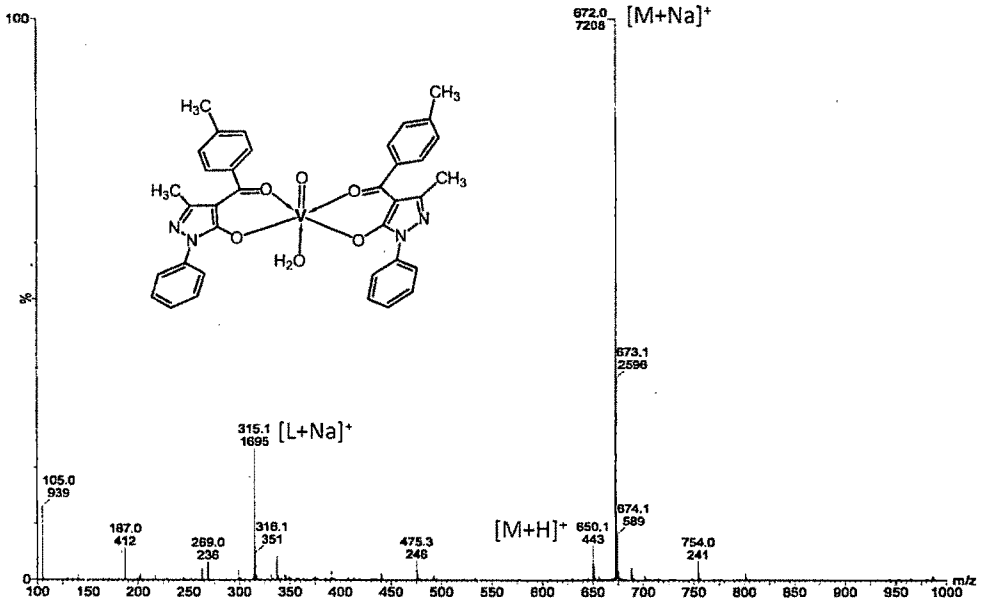

Figure 1.1.9. ESI-MS of complex $VO(L^1)_2$.

FT-IR spectrum of the complexes shows absorptions between 1565 to 1585 cm^{-1} and 1475-1497 cm^{-1} which are assigned to $\nu_{C=N}$ of the pyrazolone ring and ν_{C-O}, respectively. An additional information from IR spectra arises from the strong band observed in the range 945-970 cm^{-1} due to $\nu_{V=O}$ stretching. The bands within 470-485 cm^{-1} are assigned to the ν_{V-O} stretching. The IR spectra of complexes exhibit a band in

the range 3390-3435 cm^{-1}, which can be assigned to coordinate water molecule (*see* Figure 1.1.10).

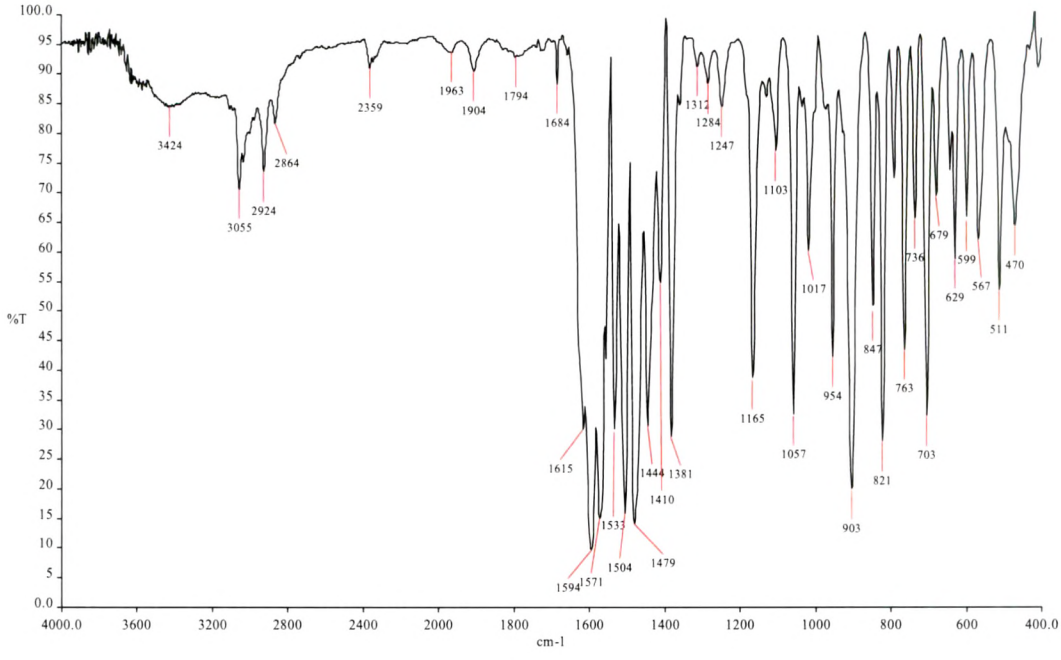

Figure 1.1.10. FT-IR spectrum of the complex $VO(L^2)_2$.

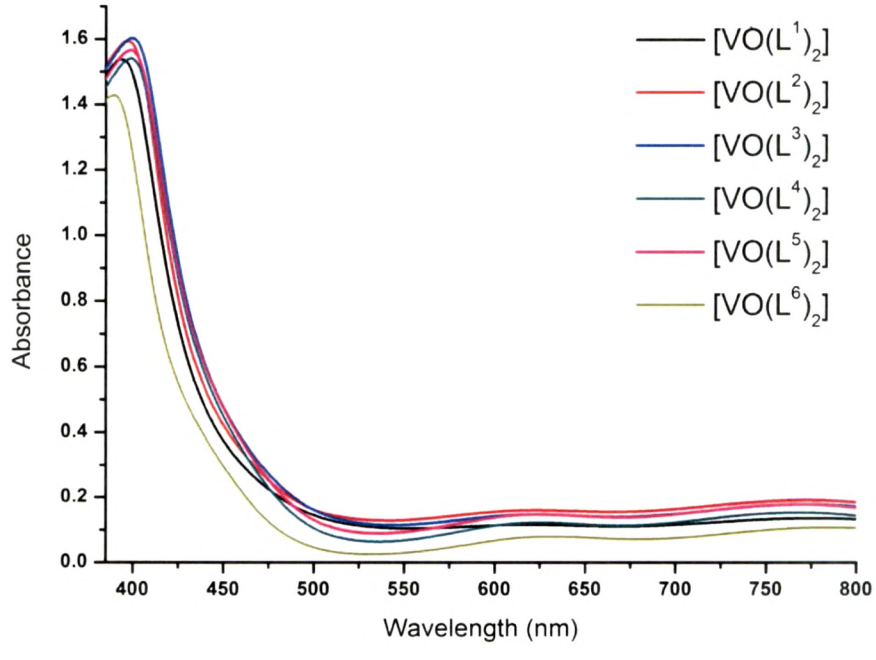

Figure 1.1.11. Electronic Spectra of the oxovanadium(IV) complexes.

The oxovanadium complexes show three absorption bands in the electronic spectra. The bands appear in the range 392-401 nm was assigned to ligand to metal charge transfer (LMCT). The two bands appear in the range 616-632 nm and 772-783 nm were assigned to $d \rightarrow d$ transitions. The electronic spectra reveal that in the complexes vanadium is present in +4 oxidation state (*see* Figure 1.1.11). The electronic spectral data of the complexes are provided in the Table 1.1.8.

Table 1.1.8. Electronic spectral data of the oxovanadium(IV) complexes [**1-6**].

Complex	UV-Vis data (nm)
Complex 1	394 (LMCT), 616($d \rightarrow d$), 775($d \rightarrow d$)
Complex 2	398 (LMCT), 621($d \rightarrow d$), 772($d \rightarrow d$)
Complex 3	401 (LMCT), 621($d \rightarrow d$), 773($d \rightarrow d$)
Complex 4	399 (LMCT), 626($d \rightarrow d$), 768($d \rightarrow d$)
Complex 5	392 (LMCT), 628($d \rightarrow d$), 775($d \rightarrow d$)
Complex 6	390 (LMCT), 632($d \rightarrow d$), 783($d \rightarrow d$)

The full range (3200 – 2000 G) X-band EPR spectra for $VO(L^1)_2$ (frozen solution state and room temperature solid state) were recorded. The EPR spectra of the complex $VO(L^1)_2$ at liquid nitrogen temperature and at room temperature are shown in Figure 1.1.12*a*. X-band EPR spectra were recorded in DMF for the $VO(L^1)_2$. The EPR spectrum of metal complex provide information about hyperfine and super hyperfine structure which is important in studying the metal ion environment in the complexes, i.e. the geometry, nature of the ligating sites from the ligand of the metal and the degree of covalency of the metal-ligand bonds.

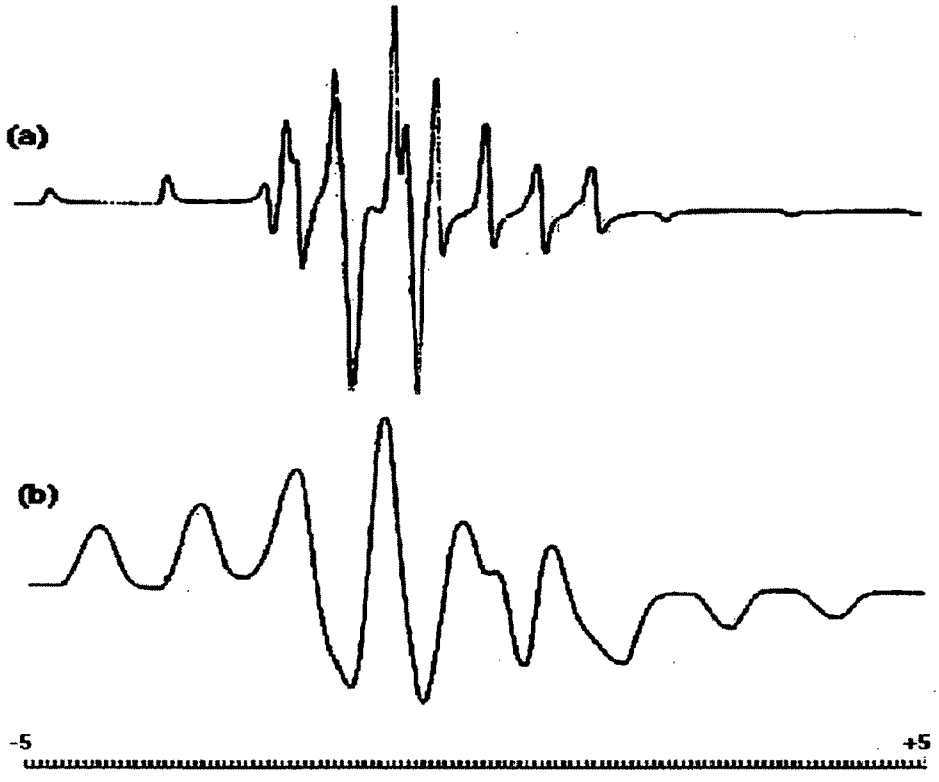

Figure 1.1.12. EPR spectra of (*a*) $VO(L^1)_2$ (in DMF at liquid nitrogen temperature) (*b*) $VO(L^1)_2$ (in polycrystalline state at room temperature).

The room temperature (300 K) spectrum of $VO(L^1)_2$ (Figure 1.1.12*b*) is a typical eight line pattern which shows that single vanadium is present in the molecule, i.e. it is mononuclear. In the frozen solution state, the spectrum shows two types of resonance components, one set due to the parallel feature and the other set due to the perpendicular features, which indicates axially symmetric anisotropy with well-resolved 16-line hyperfine splitting, characteristic of interaction between the electron and vanadium nuclear spins. The *g*-value (1.976) was computed from the spectra using TCNE free- radical as *g* marker.

The room temperature (300 K) spectrum of $VO(L^1)_2$ (Figure 1.1.12*b*) is a typical eight line pattern which shows that single vanadium is present in the molecule, i.e. it is mononuclear. In the frozen solution state, the spectrum shows two types of resonance components, one set due to the parallel feature and the other set due to the perpendicular features, which indicates axially symmetric anisotropy with well-resolved 16-line hyperfine splitting, characteristic of interaction between the electron

and vanadium nuclear spins. The *g*-value (1.976) was computed from the spectra using TCNE free- radical as *g* marker.

An EPR spectrum of frozen (77 K) solution (in DMF) of $VO(L^2)_2$ was recorded. The spectrum of $VO(L^1)_2$ is a 8-line pattern of free electron ($3d^1$) with the magnetic nuclear moment of $^{51}V(I = 7/2)$, which shows that a single vanadium is present in the molecule, i.e., it is mononuclear. The value of $g_{iso} = 1.981$ and $A_{iso} = 104.5 \times 10^{-4}$ confirms the presence of vanadium(V^{4+}, $3d^1$) in distorted octahedral geometry of the complex. The g value was computed from the spectrum using a tetracyanoethylene free radical as the *g* marker. The EPR spectra of $VO(L^2)_2$ is illustrated in the Figure 1.1.13.

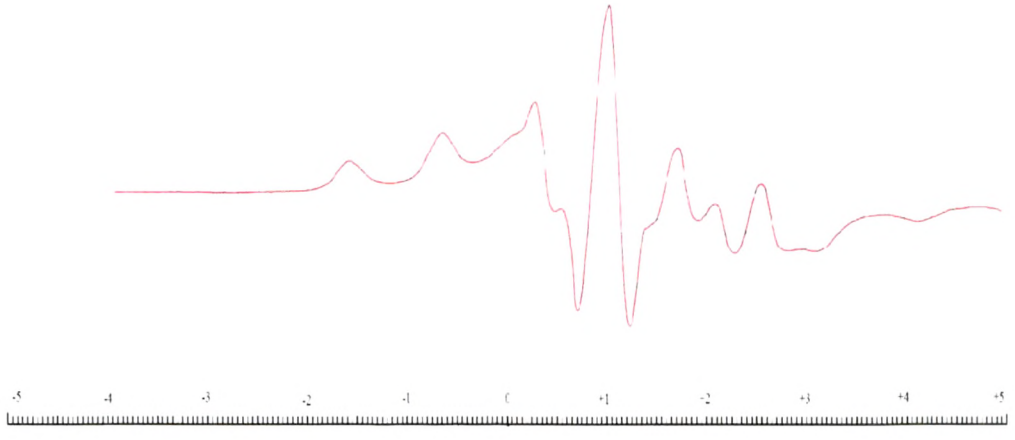

Figure 1.1.13. EPR spectrum of the complex $VO(L^2)_2$ at liquid nitrogen temperature in DMF.

On the basis of the results of various spectroscopic and analytical techniques including single crystal XRD, structures of the oxovanadium(IV) complexes were proposed and illustrated in the Figure 1.1.14. It is suggested that the oxovanadium(IV) complexes of 4-acylpyrazolones can exist in *syn*, *anti* or *twisted* conformations/geometries.

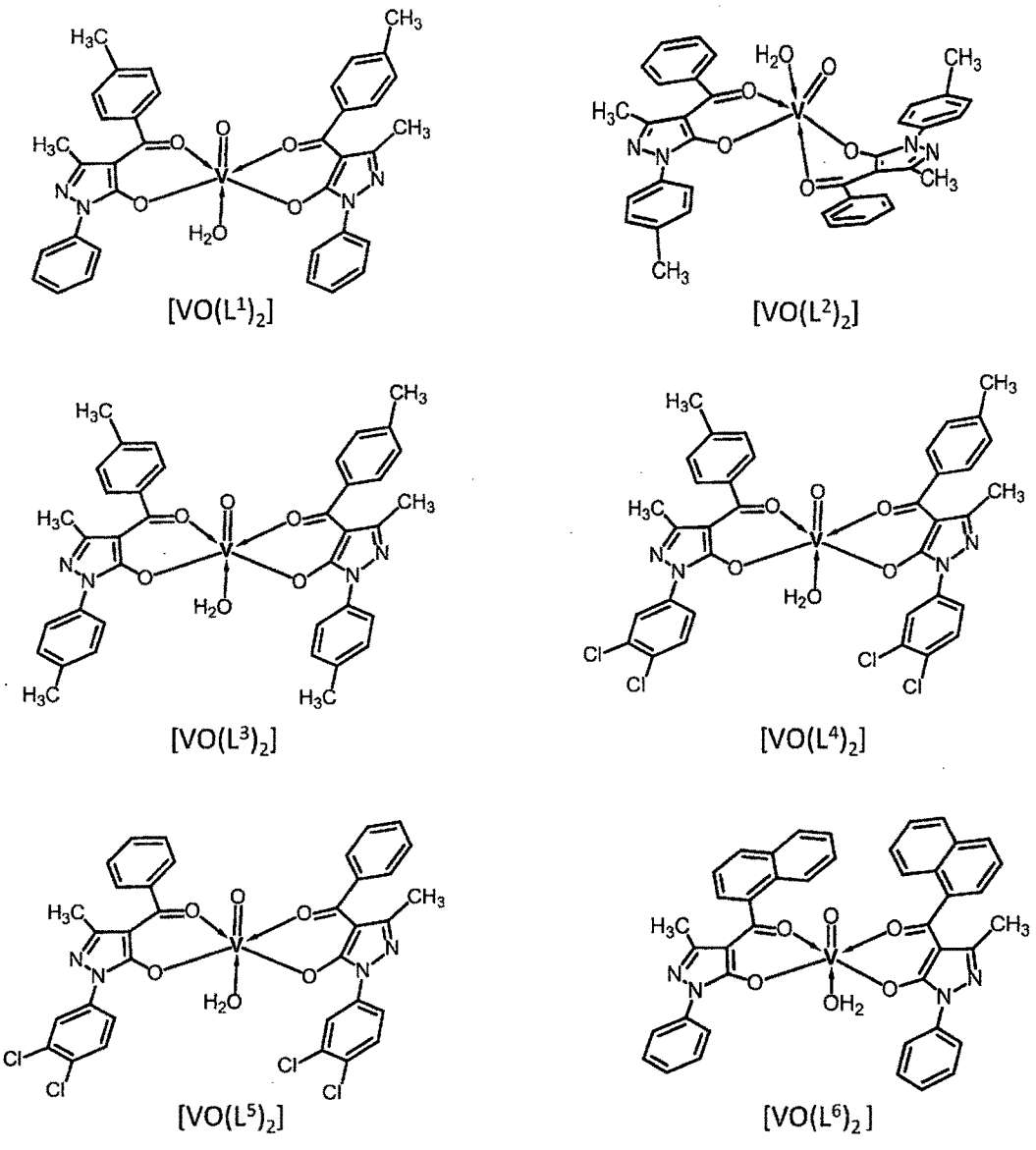

Figure 1.1.14. Structures of oxovanadium(IV) complexes [**1-6**].

1.1.3.3. Catalytic activity studies

The oxidation of benzyl alcohol, catalyzed by oxovanadium(IV) complexes was carried out using H_2O_2 as an oxidant to give benzaldehyde, benzoic acid and benzyl benzoate as products. The formation of all these products is represented by Scheme 1.1.3. These are common products and have been identified by others as well [10].

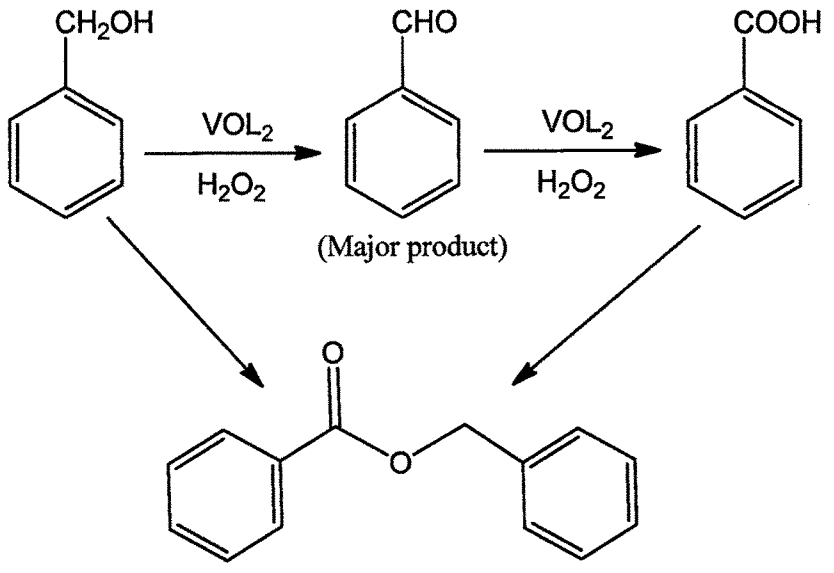

Scheme 1.1.3. Representation of benzyl alcohol oxidation and its products.

The optimization was carried out by varying different parameters such as effect of molar ratios of H_2O_2, amount of catalyst, reaction time and solvent. The progress of the reaction was monitored by GC-MS analysis and products formed in the reactions were matched with those reported in the literature. The complex $VO(L^2)_2$ was chosen for the optimization. The optimizations of effect of catalyst amount, reaction time and molar ratio of H_2O_2 were done without solvent.

Effect of catalyst amount

The amount of catalyst has a significant effect on the oxidation of benzyl alcohol. Four different amounts of catalyst viz. 0.015, 0.03, 0.045 and 0.06 mmol were used, keeping all other parameters fixed: namely, temperature (90 °C), benzyl alcohol (10 mmol), 30% H_2O_2 (30 mmol) and reaction time (24 h). The results are shown in Figure 1.1.15, indicating 68, 78, 93 and 94% conversion corresponding to 0.015 mmol, 0.03 mmol, 0.045 mmol and 0.06 mmol, respectively. The maximum percentage conversion was observed with 0.06 mmol catalyst but there was no remarkable difference in the reaction when 0.045 or 0.06 mmol catalyst was employed. Therefore, 0.045 mmol catalyst was taken to be optimum.

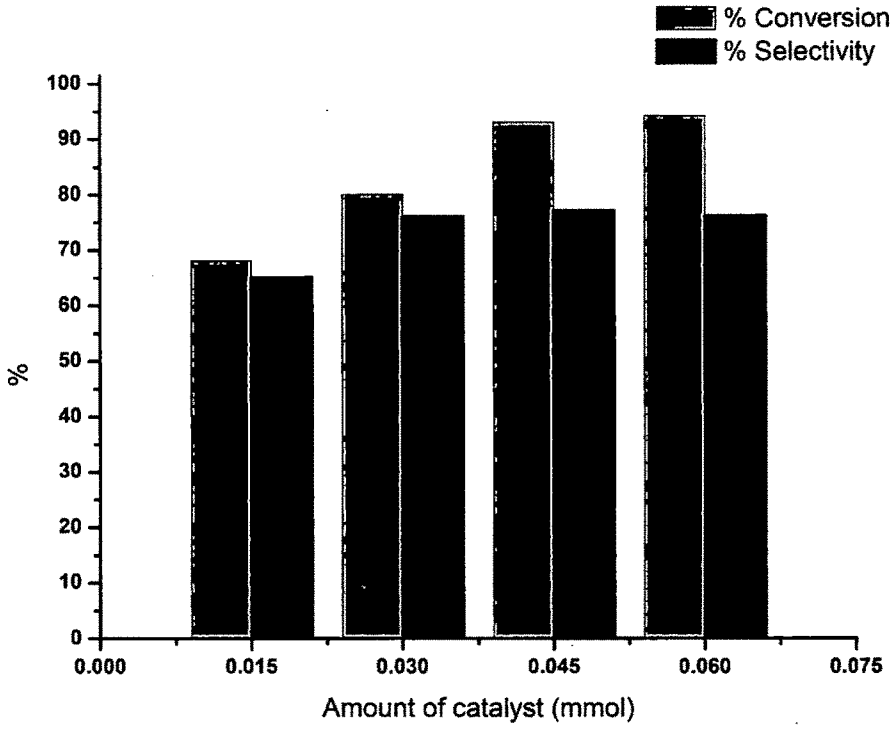

Figure 1.1.15. Effect of amount of catalyst; % conversion is based on benzyl alcohol and % selectivity with respect to benzaldehyde; reaction time = 24 h, temperature = 90 °C, benzyl alcohol = 10 mmol and H_2O_2 = 30 mmol.

Effect of H_2O_2 concentration

In order to determine the effect of H_2O_2 on the oxidation of benzyl alcohol to benzaldehyde, we studied using four different benzyl alcohol: H_2O_2 molar ratios (1:1, 1:2, 1:3 and 1:4) keeping other parameter fixed: namely, catalyst (0.045 mmol), temperature (90 °C) and reaction time (24 h). A benzyl alcohol to H_2O_2 molar ratio of 1:1 and 1:2 resulted in 24 and 53% conversion, respectively. When benzyl alcohol to H_2O_2 molar ratio was changed to 1:3, conversion increased to be nearly 93%, keeping all other conditions similar. A further increase in the ratio of 1:4 resulted, little decreases in the conversion to 88% (*see* Figure 1.1.16). The reason for this may be due to the dilution of the reaction mixture by the presence of larger amounts of water molecules in H_2O_2 solution.

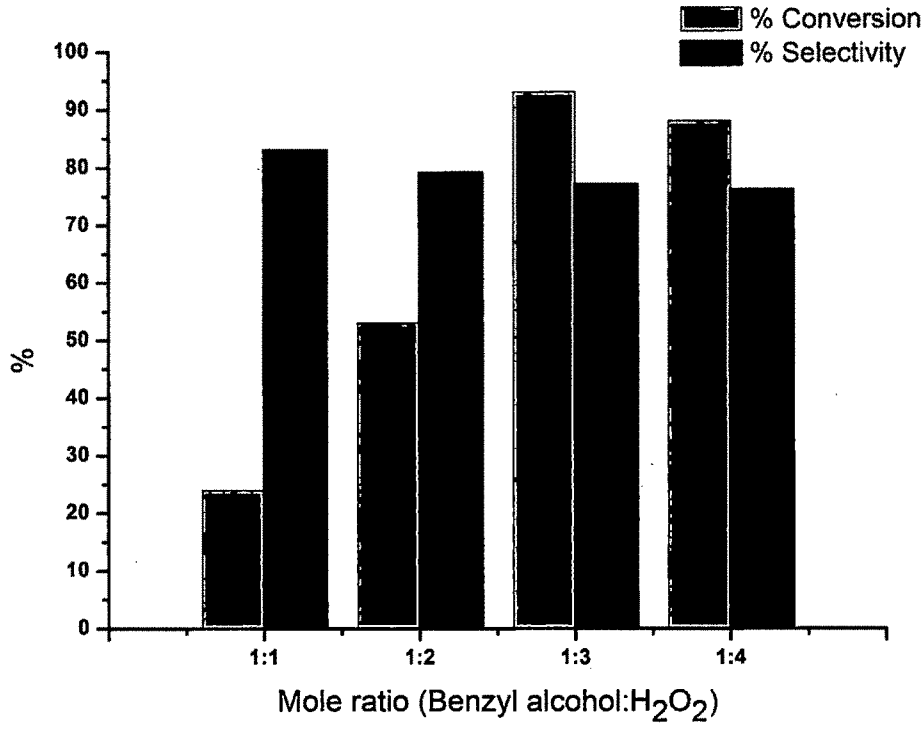

Figure 1.1.16. Effect of H_2O_2 concentration: % conversion is based on benzyl alcohol and % selectivity with respect to benzaldehyde; reaction time = 24 h, temperature = 90 °C, benzyl alcohol = 10 mmol and catalyst = 0.045 mmol.

Effect of reaction time

The time dependence of catalytic oxidation of benzyl alcohol was studied by performing the reaction of benzyl alcohol (10 mmol), 30% H_2O_2 (30 mmol) in the presence of 0.045 mmol catalyst at 90 °C temperature with constant stirring. It is seen from Figure 1.1.17 that with an increase in reaction time, the % conversion also increases. Initial conversion of benzyl alcohol increased with the reaction time. This is due to the reason that more time is required for the formation of reactive intermediate (substrate + catalyst) which is finally converted into the products. It was seen that 93% conversion was observed at 24 h; when the reaction was allowed to continue for more than 24 h, no appreciable change in conversion as well as selectivity were observed.

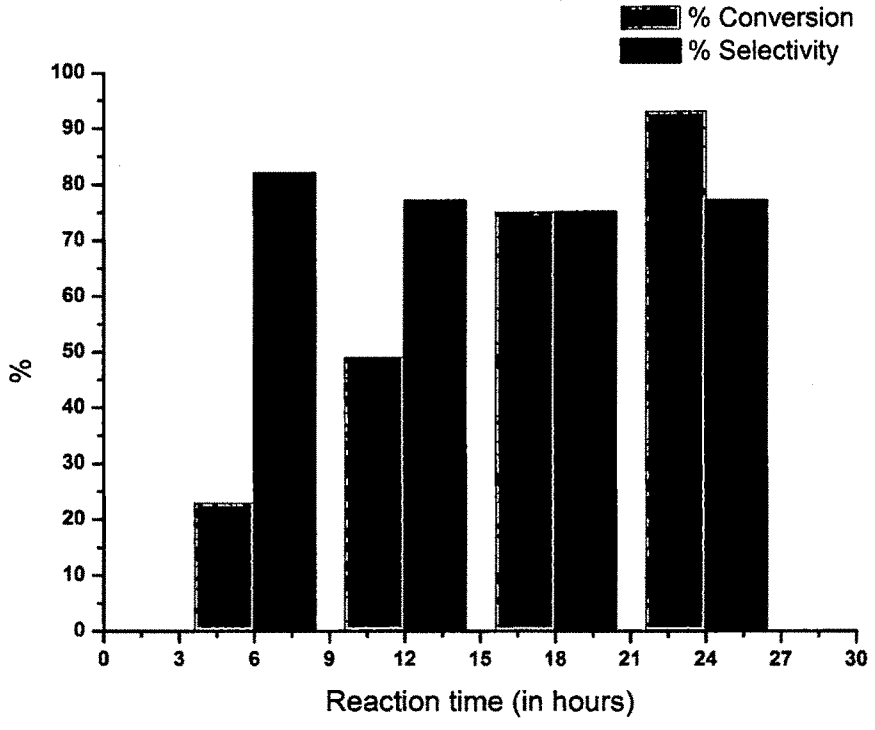

Figure 1.1.17. Effect of reaction time: % conversion is based on benzyl alcohol and % selectivity with respect to benzladehyde; amount of catalyst = 0.045 mmol, temperature = 90 °C, benzyl alcohol = 10 mmol and H_2O_2 = 30 mmol.

Effect of solvent

The selectivity in oxidation of benzyl alcohol to benzaldehyde is always an issue in this experiment. To avoid or minimize the side reactions we carried out optimization in different solvent systems keeping other parameters fixed: namely, catalyst amount (0.045 mmol), reaction temperature (90 °C), benzyl alcohol (10 mmol), 30% H_2O_2 (30 mmol), reaction time (24 h) and solvent (5 mL). The reactions were carried out in toluene, chloroform, DMF, methanol, Hexane, acetonitrile and cyclohexane (*see* Figure 1.1.18). DMF, methanol and chloroform do not lead to a remarkable % conversion of benzyl alcohol; however, toluene and hexane have some influence on the outcome of the reaction and lead to 57% and 54 % conversion with 76% and 62 % selectivity, respectively. The best results are obtained with the acetonitrile which afforded a remarkable conversion (92%) of benzyl alcohol into benzaldehyde with 80 % selectivity.

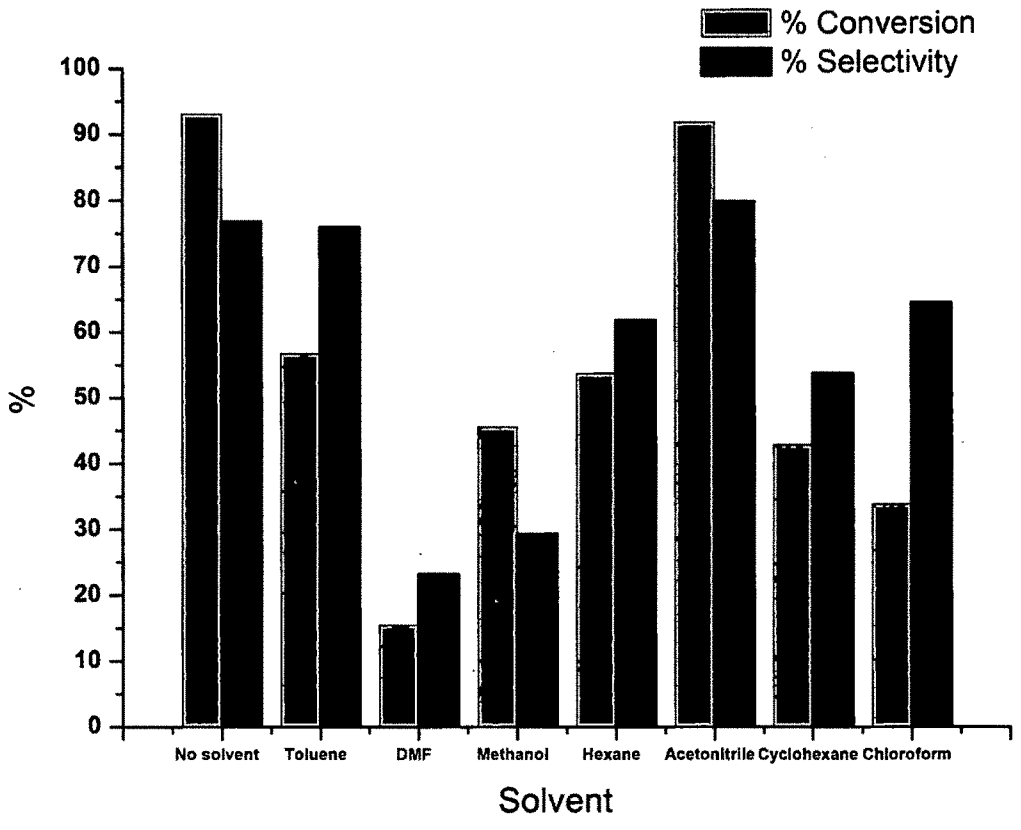

Figure 1.1.18. Effect of solvent: % conversion is based on benzyl alcohol and % selectivity with respect to benzaldehyde; reaction time = 24 h, temperature = 90 °C, benzyl alcohol = 10 mmol H_2O_2 = 30 mmol and catalyst = 0.045 mmol, solvent = 5 mL.

Thus, the optimum condition for the maximum % conversion as well as selectivity for the oxidation of benzyl alcohol to benzaldehyde is reaction temperature (90 °C), benzyl alcohol (10 mmol), 30% H_2O_2 (30 mmol), catalyst amount (0.045 mmol), reaction time (24 h) and acetonitrile (5 mL) as a solvent.

Another goal of this work was to compare the catalytic activities of oxovanadium(IV) complexes of various derivatives of 4-acylpyrazolone ligands. Thus, all the synthesized complexes were used as a catalyst for the oxidation of benzyl alcohol under the same optimized condition. From the data reported in Table 1.1.9, we observed that $VO(L^1)_2$, $VO(L^2)_2$, $VO(L^4)_2$, $VO(L^5)_2$ and $VO(L^6)_2$ showed 92%, 91%, 91%, 92% and 98% conversion, respectively. However, $VO(L^3)_2$ showed a little decrease in conversion (86%) in comparison to the other catalysts. The catalyst $VO(L^6)_2$ showed highest conversion in this series of the catalysts. Among these

catalysts, $VO(L^1)_2$ showed good selectivity (80%) for benzaldehyde in comparison to catalyst $VO(L^3)_2$, $VO(L^4)_2$ $VO(L^5)_2$ and $VO(L^6)_2$. The catalyst $VO(L^2)_2$ and $VO(L^6)_2$ resulted in 77% and 78% selectivity, respectively, which is comparable with the selectivity obtained with $VO(L^1)_2$. The results show that selectivity decreases on increasing the amount of substitution over the phenyl ring of acylpyrazolone ligands in their oxovanadium(IV) complexes. However, conversion increases on increasing aromatic character in the complexes. As $VO(L^1)_2$ shows better catalytic performance to obtained higher conversion and selectivity in compare to other complexes, further investigations were carried out using $VO(L^1)_2$ as an oxidizing catalyst.

Table 1.1.9. Oxidation of benzyl alcohol using various catalysts oxovanadium(IV) complexes [**1-6**].

Catalyst	% Conversion	% Selectivity	TON
$VO(L^1)_2$	92	80	160
$VO(L^2)_2$	91	77	156
$VO(L^3)_2$	86	66	132
$VO(L^4)_2$	91	68	146
$VO(L^5)_2$	92	68	169
$VO(L^6)_2$	98	78	184

To explore the scope of the present catalyst $VO(L^1)_2$ to act as an oxidizing catalyst, the reactions of a wide array of substituted benzyl alcohols were also conducted under the same optimized conditions. The results of the oxidation of various benzylic alcohols to the corresponding aldehydes are shown in Table 1.1.10.

Table 1.1.10. Oxidation of alcohols using VOL_2 catalyst[a]

No.	Substrate	Product	% Conversion	% Selectivity	TON
1.	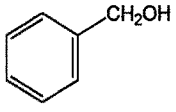	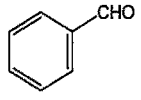	92	80	160
2.	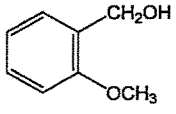	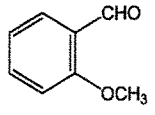	66	85	120
3.	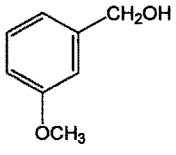	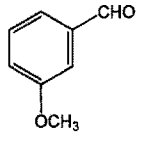	72	100	160
4.	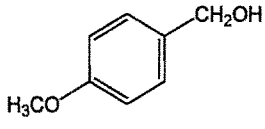	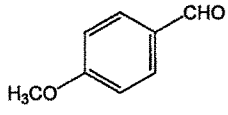	94	100	209
5.	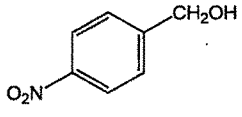	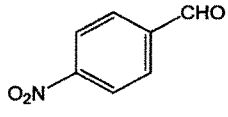	63	79	112
6.	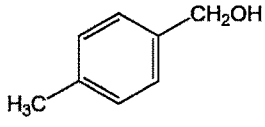	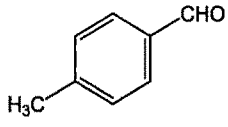	90	100	199
7.	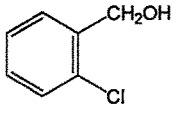	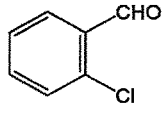	49	100	109
8.	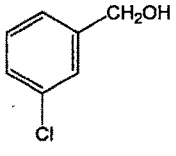	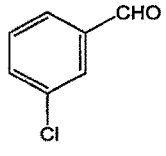	40	100	89

[a] Reaction condition: Catalyst = 0.045 mmol, benzylic alcohol = 10 mmol, 30% H_2O_2 = 30 mmol, acetonitrile solvent = 5 mL, temperature = 90 °C and reaction time = 24 h.

The reactions of benzylic alcohols (entries 1-8) bearing electron-donating and electron-withdrawing substituent at the aromatic ring proceeded smoothly to give the corresponding aldehydes in good to high conversion as well as selectivity. The conversion with 4-methoxy benzyl alcohol was comparatively higher than that of 3-methoxy and 2-methoxy benzyl alcohol and selectivity for 4-methoxy benzaldehyde is 100%. The conversion of 4-methoxy benzyl alcohol was observed to be slightly higher than that of benzyl alcohol under identical experimental conditions. Conversion of 4-methyl benzyl alcohol is also comparable with that of 4-methoxy benzyl alcohol with 100% selectivity. The conversion of 4-nitro benzyl alcohol was lower in comparing with benzyl alcohol and methoxy derivatives of benzyl alcohol. The 2-chloro & 3-chloro benzyl alcohol shows a poor conversion but high selectivity for their corresponding aldehydes. The catalyst shows a higher turnover number (TON) for 4-methoxy benzyl alcohol while the lowest TON is obtained for 3-chloro benzyl alcohol.

Possible pathway of the catalyzed reactions

Several mechanisms have been proposed in the literatures for the oxidation of alcohols catalyzed by the vanadium complexes [9*a*, 19]. To establish the possible pathway of present reaction and to evaluate intermediate species formed during catalytic oxidation, a 3 mmol solution of $VO(L^1)_2$ was prepared in acetonitrile and its electronic spectrum was recorded using UV-Vis spectrophotometer. The electronic spectral data of the neat complex exhibit band at 393 nm, which was assigned to ligand to metal charge transfer (LMCT). The lower energy and less intense bands appearing at 617 and 772 nm, were assigned to $d \rightarrow d$ transitions. After that 30% H_2O_2 was added to the solution of $VO(L^1)_2$. The color of solution rapidly changes from green to brown due to the change in the oxidation state of vanadium from +4 to +5. The electronic spectra of this solution exhibit only one band at 398 nm (LMCT). As V^V complexes have $3d^0$ configuration, $d \rightarrow d$ transitions are not expected to appear in the electronic spectrum (*see* Figure 1.1.19).

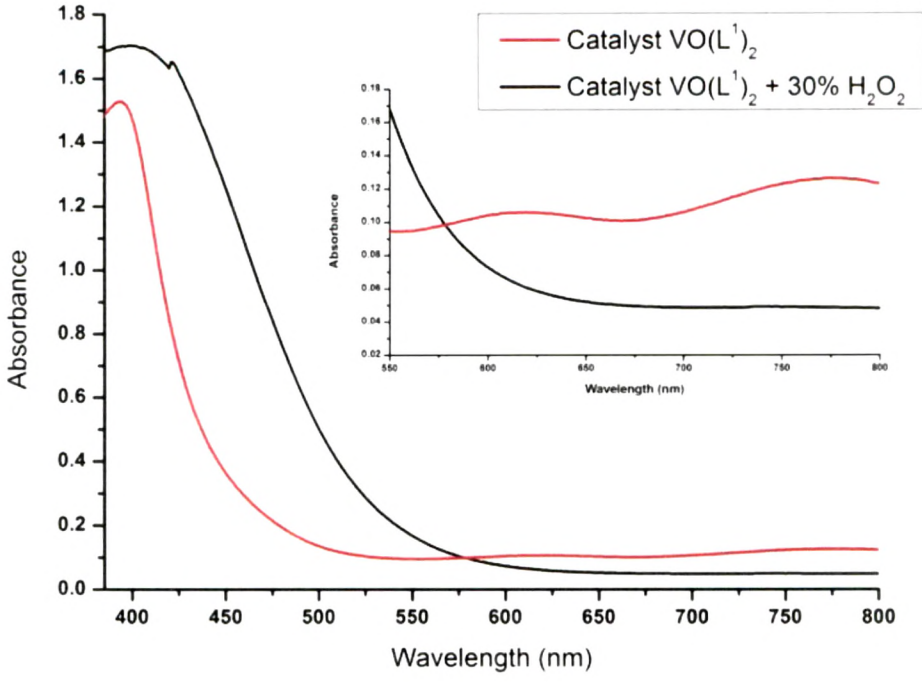

Figure 1.1.19. UV-Vis spectra of neat catalyst $VO(L^1)_2$ (in red) and catalyst $VO(L^1)_2$ with 30% H_2O_2 (in black).

The mechanism of alcohol oxidation catalyzed by $VO(L^1)_2$ may be viewed as an oxidative dehydrogenation involving the formation of high valent peroxovanadium intermediate. The results of electronic spectra show that a higher vanadium(V) species might be produced and for its formation, the presence of H_2O_2 is necessary [20]. Thus, based on UV-Vis study and literature reports it is proposed that first, a vanadium(IV) species reacts with H_2O_2 to form vanadium(V) species. This species reacts with benzylic alcohol to afford a vanadium-alcoholate. Next, the product carbonyl compound is formed, and vanadium(IV) species is reproduced.

1.1.4. Conclusions

A series of novel oxovanadium(IV) complexes with a variety of different substituted 4-acylpyrazolone ligands were synthesized, and characterized by various analytical and spectroscopic techniques. The geometry and molecular structure of the complexes $[VO(L^1)_2]$ and $[VO(L^1)_2]$ were resolved by single-crystal XRD. Interestingly, contrary results were obtained with the previous reported geometries of the oxovanadium (IV) complexes of acylpyrazolone ligands. The conformation of the

ligands with the centre metal has been changed and the ligands are in *syn* configuration to each other in the complex $[VO(L^1)_2]$. The coordination mode of ligands with centre metal has been changed in the complex $[VO(L^1)_2]$ and V-O(oxo) group is located *cis* to the coordinated water molecule in $[VO(L^2)_2]$, thus forming a *twisted* octahedral structure with the metal centre. It is concluded from the results of single crystal XRD data that oxovanadium(IV) complexes of 4-acylpyrazolones can exist in *syn*, *anti* and *twisted* geometries. The synthesized oxovanadium(IV) complexes were used for the oxidation of benzyl alcohol using H_2O_2 as an oxidant and proved to be successful as an oxidation catalyst. Various parameters such as effect of catalyst amount, solvent, H_2O_2 concentration and reaction time were tested in order to optimize both the conversion as well as selectivity. Under optimized conditions, $VO(L^1)_2$ has provided high value of conversion (92%) as well as selectivity (80%) for benzaldehyde in compare to other complexes. The catalyst shows the high catalytic conversion as well as selectivity towards benzyl alcohol and substituted benzylic alcohols (4-methoxy & 4-methyl benzyl alcohols). To the best of our knowledge, the present catalytic system is the first example of the oxidation of alcohols by oxovanadium(IV) complex of acylpyrazolone ligand. Mechanistic details were provided for the oxidation of benzylic alcohols by oxovanadium(IV) complex using H_2O_2 as an oxidant.

1.1.5. References

[1] P. W. N. M. van Leeuwen, *Homogeneous catalysis understanding the art*, Kluwer Academic Publishers, Netherlands, **2004**.

[2] M. Lancaster, *Green Chemistry: An Introductory Text*, Royal Society of Chemistry, UK, **2002**.

[3] (*a*) D. Rehder, *Coord. Chem. Rev.*, **1999**, *182*, 297-322; (*b*) Y. Shechter, S. J. D. Karlish, *Nature*, **1980**, *286*, 556-558; (*c*) D. Rehder, *Bioinorganic Vanadium Chemistry*, John Wiley & Sons: Chichester, U.K., **2008**; (*d*) R. R. Eady, *Coord. Chem. Rev.*, **2003**, *237*, 23-30; (*e*) K. H. Thompson, C. Orvig, *Coord. Chem. Rev.*, **2001**, *219*, 1033-1053; (*f*) I. Osinska-Krolicka, H. Podsiadly, A. Bukietynska, *J. Inorg. Biochem.*, **2004**, *98*, 2087-2098.

[4] (*a*) T. Hirao, *Chem. Rev.*, **1997**, *97*, 2707-2724; (*b*) C. Bolm, *Coord. Chem. Rev.* **2003**, *237*, 245-256; (*c*) A.G. J. Ligtenbarg, R. Hage, B.L. Feringa, *Coord. Chem. Rev.*, **2003**, *237*, 89-101; (*d*) F. Cavani, N. Ballarini, A.

Cericola, *Catal. Today*, **2007**, *127*, 113-131; (*e*) S. Takizawa, T. Katayama, H. Sasai, *Chem. Commun.*, **2008**, 4113-4122; (*f*) S. K. Hanson, R. Wu, L. A. P. Silks, *Org. Lett.* **2011**, *13*, 1908-1911; (*g*) N. Mizuno, K. Kamata, *Coord. Chem. Rev.*, **2011**, *255*, 2358– 2370; (*h*) M. Kirihara, *Coord. Chem. Rev.*, **2011**, *255*, 2281-2302; (*i*) J. A. L. da Silva, J. J. R. F. da Silva, A. J. L. Pomberio, *Coord. Chem. Rev.*, **2011**, *255*, 2232-2248; (*j*) J. -Q. Wu, Y. -S. Li, *Coord. Chem. Rev.*, **2011**, *255*, 2303-2314; (*k*) M. R. Maurya, A. Kumar, J. C. Pessoa, *Coord. Chem. Rev.*, **2011**, *255*, 2315-2344.

[5] (*a*) H.-L. Wu, B.-J. Uang, *Tetrahedron: Asymmetry*, **2002**, *13*, 2625–2628; (*b*) M. Bühl, R. Schurhammer, P. Imho, *J. Am. Chem. Soc.*, **2004**, *126*, 3310-3320; (*c*) M. L. Kuznetsova, J. C. Pessoa, *Dalton Trans.*, **2009**, 5460–5468.

[6] (*a*) G. Santoni, G. Licini, D. Rehder, *Chem.-Eur. J.*, **2003**, *9*, 4700-4708; (*b*) C. Drago, L. Caggiano, R. F. W. Jackson, *Angew. Chem., Int. Ed.*, **2005**, *44*, 7221-7223; (*c*) A. Basak, A. U. Barlan, H. Yamamoto, *Tetrahedron: Asymmetry*, **2006**, *17*, 508-511; (*d*) S.-H. Hsieh, Y.-P. Kuo, H.-M. Gau, *Dalton Trans.*, **2007**, 97–106; (*e*) S. L. Jain, B. S. Rana, B. Singh, A. K. Sinha, A. Bhaumik, M. Nandi, B. Sain, *Green Chem.*, **2010**, *12*, 374–377.

[7] (*a*) M. R. Maurya, U. Kumar, I. Correia, P. Adão, J. C. Pesoa, *Eur. J. Inorg. Chem.*, **2008**, 577–587; (*b*) M. R. Maurya, A. Arya, U. Kumar, A. Kumar, F. Avecilla, J. C. Pessoa, *Dalton Trans.*, **2009**, 9555–9566.

[8] (*a*) P. J. Figiel, J. M. Sobczak, J. J. Ziólkowski, *Chem. Commun.*, **2004**, 244–245; (*b*) T. Waters, G. N. Khairallah, S. A. S. Y. Wimala, Y. C. Ang, R. A. J. O'Hair, A. G. Wedd, *Chem. Commun.*, **2006**, 4503–4505; (*c*) S. Kodama, Y. Ueta, J. Yoshida, A. Nomoto, S. Yano, M. Ueshima, A. Ogawa, *Dalton Trans.*, **2009**, 9708–9711; (*d*) A. Dewan, T. Sarma, U. Bora, D. K. Kakati, *Tetrahedron Lett.*, **2011**, 52, 2563–2565.

[9] (*a*) A. Butler, M. J. Clague, G. E. Meister, *Chem. Rev.*, **1994**, *94*, 625-638; (*b*) V. Conte, F. Di Furia, S. Moro, *J. Phys. Org. Chem.*, **1996**, *9*, 329-336.

[10] (*a*) C. Li, P. Zheng, J. Li, H. Zheng, Y. Cui, Q. Shao, X. Ji, J. Zheng, P. Zhao, Y. Xu, *Angew. Chem. Int. Ed.*, **2003**, *42*, 5063 –5066; (*b*) A. Jia, L.-L. Lou, C. Zhang, Y. Zhang, S. Liu, *J. Mol. Catal. A: Chem.*, **2009**, *306*, 123–129; (*c*) A. Podgoršek, M. Zupan, J. Iskra, *Angew. Chem. Int. Ed.*, **2009**, *48*, 8424-8450; (*d*) V. K. Bansal, P. P. Thankachan, R. Prasad, *Appl. Catal. A:*

Gen., **2010**, *381*, 8–17; (*e*) G.D. Faveri, G. Ilyashenko, M. Watkinson, *Chem. Soc. Rev.*, **2011**, *40*, 1722–1760.

[11] (*a*) *Peroxide Chemistry. Mechanistic and Preparative Aspects of Oxygen Transfer*, (Ed: W. Adam), Wiley-VCH Verlag GmbH, Weinheim, **2000**; (*b*) *The Chemistry of Peroxides- Transition Metal Peroxides. Synthesis and Role in Oxidation Reactions*, (Eds: V. Conte, O. Bortolini, Z. Rappoport), Wiley Interscience, **2006**, p.1053, and references cited therein.

[12] (*a*) R. A. Sheldon, I. W. C. E. Arends, G. J. ten Brink, A. Dijksman, *Acc. Chem. Res.*, **2002**, *35*, 774-781; (*b*) K. Yamaguchi, N. Mizuno, *Chem. Eur. J.*, **2003**, *9*, 4353- 4361; (*c*) A. Dhakshinamoorthy, M. Alvaro, H. Garcia, *ACS Catal.*, **2011**, *1*, 48–53; (*d*) R. Kwahara, K.-i Fujita, R. Yamaguchi, *J. Am. Chem. Soc.*, **2012**, *134*, 3643-3646.

[13] (*a*) H. -J. Arpe, Ulmann's, Encyclopedia of Industrial Chemistry, 5th ed.; VCH: Weinheim, **1985**; (*b*) V. R. Choudhary, D. K. Dumbre, V. S. Narkhede, S. K. Jana, *Catal. Lett.*, **2003**, *86*, 229-233.

[14] F. Marchetti, C. Pettinari, C. D. Nicola, R. Pettinari, A. Crispini, M. Crucianelli, A. D. Giuseppe, *Appl. Catal. A: Gen.*, **2010**, *378*, 211-233.

[15] W. L. F. Armarego, C. L. L. Chai, *Purification of Laboratory Chemicals*, 5th *ed.*, Butterworth-Heinemann, Elsevier Science (USA), **2003**.

[16] G. M. Sheldrick, *SHELX97*, University of Göttingen: Göttingen, Germany **1997**.

[17] L. J. Farrugia, *J. Appl. Cryst.*, **1999**, *32*, 837-838.

[18] M. Nardelli, *J. Appl. Cryst.*, **1995**, *28*, 659.

[19] (*a*) Y. Maeda, N. Kakiuchi, S. Matsumura, T. Nishimura, T. Kawamura, S. Uemura, *J. Org. Chem.*, **2002**, *67*, 6718-6724; (*b*) S.R. Reddy, S. Das, T. Punniyamurthy, *Tetrahedron Lett.*, **2004**, *45*, 3561-3564; (*c*) S. K. Hanson, R. T. Baker, J. C. Gordon, B. L.Scott, L. A. Silks, D. L. Thorn, *J. Am. Chem. Soc.*, **2010**, *132*, 17804-17816; (*d*) V. Conte, A. Coletti, B. Floris, G. Licini, C. Zonta, *Coord. Chem. Rev.*, **2011**, *255*, 2165-2177.

[20] (*a*) D. Rehder, M. Ebel, C. Wikete, G. Santoni, J. Gätjens, *Pure Appl. Chem.* **2005**, *77*, 1607–1616; (*b*) M. R. Maurya, A. K. Chandrakar, S. Chand, *J. Mol. Catal. A: Chem.*, **2007**, *270*, 225-235; (*c*) M. R. Maurya, A. K. Chandrakar, S. Chand, *J. Mol. Catal. A: Chem.*, **2007**, *274*, 192-201.

RSC Advances

PAPER

Novel oxovanadium(IV) complexes with 4-acyl pyrazolone ligands: synthesis, crystal structure and catalytic activity towards the oxidation of benzylic alcohols†

Cite this: *RSC Adv.*, 2014, 4, 10295

Sanjay Parihar,[a] R. N. Jadeja*[a] and Vivek K. Gupta[b]

Received 22nd November 2013
Accepted 20th December 2013

DOI: 10.1039/c3ra46896h

www.rsc.org/advances

A series of oxovanadium(IV) complexes of 4-acylpyrazolone ligands were synthesized and characterized by elemental analyses, FT-IR, UV-Vis, EPR spectroscopy and single crystal XRD. The single-crystal X-ray analysis of the complex $VO(L^1)_2$ shows that the ligands were coordinated with the vanadium atom in a twisted form to create a distorted octahedral geometry and two *O*,*O*-chelating acylpyrazolonate ligands constitute two six-membered rings with the vanadium atom. The catalytic activity of all the complexes was evaluated for the oxidation of benzylic alcohols with H_2O_2 as an oxidant. The conditions for maximum conversion as well as selectivity for the desired product were optimized by varying different parameters such as the molar ratio of substrate to H_2O_2, the amount of the catalyst, reaction time and solvent. A possible pathway for the oxidation of benzylic alcohols was also proposed on the basis of the spectral evidence.

Introduction

Vanadium compounds have attracted much attention because of their involvement in various biological processes[1] and for their use as homogeneous and heterogeneous catalysts in various reactions and in industrial processes.[2] Vanadium based oxidants are effectively used for various oxidation reactions such as the epoxidation of alkenes,[3] the oxidation of sulfides,[2b,4] hydro and oxidative amination[5] and the oxidation of alcohols[6] to aldehydes and ketones, thus showing their influence on the yield and selectivity in chemical transformations. Oxo and peroxo derivatives of vanadium complexes play an important role in such catalytic oxidations, acting as oxo-transfer agents.[7] Aqueous hydrogen peroxide is a highly attractive oxidant because it is a cheap, mild and environmentally benign reagent with a high content of 'active' oxygen, and water is the only by-product. Thus, many catalytic systems were studied for selective oxidation of alcohols with H_2O_2.[8] The catalytic species resulting from the interaction of hydrogen peroxide with suitable transition metal ions, are considered among the most active oxidants[9] toward a number of organic and inorganic substrates.

The selective oxidation of alcohols to carbonyl compounds is one of the most important organic transformations, with recognized importance to fundamental organic synthesis, but also to the fine chemical industry.[6,10] Selective oxidation of benzyl alcohol to benzaldehyde is a practically important reaction for the production of chlorine-free benzaldehyde, required in the perfumery and pharmaceutical industries.[11] Benzaldehyde is an attractive target because it is an important intermediate in the production of derivatives for perfumery, pharmaceutical, dyestuff and agrochemical industries.

Recently, we have reported the synthesis and crystal structure of a novel oxovanadium(IV) complex with 1-phenyl-3-methyl-4-toluoyl-5-pyrazolone ligand and immobilized it over hydrous zirconia to use as a heterogeneous catalyst for the oxidation of styrene with H_2O_2.[12] To the best of our knowledge no report is available in the literature for the selective oxidation of alcohols with the oxovanadium(IV) complexes of acylpyrazolone ligands. The objective of the present study is to emphasis the geometry of oxovanadium(IV) complexes of acylpyrazolone ligands and to establish the viability of the newly synthesized oxovanadium(IV) complexes (Scheme 1) in oxidation reactions. The catalytic properties of the new mononuclear complexes have been thoroughly studied, in the hydrogen peroxide promoted oxidation of benzylic alcohols, under homogeneous conditions. To investigate the effectiveness of the synthesized complexes in oxidation reactions, benzyl alcohol was chosen as a model substrate. The oxidation of benzyl alcohol was studied in more detail to optimize the reaction variables such as the amount of catalyst, alcohol/oxidant molar

[a]*Department of Chemistry, Faculty of Science, The Maharaja Sayajirao University of Baroda, Vadodara 390 002, India. E-mail: rajendra_jadeja@yahoo.com; Tel: +91-265-2795552*

[b]*Post-Graduate Department of Physics, University of Jammu, Jammutawi 180 006, India*

† Electronic supplementary information (ESI) available: Fig. S1 to S26. CCDC reference number 859107 (for complex $VO(L^1)_2$). For ESI and crystallographic data in CIF or other electronic format see DOI: 10.1039/c3ra46896h

Chapter – 1

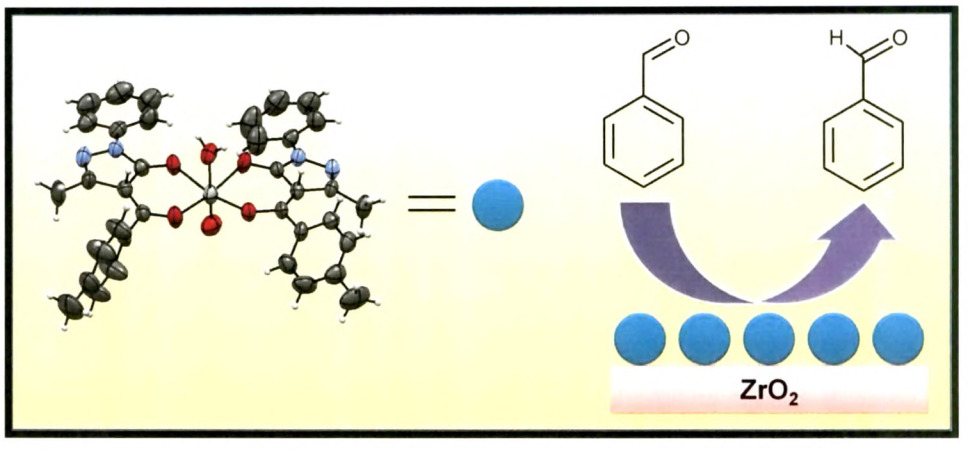

Part 2

Heterogeneous catalysis using oxovanadium(IV) complexes

1.2.1. Introduction

Catalysis is the key to chemical transformations. Most industrial syntheses and nearly all biological reactions require catalysts. Furthermore, catalysis is the most important technology in environmental protection, *i. e.*, the prevention of emissions. A well-known example is the catalytic converter for automobiles [1]. In recent years increasingly stringent environmental constraints have led to a great interest in the application of new catalytic methods in the synthesis of fine and intermediate chemicals.

Heterogeneous catalysts have been used industrially for well over 100 years. In 1908, the German chemist Fritz Haber succeeded in synthesizing ammonia by feeding N_2 and H_2 at high pressures over an osmium catalyst. This discovery was picked up by Carl Bosch and Alwin Mittasch at BASF, who tested over 2500 different materials until they found an iron-based compound which was active enough and cheap enough to serve as a commercial catalyst. The Haber–Bosch ammonia synthesis has become one of the most important chemical processes worldwide, earning Haber the Nobel Prize in chemistry in 1918. Nitrogen fixation provided mankind with a much-needed fertilizer, improving crop yields for the world's growing population [2].

Another important catalytic process was the Fischer-Tropsch synthesis. Germany and Japan had an abundance of coal, but no reliable source of petroleum. The Co/Fe-catalyzed Fischer-Tropsch process converted coal to syngas, further reaction of which gave a liquid mixture rich in C olefins and paraffins. Today, heterogeneous catalysis dominates the petrochemicals and the bulk chemicals industry [3]. Modern industrial chemistry is based on catalytic processes.

There is a whole spectrum of heterogeneous catalysts, but the most common types consist of an inorganic or polymeric support, which may be inert or have acid or basic functionality, together with a bound metal [4]. The issue of leaching and the avoidance of trace catalyst residues are still important aspects of research from both economic and environmental points of view. Even if the support is inert its structure is of vital importance to the efficiency of the catalytic reaction. Since the reactants are in a different phase to the catalyst both diffusion and adsorption influence the overall rate, these factors to some extent depending on the nature and structure of the support.

In contrast to homogeneous catalysts, heterogeneous catalysts bear specific advantages concerning especially the workup procedures. The separation of the catalyst from reactants and products can be facilitated by using simple mechanical techniques as filtration or centrifugation. The immobilization of homogeneous catalysts is a reasonable idea, combining the positive effects of catalytical performance and practical use.

The coordination chemistry of vanadium, in particular with multidentate ligands, is receiving much attention on account of its involvement in various biological processes: in the active site of metalloenzymes such as vanadium nitrogenase [5] and haloperoxidases [6], as a metabolic regulator [7], as a mitogenic activator and especially as an insulin-mimicking agent [8]. Vanadium complexes can also affect the cardiac abnormality associated with diabetes mellitus [9] and exhibit anticancer activity [10].

Moreover, catalytic applications have also stimulated the coordination chemistry of vanadium, and the search for novel vanadium complexes with pharmacological and catalytic significance is a matter of a high current interest. Oxovanadium peroxo complexes efficiently oxygenate organic compounds. Vanadium complexes possess versatile oxidation states and unusual redox ability. Usually, vanadium can exist in +3, +4 and +5 oxidation states. In +4 and +5 oxidation states vanadium has strong redox ability which can lead to some important reactions [11]. Oxovanadium complexes were illustrated to be catalysts [12] in a variety of asymmetric reactions such as the cyanation reaction [13], epoxidation of allyl alcohols [14], oxidative coupling of 2-naphthol [15], oxidation of organic sulfides [16], alkynyl addition to aldehydes [17] and others [18].

Immobilization of metal complexes onto the surfaces of solid supports is highly desirable in the development of reusable catalysts [19]. Supported vanadium oxide catalysts constitute a very important class of catalytic materials. They have become the model for catalytic systems for fundamental studies of supported metal oxides and they are widely used as selective oxidation catalysts in the industrial production of economically attractive redox reactions. These heterogeneous catalysts, mostly deposited on a porous support, have the advantage of mechanical strength and the easy recovery and recycling, in comparison with their analogous homogeneous

counterparts. Recently, Maurya *et al* reported a review on the Vanadium complexes immobilized on solid supports and their use as catalysts for the oxidation and functionalization of alkanes and alkenes [20]. The immobilization of complexes on various solid supports is a beneficial process as in many cases these catalysts are more active and easily recyclable and can maintain their catalytic activity after numerous cycles of the reaction. Moreover, these catalysts exhibit increased stability and improved selectivity. A number of publications and numerous reviews have been reported on the heterogenization of the catalysts [21].

Catalytic oxidation of alkenes into more valuable epoxides as well as oxygen containing carbonyl compounds is one of the important synthetic reactions. Carbonyl compounds have industrial significance and are widely used as solvents, perfumes, and flavoring agents or as intermediates in the manufacture of plastics, dyes, and pharmaceuticals.

As per our knowledge, only one report on the use of oxovanadium complex with pyrazolone ligand as homogeneous catalyst is available [22]. A literature survey shows that, no reports on the catalytic aspects of supported oxovanadium complexes with pyrazolone ligands are available. In this part of the chapter **1**, we report the synthesis and characterization of oxovanadium complex $[VO(L^1)_2]$. The synthesized complex was heterogenized by supporting onto hydrous zirconia (ZrO_2). The reason for selecting ZrO_2 as support is the available surface hydroxyl groups of ZrO_2 which are able to undergo a chemical reaction or strong interaction with supported species [23].

Supported catalyst $(VO(L^1)_2/ZrO_2)$ was characterized by various physicochemical techniques and its catalytic activity was evaluated for solvent free oxidation of styrene with H_2O_2 as an oxidant under mild reaction conditions. The conditions for maximum conversion as well as selectivity for desired product were optimized by varying different parameters such as % loading, molar ratio of substrate to H_2O_2, amount of the catalyst and reaction time. The catalytic property for recycled catalyst was also evaluated for the oxidation of styrene under optimized condition. A reaction mechanism for oxidation of styrene with H_2O_2 as an oxidant was proposed.

1.2.2. Experimental

1.2.2.1. Materials and Physical measurments

All reagents and solvents were purchased from commercial sources and were further purified by the standard methods, if necessary. 1-Phenyl-3-methyl-5-pyrazolone was obtained from Nutan Dye Chem. Sachin, Surat. Zirconium oxychloride (Loba chemie, Mumbai), Oxovanadium sulphate, dichloromethane, 30% aqeous H_2O_2 and styrene were obtained from Merck and used as received.

The synthesized materials were characterized by ^1H NMR, GC-MS, Single crystal XRD, TGA, FT-IR, EPR, BET surface area and SEM. ^1H NMR spectra of ligand L^1 was recorded with AV 400 MHz Bruker FT-NMR instruments. Mass spectra of the ligand L^1 was recorded on Trace GC ultra DSQ II. Elemental analyses of C, H and N were determined using a Perkin Elmer series-II 2400 elemental analyzer. X-ray intensity data of 34372 reflections (of which 5527 unique) were collected on Bruker CCD area-detector diffractometer equipped with graphite monochromated MoKα radiation (λ = 0.71073 Å). A simultaneous TG-DTA of $VO(L^1)_2$ and 30% $VO(L^1)_2$/ ZrO_2 were carried out on a SII EXSTAR6000 TG/DTA 6300. The experiments were performed in N_2 at a heating rate of 10 °C min-1 in the temperature range 25–500 °C using an aluminium pan. FT-IR spectra of $VO(L^1)_2$ and 30% $VO(L^1)_2/ZrO_2$ were recorded as the KBr pellet on the Perkin Elmer Fourier transform (FT-IR) spectrum RX 1 spectrometer. EPR spectra of $VO(L^1)_2$, 30% $VO(L^1)_2$ /ZrO_2 were recorded on X-band instrument at EPR laboratory, SAIF, IIT, Bombay, at room temperature and liquid nitrogen temperature. ESI-mass spectra were recorded on Waters Q-ToF micromass. The BET specific surface area of $VO(L^1)_2$ and 30% $VO(L^1)_2$/ ZrO_2 was calculated by using the standard Bruanuer, Emmett and Teller method on the basis of the adsorption data. Metal contents were measured by inductively coupled plasma-atomic emission spectroscopy (Perking Elmer Optima 2000). Adsorption-desorption isotherms of samples were recorded on a micromeritics ASAP 2010 surface area analyzer at -196 °C. SEM analysis of ZrO_2, $VO(L^1)_2$ and 30% $VO(L^1)_2$/ ZrO_2 were carried out using JSM 5610 LV combined with INCA instrument for EDX-SEM.

1.2.2.2. Synthesis of oxovanadium(IV) complex $[VO(L^1)_2]$

The synthesis of complex $VO(L^1)_2$ have been provided in the part 1 of Chapter 1.

1.2.2.3. Synthesis of support, hydrous zirconia (ZrO_2)

Hydrous zirconia (ZrO_2) was synthesized according to the procedure reported by Bhatt and Patel [24]. It was prepared by adding an aqueous ammonia solution to an aqueous solution of $ZrOCl_2 \cdot 8H_2O$ up to pH 8.5. The resulted precipitates were aged at 100 °C over a water bath for 1 h, filtered, washed with conductivity water until chloride free water was obtained and dried at 100 °C for10 h.

1.2.2.4. Synthesis of Catalyst, Supporting $VO(L^1)_2$ onto ZrO_2

A series of catalysts containing $VO(L^1)_2$ (10-40%) were synthesized by impregnating ZrO_2 (1 g) with an aqueous solution of $VO(L^1)_2.H_2O$ (0.1-0.4 g/10-40 mL of conductivity water) and dried at 100 °C for 10 h. The obtained materials were designated as 10%, 20%, 30% and 40% $VO(L^1)_2$ /ZrO_2.

1.2.2.5. Catalytic reaction

The oxidation reaction was carried out in a borosilicate glass reactor provided with a double walled condenser containing catalyst, styrene and H_2O_2 at 80 °C with constant stirring for 24 h. Similar reactions were carried out by varying different parameters such as effect of % loading, molar ratio of substrate to H_2O_2, amount of the catalyst and reaction time. After completion of the reaction, catalyst was removed and the product was extracted with dichloromethane. The product was dried with magnesium sulphate and analyzed on Gas Chromatograph using BP-5 capillary column. Product was identified by comparison with the authentic samples and finally by Gas Chromatography–Mass Spectrometry (GC–MS).

1.2.3. Results and Discussion

1.2.3.1. Synthesis and characterization of the catalyst

The synthesized ligand was characterized by IR, ^1H, ^{13}C NMR, elemental analyses and Mass spectra. All spectral data were agreed with the ligand structure. The oxovanadium(IV) complex having the general composition $VO(L^1)_2 \cdot H_2O$ has been synthesized by a general procedure based on the mixing of an aqueous solution

of $VOSO_4 \cdot 5H_2O$ with a ethanol solution of the ligand in 1:2 molar ratio, and isolation of final precipitate by filtration. The complex is stable to air and moisture, without any kind of decomposition also after several months. The complex is insoluble in water, but soluble in chlorinated solvents, alcohols, acetonitrile, DMF and DMSO. The structure of the complex $VO(L^1)_2$ is depicted in Figure 1.2.1.

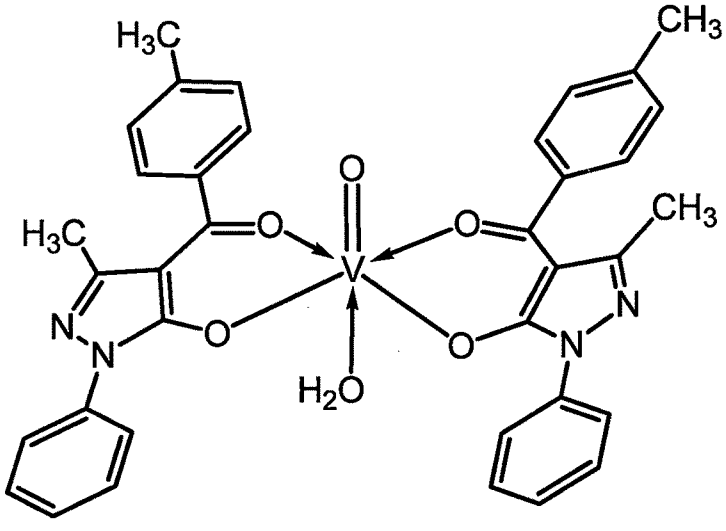

Figure 1.2.1. Structure of oxovanadium(IV) complex $VO(L^1)_2$.

TGA was performed for the $VO(L^1)_2$ and 30% $VO(L^1)_2$/ ZrO_2. TGA of $VO(L^1)_2$ shows weight loss of 2.96 % within the range of 50-150 °C, corresponds to a loss of coordinated water molecule. The decomposition of $VO(L^1)_2$ complex was observed in several steps from 300 °C. The data indicate that complex is stable to decomposition up to 300 °C.

The TGA of 30% $VO(L^1)_2$ /ZrO_2 shows initial weight loss up to 150 °C, may be due to the removal of adsorbed water molecules. No significant loss occurs up to 350 °C, which indicates an increase in the stability of $VO(L^1)_2$ after supporting ZrO_2. DTA of $VO(L^1)_2$ shows endothermic peaks at 80 °C and 235 °C, due to the loss of adsorbed water and coordinating water, respectively. In addition, DTA of $VO(L^1)_2$ shows decomposition temperature at 300 °C. DTA of 30% $VO(L^1)_2$/ZrO_2 shows a small endotherm due to the loss of adsorbed water. No significant loss up to 350 °C is observed, which indicates that present material is stable up to 350 °C. TG-DTA thermograms are shown in Figure 1.2.2.

The vanadium and zirconium contents in 30% $VO(L^1)_2/ZrO_2$ were measured by ICP analysis. Found: Zr, 49.88; V, 1.72 (calcd: Zr, 49.69; V, 1.76).

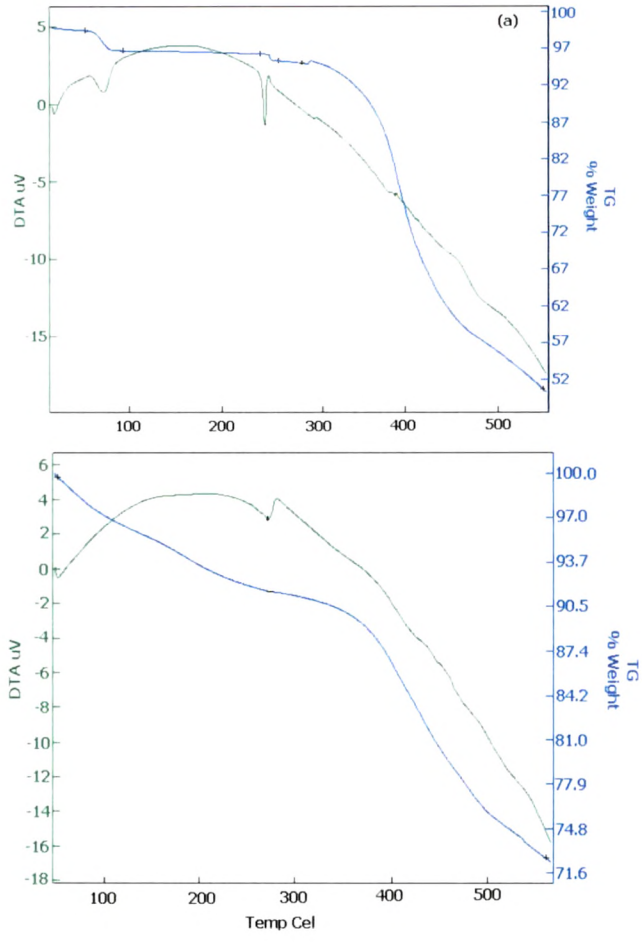

Figure 1.2.2. TG-DTA thermograms of (*a*) $VO(L^1)_2$ and (*b*) 30% $VO(L^1)_2/ZrO_2$

FT-IR was recorded to confirm the presence of reactive undegraded $VO(L^1)_2$ species present on the surface of ZrO_2 (*see* Figure 1.2.3). FT-IR spectrum of $VO(L^1)_2$ exhibits the bands at 3395 cm^{-1} which can be assigned to the coordinated water. The complex shows the absorptions at 1567 cm^{-1} and 1476 cm^{-1} which are due to $\upsilon_{C=N}$ of the pyrazolone ring and due to υ_{C-O}. The vanadium complex shows a strong band at 966 cm^{-1} due to $\upsilon_{V=O}$ stretching. The band at 476 cm^{-1} is assign to the υ_{V-O}. FT-IR spectrum of 30% $VO(L^1)_2/ ZrO_2$ shows that all of the bands correspond to functional groups of $VO(L^1)_2$, indicating the presence of $VO(L^1)_2$ over the surface of catalyst. The shifting of the bands value may be due to interaction of oxygen of $VO(L^1)_2$ with hydrogen of surface hydroxyl groups of ZrO_2.

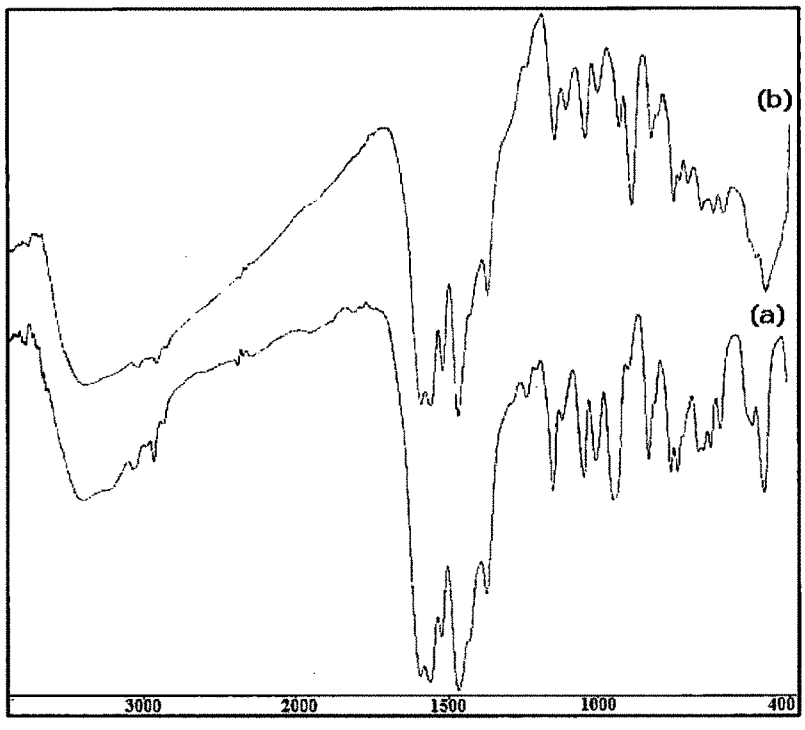

Figure 1.2.3. FT-IR spectra of (*a*) $VO(L^1)_2$ and (*b*) 30% $VO(L^1)_2$/ ZrO_2.

The full range (3200-2000 G) X-band EPR spectra for $VO(L^1)_2$ (frozen solution state and room temperature solid state) and $VO(L^1)_2/ZrO_2$ (Room temperature) were recorded (*see* Figure 1.2.4). The EPR spectra of the $VO(L^1)_2$ at liquid nitrogen temperature and at room temperature are shown in Figure 1.2.4*a*. X-band EPR spectra were recorded in DMF for the $VO(L^1)_2$. The EPR spectrum of metal complex provide information about hyperfine and super hyperfine structure which is important in the study of the metal-ion environment in the complexes, i.e. the geometry, nature of the ligating sites from the ligand of the metal and the degree of covalency of the metal-ligand bonds.

The room temperature (300 K) spectrum of $VO(L^1)_2$ (*see* Figure 1.2.4*b*) is a typical eight line pattern, which shows that a single vanadium is present in the molecule, i.e. it is mononuclear. In the frozen solution state, the spectrum shows two types of resonance components, one set due to the parallel feature and the other set due to the perpendicular features, which indicates axially symmetric anisotropy with well-resolved 16-line hyperfine splitting, characteristic of interaction between the electron and vanadium nuclear spins. The *g*-values were computed from the spectra using TCNE free- radical as *g* marker. The room temperature EPR of $VO(L^1)_2/ZrO_2$ (*see* Figure 1.2.4*c*) shows single line spectra (V^{4+}; $3d^1$) with a *g* value of 1.976

confirming the presence of V(IV) in octahedral symmetry on the surface of the support. The absence of hyperfine lines may be due to support of $VO(L^1)_2$ onto ZrO_2.

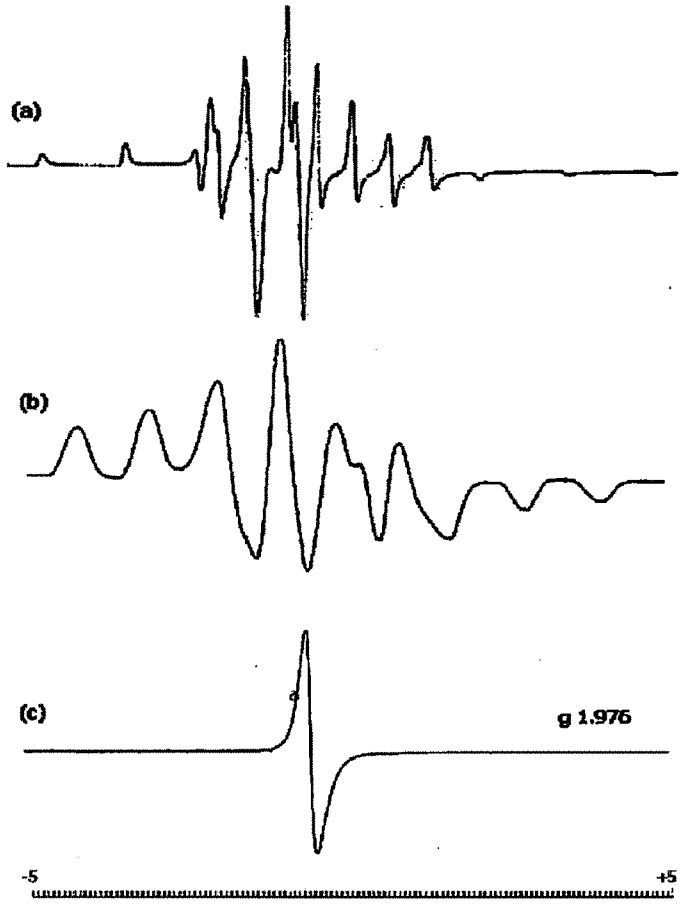

Figure 1.2.4. EPR spectra of (*a*) $VO(L^1)_2$ (in DMF at liquid nitrogen temperature) (*b*) $VO(L^1)_2$ (in a polycrystalline state at room temperature) and (*c*) $VO(L^1)_2/ZrO_2$ (in a polycrystalline state at room temperature).

The larger surface area of the 30% $VO(L^1)_2$ /ZrO_2 (85.97 $m^2\ g^{-1}$) compared to that of $VO(L^1)_2$ (2.13 $m^2\ g^{-1}$) was due to support of $VO(L^1)_2$ and it is as expected.

The nitrogen adsorption isotherm of 30% $VO(L^1)_2$ /ZrO_2 (*see* Figure 1.2.5*a*) presents a type-II isotherm with a hysteresis loop in the desorption isotherm in the high range of relative pressure. The type-II isotherm is obtained when adsorption occurs on non-porous powders or on powders with pore diameters larger than the micropores. The inflection point or knee of the isotherm usually occurs near completion of the first adsorbed monolayer and, with increasing relative pressure,

second and higher layers are completed until at saturation the number of adsorbed layers becomes infinite.

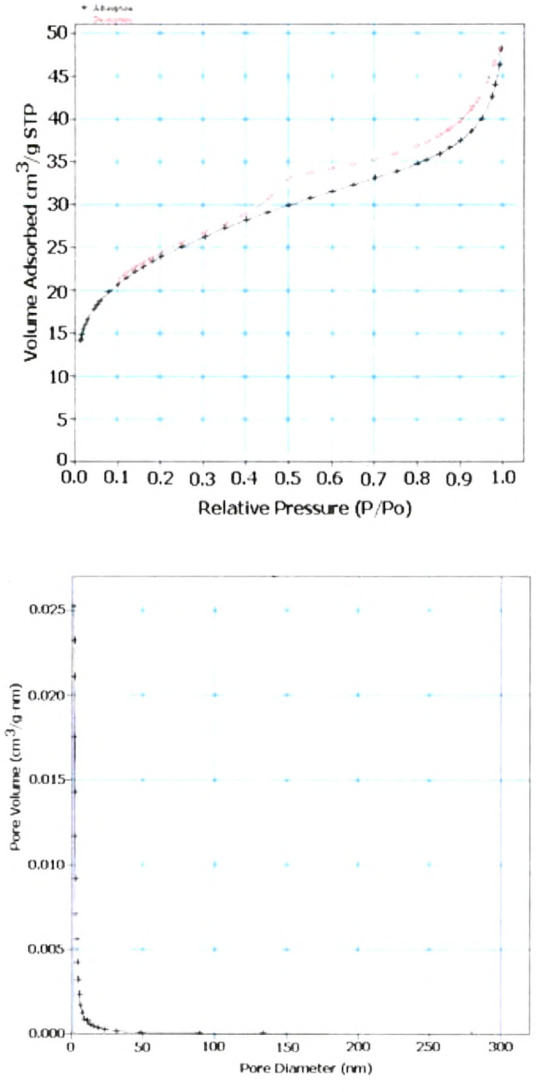

Figure 1.2.5. BET isotherm of 30% $VO(L^1)_2$ /ZrO_2 (*a*) adsorption-desorption isotherm and (*b*) pore-size distribution.

The pore size distribution curve for 30% $VO(L^1)_2$ /ZrO_2 shows a maximum at 10-15 nm (*see* Figure 1.2.5*b*), which indicates pores with sizes belonging to the entire range of characteristic mesoporosity. The sharp pore size distribution in the maximum range shows the uniformity of the porous structure.

The SEM images of ZrO_2, $VO(L^1)_2$ and 30% $VO(L^1)_2$/ZrO_2 at a magnification of 100× are reported in Figure 1.2.6. Figure 1.2.6*b* shows the crystalline nature of $VO(L^1)_2$ (block shaped). It is seen from the SEM image of 30% $VO(L^1)_2$/ ZrO_2 (*see*

Figure 1.2.6*c*) that the surface of the support is distinctly altered after support of $VO(L^1)_2$ onto ZrO_2. The SEM of 30% $VO(L^1)_2$/ ZrO_2 shows a uniform dispersion of particles. SEM confirms the uniform as well as high dispersion of $VO(L^1)_2$ in a noncrystalline form onto the surface of the support.

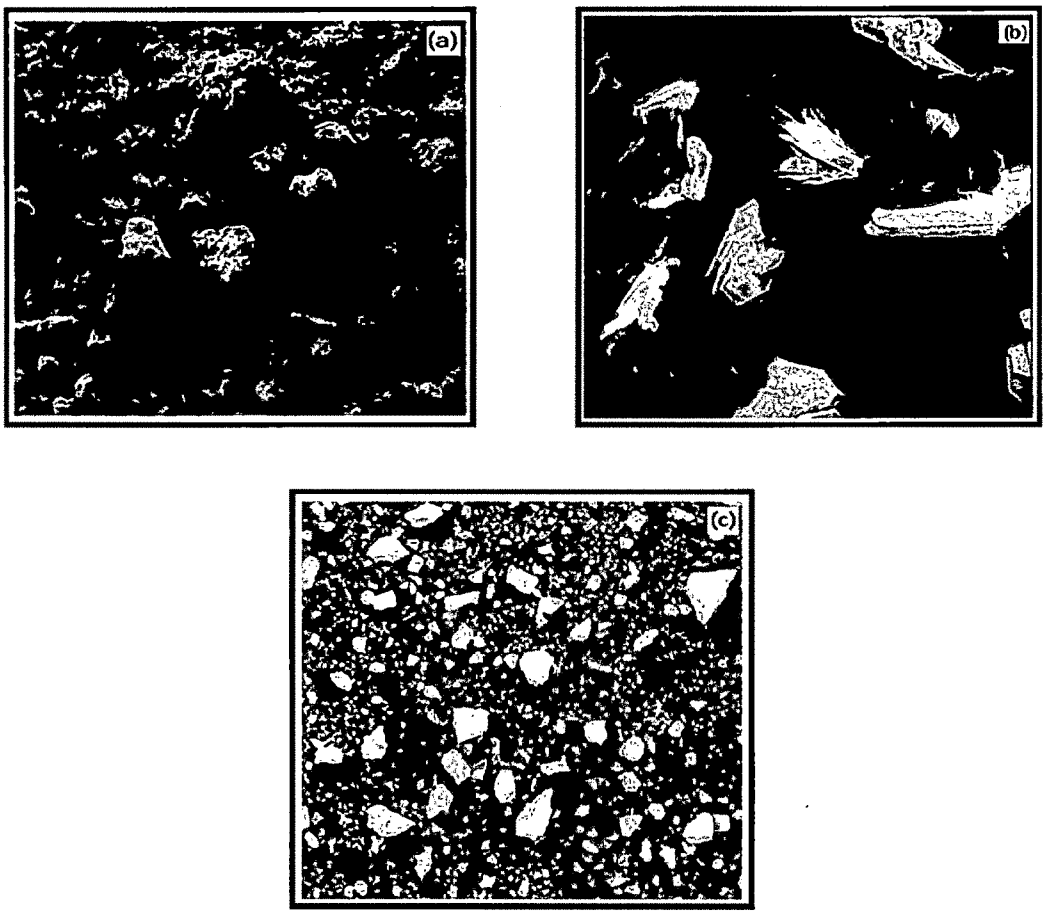

Figure 1.2.6. SEM of (*a*) ZrO_2, (*b*) $VO(L^1)_2$ and (*c*) 30% $VO(L^1)_2$ /ZrO_2 at a magnification 100x.

1.2.3.2. Oxidation of styrene using hydrogen peroxide

The reaction was carried out by varying the mole ratio of styrene to H_2O_2 with 25 mg of the catalyst for 24 h at 80 °C. Generally, styrene oxidation gives styrene oxide, benzaldehyde, benzyl alcohol, acetophenone and benzoic acid. However in the present reaction conditions, the major oxidation product obtained was benzaldehyde may be because of (i) direct oxidative cleavage of C=C of styrene and (ii) the fast conversion of styrene oxide to benzaldehyde.

With a 1: 3 molar ratio the conversion of styrene was >99% and the selectivity for benzaldehyde was 99.1%, While with a 1: 4 molar ratio the conversion was >99% with 78% selectivity for benzaldehyde. Hence, further optimization of the conditions was carried out with a 1: 3 molar ratio.

Effect of % loading of $VO(L^1)_2$

The oxidations of styrene carried out with H_2O_2 in 1:3 molar ratios by using 25 mg of fresh catalysts for 24 h at 80 °C are presented in Figure 1.2.7. The Figure shows, an increase in the conversion with an increase in the % loading of $VO(L^1)_2$ from 10% to 30%.

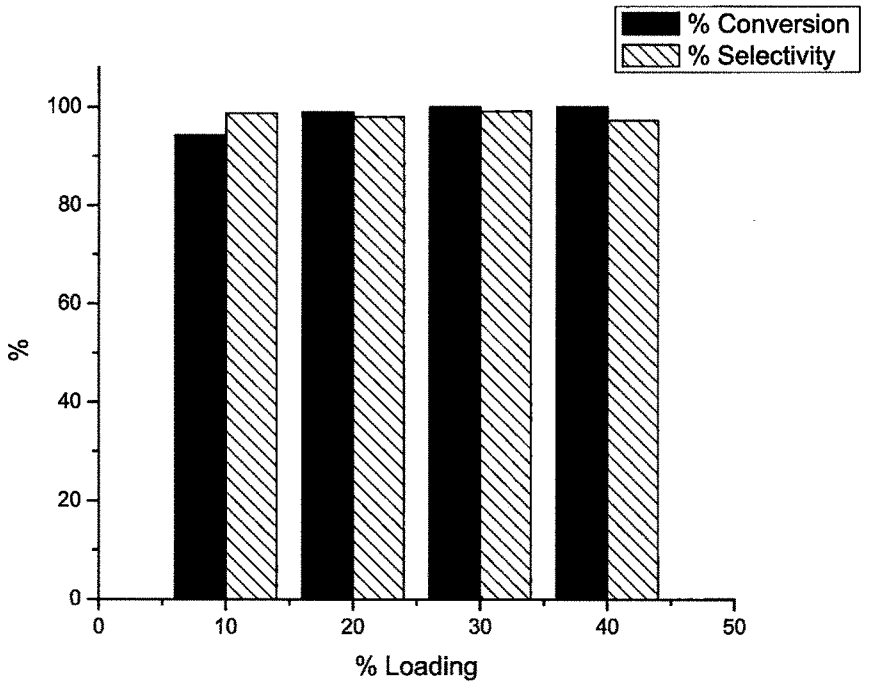

Figure 1.2.7. Effect of % loading; % Conversion is based on styrene; time = 24 h; temperature = 80 °C; amount of catalyst = 25 mg, molar ratio of styrene to H_2O_2: 1:3.

Further, with an increase in the percent loading from 30% to 40%, a small decrease in conversion was found. This may be due to blocking of the active sites. Thus the loading of $VO(L^1)_2$ on the support was fixed at 30%. A detailed study was carried out at 80 °C over 30% $VO(L^1)_2$/ ZrO_2.

Effect of mole ratio of styrene to H_2O_2

In order to determine the effect of H_2O_2 on the oxidation of styrene to benzaldehyde, the mole ratio of styrene to H_2O_2 was varied (1:1, 1:2, 1:3, and 2:1), keeping other parameters fixed: namely catalyst (25 mg), temperature (80 °C) and reaction time (24 h). The results are shown in Figure 1.2.8. Styrene to H_2O_2 molar ratio of 1:1 and 1:2 resulted in 33.2 and 73.8% conversion, respectively, and when the styrene to H_2O_2 molar ratio was changed to 1:3, conversion increased to 100%, keeping all other conditions similar.

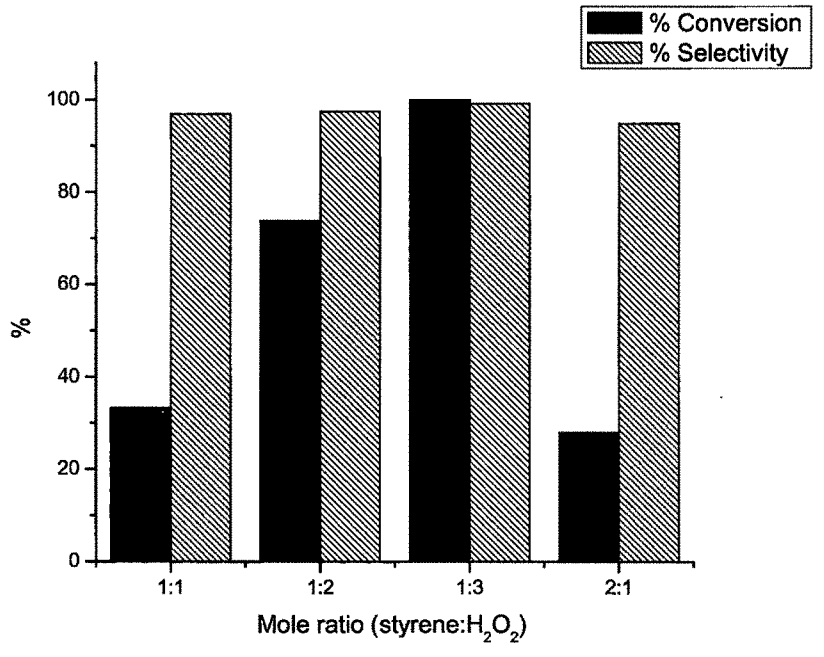

Figure 1.2.8. Effect of mole ratio; % Conversion is based on styrene; time = 24 h; temperature = 80 °C; amount of catalyst =25 mg.

However, conversion was found to be decrease for a styrene to H_2O_2 molar ratio of 2:1. Therefore, a 1:3 molar ratio of styrene to H_2O_2 was found to be the optimum in terms of conversion of styrene.

Effect of the amount of catalyst

The amount of catalyst has a significant effect on the oxidation of styrene. Five different amounts of 30% $VO(L^1)_2$/ ZrO_2 *viz.*, 10, 15, 20, 25 and 30 mg were used, keeping all other reaction parameters fixed: namely temperature (80 °C), styrene (10 mmol), 30% H_2O_2 (30 mmol) and reaction time (24 h). The results are shown in

Figure 1.2.9, indicating 72.4, 88.7, 93.9, 100 and 100% conversion corresponding to 10, 15, 20, 25 and 30 mg catalyst, respectively.

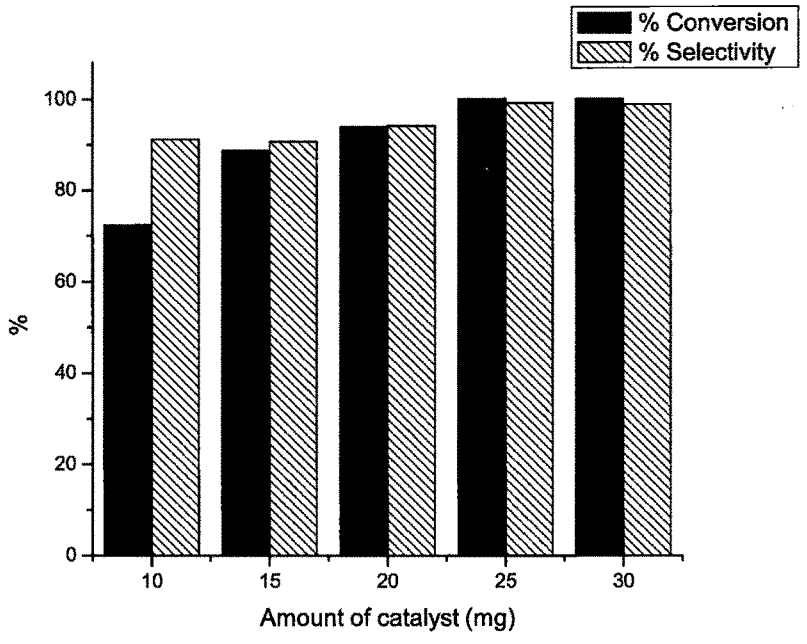

Figure 1.2.9. Effect of amount of catalyst; % Conversion is based on styrene; time = 24 h; temperature = 80 °C; molar ratio of styrene to H_2O_2: 1:3.

The lower conversion of styrene into benzaldehyde with 10- 20 mg catalyst may be due to fewer catalytic sites. The maximum percentage conversion was observed with 25 mg of catalyst, but there was no remarkable difference in the progress of reaction when 25 or 30 mg of catalyst was employed. Therefore, 25 mg of catalyst was taken to be optimal.

Effect of the reaction time

The time dependence of catalytic solvent free oxidation of styrene was studied by performing the reaction of styrene (10 mmol) with 30% H_2O_2 (30 mmol) in the presence of 25 mg of catalyst at 80 °C with constant stirring. The percentage conversion was monitored at different reaction times.

It is seen from Figure 1.2.10 that, with an increase in the reaction time, percent conversion also increases. The initial conversion of styrene increased with the reaction time. This is because more time is required for the formation of reactive

intermediate (substrate + catalyst), which is finally converted into the products. It is seen that maximum conversion of styrene was observed within 24 h.

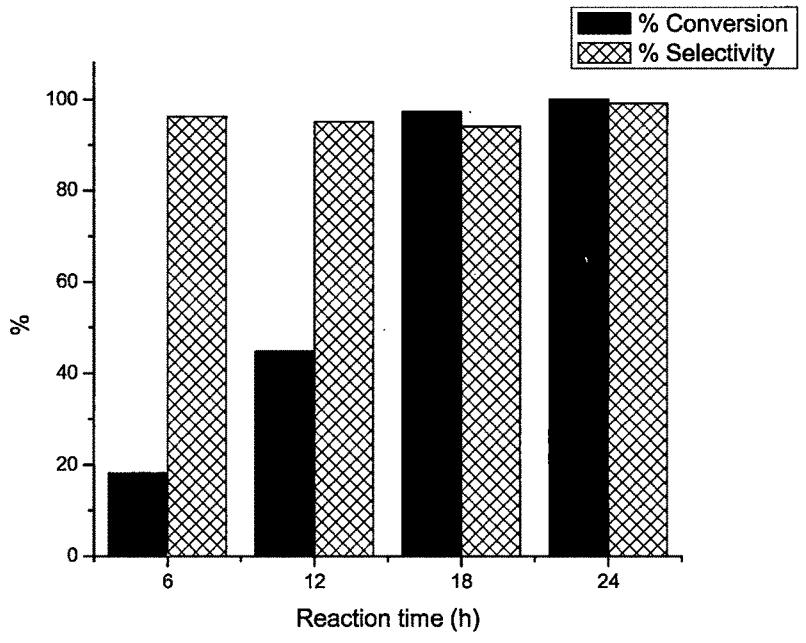

Figure 1.2.10. Effect of reaction time; % Conversion is based on styrene; amount of catalyst = 25 mg; temperature = 80 °C; molar ratio of styrene to H_2O_2: 1:3.

The optimum conditions for maximum percent conversion of styrene to benzaldehyde are a mole ratio of styrene to H_2O_2 of 1:3, with 25 mg of catalyst and 24 h reaction time at 80 °C.

The control experiments with ZrO_2 and $VO(L^1)_2$ were also carried out under optimized conditions with styrene and H_2O_2. It can be seen from Table 1.2.1 that ZrO_2 is inactive towards the oxidation of styrene, indicating that the catalytic activity is due to only $VO(L^1)_2$. The same reaction was carried out by taking the active amount of $VO(L^1)_2$ (5.8 mg). It was found that the active catalyst gives, 97% conversion of styrene with >96% selectivity of benzaldehyde. Almost the same obtained activity for supported catalyst indicates that $VO(L^1)_2$ is the real active species. Thus, we are successful in supporting $VO(L^1)_2$ onto ZrO_2 without any significant loss in activity and hence in overcoming the traditional problems of homogeneous catalysis.

Table 1.2.1. Control experiments for the oxidation of styrene

Catalyst	% Conversion	% Selectivity for benzaldehyde
ZrO_2	-	-
$VO(L^1)_2$	97.1	96.4

% Conversion is based on styrene; Amount of $VO(L^1)_2$ = 5.8 mg, amount of ZrO_2 = 19.2 mg; molar ratio of styrene to H_2O_2 = 1 : 3; Time = 24 h; temperature = 80 °C.

1.2.3.3. Heterogeneity test

A heterogeneity test was carried out for the oxidation of styrene. For the rigorous proof of heterogeneity, a test [25] was carried out by filtering the catalyst from the reaction mixture at 80 °C after 2 h and, then the filtrate was allowed to react up to 4 h. The 2 h reaction mixture and the filtrate were analyzed by gas chromatography. No change in percent conversion as well as % selectivity was found, indicating that the present catalyst falls into category C [26]. The results are presented in Table 1.2.2.

Table 1.2.2. Heterogeneity test

Catalyst	% Conversion	% Selectivity for benzaldehyde
30% $VO(L^1)_2$ / ZrO_2 (2h)	15.4	90.3
Filtrate (4h)	15.6	89.7

% Conversion is based on styrene; amount of catalyst = 25 mg; molar ratio of styrene to H_2O_2 = 1:3, temperature = 80 °C.

1.2.3.4. Recycling of the catalyst

The oxidation of styrene was carried out with the recycled catalyst, under optimized conditions. The catalyst was removed from the reaction mixture after completion of the reaction by simple filtration, washed with dichloromethane and dried at 100 °C. The catalyst was recycled in order to test its activity as well as stability. The obtained results are presented in Table 1.2.3. As can be seen from table, there was no appreciable change observed in selectivity; however, a small decrease in

conversion was observed, which shows that the catalysts are stable and can be regenerated for repeated use.

Table 1.2.3. Oxidation of styrene with fresh and recycled catalysts

Catalyst	Cycle	% Conversion	% Selectivity for benzaldehyde	TON
30% $VO(L^1)_2$/ ZrO_2	Fresh	100	99.1	1151
	1	99.8	98.9	1148
	2	99.2	97.0	1116

% Conversion is based on styrene; amount of catalyst = 25 mg; molar ratio of styrene to H_2O_2 = 1:3, Time = 24 h; temperature = 80 °C.

1.2.3.5. Reaction mechanism

A reaction mechanism for the oxidation of styrene is proposed in Scheme 1.2.1. For the catalytic reaction to proceed, activation of V^{4+} is required. The activation of V^{4+} species takes place through the attack of H_2O_2 followed by the formation of intermediate $HOOV^{5+}(OH)L_2/ZrO_2$. Upon rearrangement of this intermediate, an active species $\bullet OOV^{5+}OL_2/ZrO_2$ is formed. This formed active species is responsible for the activation of alkenes.

This activated species $\bullet OOV^{5+}OL_2/ZrO_2$ radical (i.e. V-O_2 metal-superoxo intermediate), which then attacks the substrate reversibly, binds to the alkene attacking the reaction site, resulting in the oxidation of substrate to form products. Further, the oxidation of alkenes *via* a radical chain mechanism is a known process [27]. In order to confirm the role of formed active intermediate $\bullet OOV^{5+}OL_2/ZrO_2$, it was isolated and characterized by EPR. The room temperature X-band EPR of $V^{4+}OL_2/ZrO_2$ shows an EPR signal with a *g* value of 1.975, which may correspond to V^{4+} in octahedral symmetry. The room temperature X-band EPR of the active intermediate ($\bullet OOV^{5+}OL_2/ZrO_2$) shows a typical anisotropic EPR with splitting of the EPR signalm which may be due to the presence of a radical electron.

The broadening of the signal may be due to the presence of a transition metal ion. The anisotropic EPR signal is indicative of the presence of a free radical. The free radical resides on O atom, and it is strongly coupled with V^{5+}. The average *g* value calculated for the present system ($\bullet OOV^{5+}OL_2/ZrO_2$) is 2.006, which are in good agreement with the reported *g* value of organic free radicals, 2.0023 [28]. The EPR studies strongly support the proposed mechanism.

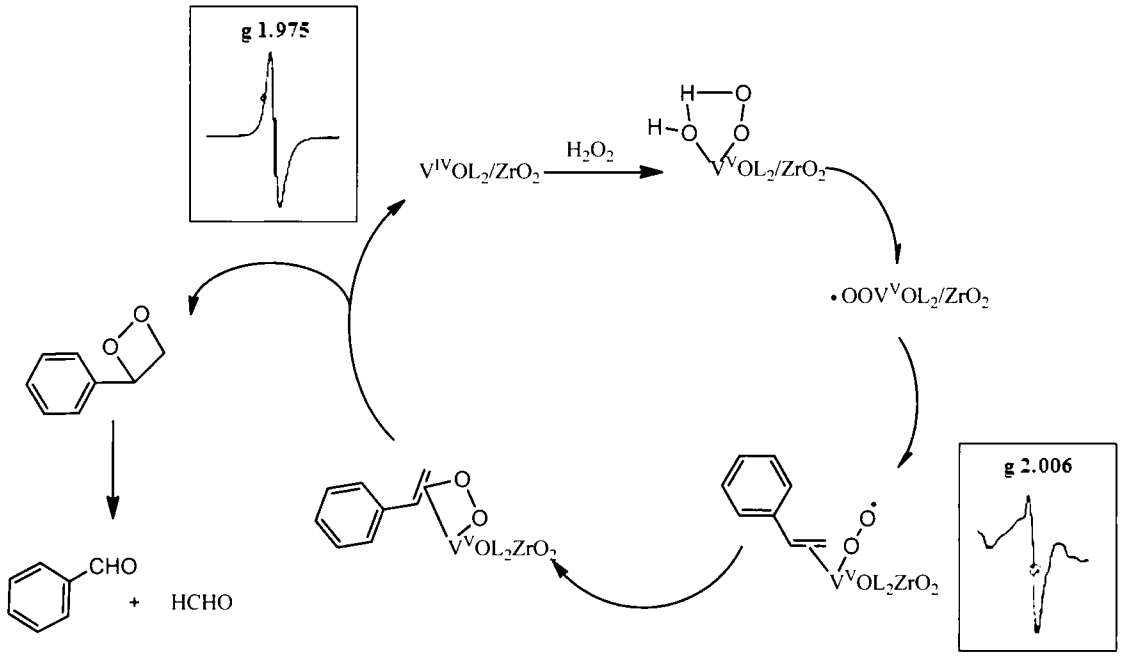

Scheme 1.2.1. Proposed reaction mechanism for the oxidation of styrene.

1.2.4. Conclusions

Oxovanadium(IV) complex containing 1-phenyl-3-methyl-4-toluoyl-5-pyrazolone donor ligand has been synthesized and its crystal and molecular structure has been resolved by single crystal X-ray diffraction, showing a distorted octahedral environment around vanadium through the coordination of two *O, O*-chelating acylpyrazolonate ligands occupying the equatorial plane in *syn* configuration to each other and a water molecule *trans* to oxo group. The catalyst comprising of oxovanadium(IV) complex and hydrous zirconia, is proved to be successful in oxidation of styrene under mild reaction condition. Superiority of catalyst lies in obtaining 100% conversion of styrene with >99% selectivity for benzaldehyde (1151 TON). In all reactions removal of the catalyst consist of single filtration and catalyst

can be reused after a simple workup. A reaction mechanism was proposed for the oxidation of styrene by the present oxovanadium(IV) complex using H_2O_2 as an oxidant. The reactive intermediate species ($•OOV^{5+}OL_2/ZrO2$) was isolated and characterized by EPR spectroscopy.

1.2.5. References

[1] J. Hagen, *Industrial Catalysis: A Practical Approach, 2nd Ed.*, Wiley-VCH, Weinheim, Germany, **2006**.

[2] G. Rothenberg, *Catalysis: Concepts and Green Applications*, Wiley-VCH, Weinheim, Germany, **2008**.

[3] J. H. Gary, G. E. Handwerk, *Petroleum Refining: Technology and Economics*, CRC Press, Boca Raton, **2001**.

[4] M. Lancaster, *Green Chemistry: An Introductory Text*, Royal Society of Chemistry, UK, **2002**.

[5] (*a*) D. Rehder, *Coord. Chem. Rev.*, **1999**, *182*, 297-322; (*b*) J. J. R. Frafflsto da Silva, R. J. P. Williams, *The Biological Chemistry of the Elements, The Inorganic Chemistry of Life, 2nd edn.*, Oxford University Press, Oxford, **2001**; (*c*) W. Kaim, B. Schwederski, *Bioinorganic Chemistry: Inorganic Elements in the Chemistry of Life*, John Wiley & Sons, Chichester, **1994**; (*d*) R. R. Eady, *Coord. Chem. Rev.*, **2003**, *237*, 23-30.

[6] (*a*) D. Rehder, *J. Inorg. Biochem.*, **2008**, *102*, 1152-1158; (*b*) M. R. Maurya, S. Agarwal, C. Bader, D. Rehder, *Eur. J. Inorg. Chem.*, **2005**, 147-157; (*c*) D. Rehder, G. Santonin, G. M. Licini, C. Schulzke, B. Meier, *Coord. Chem. Rev.*, **2003**, *237*, 53-63; (*d*) W. Plass, *Coord. Chem. Rev.*, **2003**, *237*, 205-212; (*e*) K. H. Thompson, C. Orvig, *Coord. Chem. Rev.*, **2001**, *219*, 1033-1053; (*f*) A. Butler, *Coord. Chem. Rev.*, **1999**, 187, 17-35.

[7] (*a*) I. Osinska-Krolicka, H. Podsiadly, A. Bukietynska, *J. Inorg. Biochem.*, **2004**, *98*, 2087-2098; (*b*) K. H. Thompson, J. H. McNeil, C. Orvig, *Chem. Rev.*, **1999**, *99*, 2561-2572.

[8] (*a*) D. C. Crans, *Pure Appl. Chem.*, **2005**, *77*, 1497-1527; (*b*) H. Sakurai, Y. Kojima, Y. Yoshikawa, K. Kawabe, H. Yasuri, *Coord. Chem. Rev.*, **2002**, *226*, 187-198; (*c*) Y. Shechter, I. Goldwaser, M. Mironchik, M. Fridkin, D. Gefel, *Coord. Chem. Rev.*, **2003**, *237*, 3-11.

[9] (*a*) Y. Shechter, S. J. D. Karlish, *Nature*, **1980**, *286*, 556-558; (*b*) Y. Shechter, *Diabetes*, **1990**, *39*, 1-5.

[10] (*a*) D. Rehder, *Bioinorganic Vanadium Chemistry*, John Wiley & Sons, Chichester, **2008**; (*b*) K. Kustin,; J. C. Pessoa, D. C. Crans, (Eds.), *Vanadium: The Versatile Metal, American Chemical Society*, Washinton, DC, **2007**; (*c*) R. L. Richards, in: *Encyclopedia of Inorganic Chemistry*, 2nd *edn.*, (Ed.: R. B. King), Wiley, **2005**, Vol. IX, pp 5767 – 5803; (*d*) T. Hirao, *Chem. Rev.*, **1997**, *97*, 2707-2724; (*e*) A. S. Tracey, G. R. Willsky, E. S. Takeuchi, *Vanadium Chemistry, Biochemistry Pharmacology and Practical Applications*, CRC Press, **2007**.

[11] (*a*) M. L. Kuznetsov, J. C. Pessoa, *Dalton Trans.*, **2009**, 5460-5468; (*b*) H. Mizuno, H. Sakurai, T. Amaya, T. Hirao, *Chem. Comm.*, **2006**, 5042-5044; (*c*) L. G. Cuervo, Y. N. Kozlov, G. Süss-Fink, G. B. Shul'pin, *J. Mol. Catal A: Chem.*, **2004**, *218*, 171-177.

[12] (*a*) C. Bolm, *Coord. Chem. Rev.*, **2003**, *237*, 245-256; (*b*) G. Du, J. H. Espenson, *Inorg. Chem.*, **2005**, *44*, 2465-2471.

[13] Y. N. Belokon, M. North, V. I. Maleev, N. V. Voskoboev, M. A. Moskalenko, A. S. Preegudov, A. V. Dmitriev, N. S. Ikonnikov, H. B. Kagan, *Angew. Chem., Int. Ed.*, **2004**, *43*, 4085-4089.

[14] (*a*) R. C. Michaelson, R. E. Palermo, K. B. Sharpless, *J. Am. Chem. Soc.*, **1977**, *99*, 1990-1992; (*b*) Y. Hoshino, H. Yamamoto, *J. Am. Chem. Soc.*, **2000**, *122*, 10452-10453; (*c*) C. Bolm, T. Kühn, *Synlett.*, **2000**, *6*, 899-901; (*d*) H. L. Wu, B. J. Uang, *Tetrahedron: Asymmetry*, **2002**, *13*, 2625-2628; (*e*) W. Adam, A. K. Beck, A. Pichota, C. R. Saha-Möller, D. Seebach, N. Vogl, R. Zhang, *Tetrahedron: Asymmetry*, **2003**, *14*, 1355-1361; (*f*) W. Zhang, A. Basak, Y. Kosugi, Y. Hoshino, H. Yamamoto, *Angew. Chem., Int. Ed.*, **2005**, *44*, 4389-4391; (*g*) Z. Bourhani, A. V. Malkov, *Chem.Commun.*, **2005**, 4592-4594; (*h*) A. Lattanzi, S. Piccirillo, A. Scettri, *Eur. J. Org. Chem.*, **2005**, 1669-1674.

[15] (*a*) C. -Y. Chu, D. -R. Hwang, S. -K. Wang, B. -J. Uang, *Chem. Commun.*, **2001**, 980-981; (*b*) Z. Luo, Q. Liu, L. Gong, X. Cui, A. Mi, Y. Jiang, *Angew. Chem., Int. Ed.*, **2002**, *41*, 4532-4535; (*c*) N. B. Barhate, C.-T. Chen, *Org. Lett.*, **2002**, *4*, 2529-2532; (*d*) H. Somei, Y. Asano, T. Yoshida,

S. Takizawa, H. Yamataka, H. Sasai, *Tetrahedron Lett.*, **2004**, *45*, 1841-1844.

[16] (*a*) K. Nakajima, M. Kojima, J. Fujita, *Chem. Lett.*, **1986**, 1483-1486; (*b*) D. A. Cogoa, G. Liu, K. Kim, B. J. Backes, J. A. Ellman, *J. Am. Chem. Soc.*, **1998**, *120*, 8011-8019; (*c*) B. Pelotier, M. S. Anson, I. B. Campbell, S. J. F. Macdonald, G. Priem, R. F. W. Jackson, *Synlett.*, **2002**, 1055-1060; (*d*) C. Ohta, H. Shimizu, A. Kondo, T. Katsuki, *Synlett.*, **2002**, 161-163; (*e*) G. Santoni,G. Licini, D. Rehder, *Chem. Eur. J.*, **2003**, *9*, 4700-4708; (*f*) J. Sun, C. Zhu, Z. Dai,M. Yang, Y. Pan, H. Hu, *J. Org. Chem.*, **2004**, *69*, 8500; (*g*) C.Drago, L. Caggiano, R. F.W. Jackson, *Angew. Chem., Int. Ed.*, **2005**, *44*, 7221-7223; (*h*) A. Basak, A. U. Barlan, H. Yamamoto, *Tetrahedron: Asymmetry*, **2006**, *17*, 508-511.

[17] S. -H. Hsieh, H.-M. Gau, *Synlett.*, **2006**, 1871-1874.

[18] (*a*) S. Akai, K. Tanimoto, Y. Kanao, M. Egi, T. Yamamoto, Y. Kita, *J. Am. Chem. Soc.*, **2005**, *127*, 1090-1091; (*b*) A. Blanc, F. D. Toste, *Angew. Chem., Int. Ed.*, **2006**, *45*, 2096-2099.

[19] (*a*) A. D. Pomogaĭlo, *Catalysis by Polymer-immobilized Metal Complexes*, CRC Press, New York, **1998**; (*b*) N. E. Leadbeater, M. Marco, *Chem. Rev.*, **2002**, *102*, 3217–3274; (*c*) K. Burgess, *Solid Phase Organic Synthesis*, John-Wiley, New York, **2000**.

[20] M. R. Maurya, A. Kumar, J. C. Pessoa, *Coord. Chem. Rev.*, **2011**, *255*, 2315-2344.

[21] (*a*) C. E. Song, *Annu. Rep. Prog. Chem., Sect. C*, **2005**, *101*, 143-173; (*b*) C. E. Song, S. -G. Lee, *Chem. Rev.*, **2002**, *102*, 3495-3524; (*c*) D. E. De Vos, M. Dams, B. F. Sels, P. A. Jacobs, *Chem. Rev.*, **2002**, *102*, 3615-3640.

[22] F. Marchetti, C. Pettinari, C. D. Nicola, R. Pettinari, A. Crispini, M. Crucianelli, A. D. Giuseppe, *Appl. Catal. A: Gen.*, **2010**, *378*, 211-233.

[23] (*a*) B. M. Reddy, M. K. Patil, *Chem. Rev.*, **2009**, *109*, 2185-2208; (*b*) Soyeb Pathan, Anjali Patel, *Dalton Trans.* **2011**, *40*, 348-355.

[24] N. Bhatt, A. Patel, *J. Mol. Catal. A: Chem.*, **2005**, *238*, 223-228.

[25] T. Okuhara, N. Mizuno, M. Misono, *Adv. Catal.* **1996**, *41*, 113-252.

[26] A. Sheldon, M. Walau, I. W. C. E. Arends, U. Schuchurdt, *Acc. Chem. Res.*, **1998**, *31*, 485-493.

[27] (*a*) L. Xinrong, X. Jinyu, L. Huizhang, Y. Bin, J. Songlin, X. Gaoyang, *J. Mol. Catal. A: Chem.* **2000**, *161*, 163-169; (*b*) X. Zhang, Q. Chen, D.C. Duncan, R. J. Lachicotte, C. L. Hill, *Inorg. Chem.*, **1997**, *36*, 4381-4386.

[28] M. Bersohn, J. C. Baird, *An Introduction to Electron Paramagnetic Resonance,* W. A. Benjamin, INC., New York, **1966**, p. 69 (Chapter 5).

Inorganic Chemistry

Article

pubs.acs.org/IC

Synthesis and Crystal Structure of an Oxovanadium(IV) Complex with a Pyrazolone Ligand and Its Use as a Heterogeneous Catalyst for the Oxidation of Styrene under Mild Conditions

Sanjay Parihar,[†] Soyeb Pathan,[†] R. N. Jadeja,*[,†] Anjali Patel,*[,†] and Vivek K. Gupta[‡]

[†]Department of Chemistry, Faculty of Science, The Maharaja Sayajirao University of Baroda, Vadodara 390 002, India

[‡]Post-Graduate Department of Physics, Jammu University, Jammutawi 180 006, India

Supporting Information

ABSTRACT: 1-Phenyl-3-methyl-4-touloyl-5-pyrazolone (ligand) was synthesized and used to prepare an oxovanadium(IV) complex. The complex was characterized by single-crystal X-ray analysis and various spectroscopic techniques. The single-crystal X-ray analysis of the complex shows that the ligands are coordinated in a syn configuration to each other and create a distorted octahedral environment around the metal ion. A heterogeneous catalyst comprising an oxovanadium(IV) complex and hydrous zirconia was synthesized, characterized by various physicochemical techniques, and successfully used for the solvent-free oxidation of styrene. The influence of the reaction parameters (percent loading, molar ratio of the substrate to H_2O_2, amount of catalyst, and reaction time) was studied. The catalyst was reused three times without any significant loss in the catalytic activity.

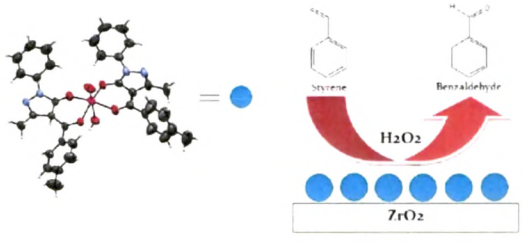

INTRODUCTION

The coordination chemistry of vanadium, in particular with multidentate ligands, is receiving much attention because of its involvement in various biological processes: in the active site of metalloenzymes such as vanadium nitrogenase[1] and haloperoxidases,[2] as a metabolic regulator,[3] as a mitogenic activator, and especially as an insulin-mimicking agent.[4] Vanadium complexes can also affect the cardiac abnormality associated with diabetes mellitus[5] and exhibit anticancer activity.[6]

Moreover, catalytic applications have also stimulated the coordination chemistry of vanadium, and the search for novel vanadium complexes with pharmacological and catalytic significance is a matter of a high current interest. Oxovanadium peroxo complexes efficiently oxygenate organic compounds. Vanadium complexes possess versatile oxidation states and unusual redox ability. Usually, vanadium can exist in 3+, 4+, and 5+ oxidation states. In 4+ and 5+ oxidation states, vanadium has strong redox ability, which can lead to some important reactions. Oxovanadium complexes were illustrated to be catalysts[8] in a variety of asymmetric reactions such as the cyanation reaction,[9] epoxidation of allyl alcohols,[8a,10] oxidative coupling of 2-naphthol,[11] oxidation of organic sulfides,[8a,12] alkynyl addition to aldehydes,[13] and others.[14]

Immobilization of metal complexes onto the surfaces of solid supports is highly desirable in the development of reusable catalysts.[15] Supported vanadium oxide catalysts constitute a very important class of catalytic materials. They have become the model for catalytic systems for fundamental studies of supported metal oxides, and they are widely used as selective oxidation catalysts in the industrial production of economically attractive redox reactions. These heterogeneous catalysts, mostly deposited on a porous support, have the advantage of mechanical strength and easy recovery and recycling, in comparison with their analogous homogeneous counterparts.

Catalytic oxidation of alkenes into more valuable epoxides as well as oxygen-containing carbonyl compounds is one of the important synthetic reactions. Carbonyl compounds have industrial significance and are widely used as solvents, perfumes, and flavoring agents or as intermediates in the manufacture of plastics, dyes, and pharmaceuticals.

As per our knowledge, only one report on the use of an oxovanadium complex with a pyrazolone ligand as a homogeneous catalyst is available.[16] Recently, the synthesis, characterization, and liquid-phase oxidation of styrene by a series of supported benzimidazole-based oxovanadium complexes have been reported by Maurya et al.[17] Thus, a literature survey shows that no reports on the catalytic aspects of supported oxovanadium complexes with pyrazolone ligands are available. In this article, we report the synthesis and characterization of an oxovanadium complex (VOL_2). The synthesized complex was heterogenized by supporting onto hydrous zirconia (ZrO_2). There are two reasons for selecting ZrO_2 as the support: (1) the available surface hydroxyl groups of ZrO_2 are able to undergo a chemical reaction or strong

Received: November 5, 2011
Published: December 21, 2011

   dx.doi.org/10.1021/ic202396q | Inorg. Chem. 2012, 51, 1152−1161

Chapter – 1

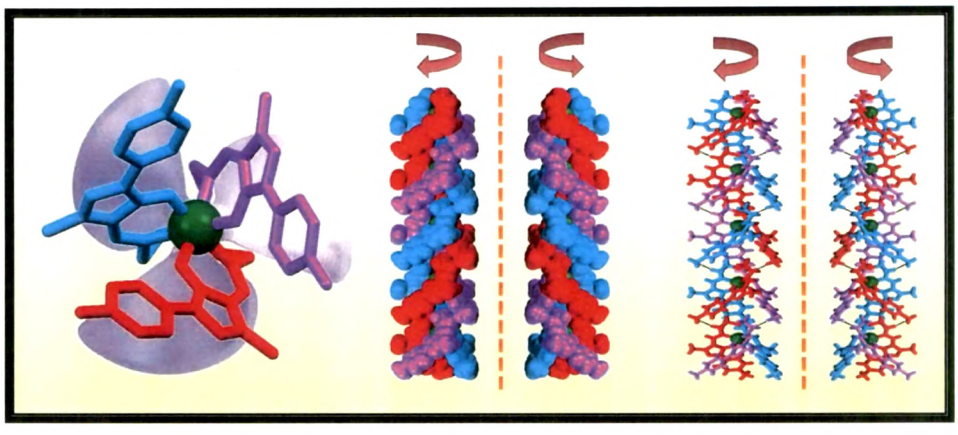

Part 3

Homogeneous catalysis using vanadium complexes of tripodal ligands

1.3.1 Introduction

Metallosupramolecular chemistry deals with the design of highly organized architectures, based upon metal-ion-directed self-assembly processes [1]. Two components are necessary in every synthetic approach leading to inorganic supramolecular architectures: the suitably designed organic ligand and the metal ion. In the language of supramolecular chemistry, the ligand is a programmed species, that is, a molecule with binding sites in a correct arrangement, whose encoded information is read by the metal ions according to their coordination algorithm [2].The synthesis of metallohelicates, by twisting multidentate organic ligands (helicands), through interaction with the appropriate metal ions, played a key role in the development of supramolecular chemistry [3].

The helix is one of the most significant structural motifs in nature due to its ubiquitous presence, from the molecular level to the astronomical scale [4]. Helicity shows important properties such as chirality and other geometric features which have attracted the attention of the scientific community [5]. The most prominent examples of natural helices are probably the double-helical B-DNA and the α-helical structure found in proteins which are responsible for the genetic information and diverse biological functions [6]. This fascinating natural motif has inspired the design and synthesis from unnatural backbones of a broad variety of artificial helices in the fields of supramolecular chemistry, asymmetric catalysis, biomimetics, etc [7]. Thus, the use of synthetic building blocks for the supramolecular assembling into helical polymers [8] has been successfully exploited in the past with metal-coordinated helical complexes [9] or self-assembled spiral nanoarchitectures from barbituric acid [10], among many others [11]. Aside from various types of polymeric organic materials, an increasing number of inorganic coordination compounds showing helical polymeric structures in the solid state have also been reported [12].

The key step for the design of helical coordination polymers is the choice of ligands. The ligands should be ditopic and thus capable of bridging metal atoms in certain directions and should also contain steric information that can be interpreted by the arrangement of the bound metal centers, resulting in the formation of helical structures [13].

Vanadium has long been an attractive transition metal for study due to its wide range of oxidation states (usually, +3, +4 and +5 oxidation states) and associated beautiful colors of its complexes [14]. Among these oxidation states, V(III) has traditionally been less studied than V(IV) or V(V), which have better defined biological/physiological and catalytic roles [15]. Vanadium complexes, including organometallic compounds, exist in a variety of configurations depending on their oxidation states and coordination numbers. Mononuclear coordination complexes of V(III) are generally six-coordinate, hydrolytically stable, and axially symmetric with an octahedral or pseudo-octahedral geometry. Helical vanadium complexes have been reported in neumerous literatures. Helical oxovanadium(IV) complexes of salen type Schiff base ligands were synthesized by Levy *et al* [16] and use as catalysts for the asymmetric oxidation of thioanisole with aqueous hydrogen peroxide (*see* Figure 1.3.1).

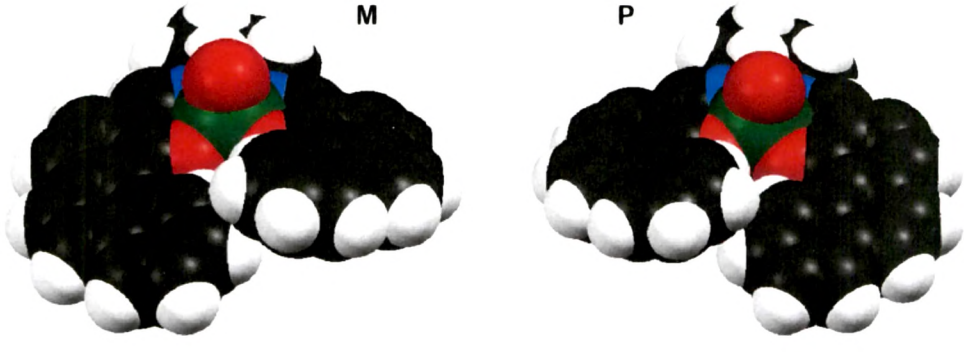

Figure 1.3.1. Space-filling plots (50 %) of the diastereomeric helical isomers of oxovanadium(IV) complex [16].

The mononuclear vanadium complexes containing 1,2-diols ligands were synthesized by the reaction of VCl_3 and $VOSO_4 \cdot 5H_2O$ with the corresponding ligands in presence of CH_3OH and CH_3CN (50:50 v/v) as a mixed solvent. The synthetsized complex was in non-chiral form but crystallizes in the chiral space group ($P6_522$), due to the symmetry elements of spiral axis (*see* Figure 1.3.2). Pharmaceutical screening of synthesized complexes were also carried out against A-549 (lung cancer), Bel-7402 (liver cancer) and HCT (colonic cancer) cell lines [17]. A series of bisimine-bridged dicatecol ligands were synthesized by Albrecht *et al* and used to prepare triple stranded helicate-type complexes with a length of upto more than 2 nm by simple mixing of ligands with the alkali metal carbonate and $VO(acac)_2$ in methanol [18].

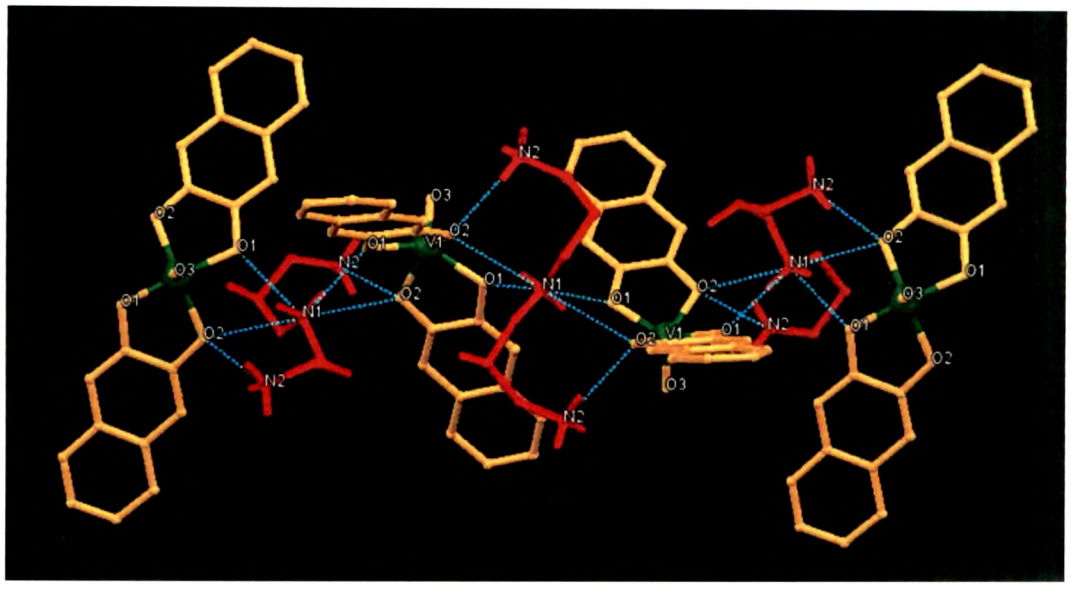

Figure 1.3.2. The helical chain intra-connected by hydrogen bonds. The cations $[1,3\text{-}H_2PDA]^{2+}$ connects anions $[VO(N\text{-}2,3\text{-}D)]^{2-}$ by hydrogen bonds [17].

Ligands with C_3 symmetry have been used extensively as building blocks in supramolecular coordination chemistry. However, very less attention was paid to the C_3 symmetric complexes of vanadium. Richards and co-workers synthesized vanadium(III) and vanadium(V) complexes of the tris(2-thiolatoethyl)amine ligand (L) containing hydrazine, hydrazide, imide, cyanide and isocyanide ligands [19]. The structures of synthesized C_3 symmetric complexes are depicted in the Figure 1.3.3.

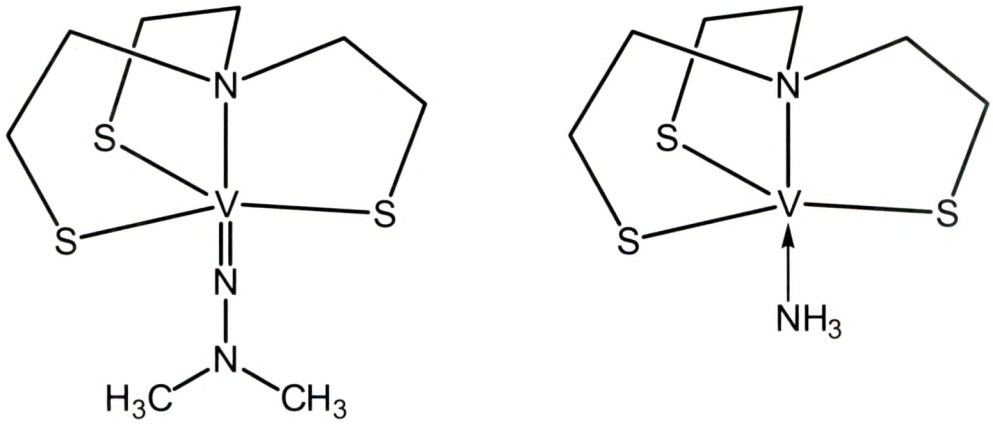

Figure 1.3.3. Structures of the complexes $[V(NNMe_2)L]$ and $[V(NH_3)L]$.

R. R. Schrock reported two vanadium complexes $[(Me_3SiNCH_2CH_2)_3N]VCl$ and $[(t\text{-}BuMe_2SiNCH_2CH_2)_3N]V$ synthesized by triamidoamine ligands [20]. The synthesized complexes exist in the C_3 symmetric environment (*see* Figure 1.3.4).

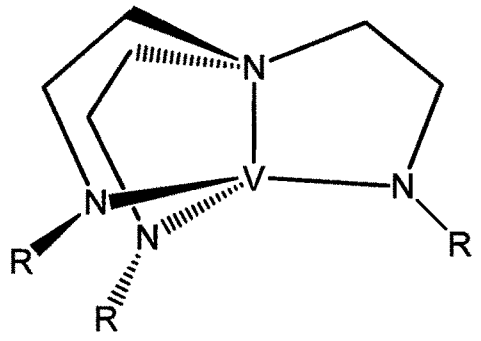

R = Me_3Si or t-$BuMe_3Si$

Figure 1.3.4. C_3 symmetric vanadium complex of triamidoamine ligands.

The C_3 symmetric vanadium(V) amine triphenolate complexes were synthesized, characterized and used as catalysts for the sulfoxidations at room temperature using hydrogen peroxide as the terminal oxidant [21]. The General structure of the complexes is shown in Figure 1.3.5.

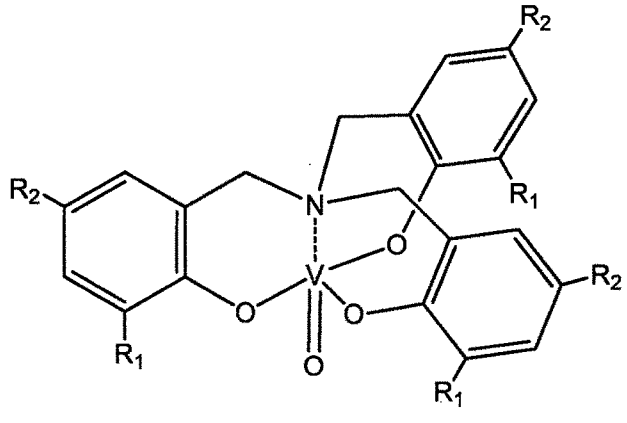

1. $R_1 = R_2 = Cl$
2. $R_1 = R_2 = Me$
3. $R_1 = R_2 = t$-Bu
4. $R_1 = R_2 = H$
5. $R_1 = Me$, $R_2 = H$
6. $R_1 = t$-Bu, $R_2 = H$

Figure 1.3.5. C_3 symmetric vanadium(V) amine triphenolate complexes (1-6).

High-valent V(IV) complexes of pyrazolones are an important structural motif that has been extensively studied due to their geometrical properties and catalytic applications. However, no attention was paid to the study of Low-valent V(III) complexes of pyrazolones [22-26]. Currently our group [24,26] in parallel with the others [23,25] have embarked on the studies of the oxovanadium(IV) complexes of pyrazolones and their catalytic applications towards the oxidation reactions. The present work has originated from our continued interest in this area.

In this part of the chapter **1**, we have focused our attention on synthesizing some new pyrazolone based tripodal ligands and their C_3 symmetric vanadium(II) complexes. The geometries of the synthesized ligands and vanadium(III) complexes were studied by the single-crystal XRD analysis along with the other spectral characterizations. The oxidation of benzyl alcohol in homogeneous rection condition was carried out by the synthesized complexes using H_2O_2 as an oxidant.

1.3.2. Exprimental

1.3.2.1. Materials and Physical measurments

All reagents and solvents were purchased from commercial sources and were further purified by the standard methods, if necessary [27]. Pyrazolone derivatives were obtained from Nutan Dye Chem. Sachin, Surat. Vanadyl sulfate, vanadyl acetylacetonate, acetonitrile, $POCl_3$, dry DMF, benzyl alcohol, hexane and 30% aqueous H_2O_2 were purchased from Merck and used as received. Tris(2-aminoethyl)amine was purchased from Sigma-Aldrich.

The synthesized ligands and their vanadium(III) complexes were characterized by ^1H & ^{13}C NMR, LC-MS, Single crystal XRD, FT-IR, elemental analysis, magnetic measurement and UV-Vis spectroscopy. ^1H and ^{13}C NMR spectra of ligands were recorded with Avance-III 400 MHz Bruker FT-NMR instrument. Elemental analyses of C, H, and N were determined using a Perkin Elmer series-II 2400 elemental analyzer. GC-MS analysis was carried out using gas chromatograph mass spectrometer (Agilent 5975 GC/MSD with 7890A GC system) having HP-5 capillary column of 60 m length and 250 μm diameter with a programmed oven temperature from 50 to 280 °C, at 1 mL min^{-1} flow rate of He as a carrier gas and ion source at 230 °C. Magnetic susceptibilities were measured using a PAR 155 vibrating sample

magnetometer fitted with a Walker Scientific L75FBAL magnet at Department of Chemistry, Jadavpur University, Kolkata. Single-crystal structures of L^1 and L^2 were determined using Bruker Smart Apex (CCD) diffractometer equipped with a graphite-monochromated Mo Kα radiation (λ = 0.71073). Crystallograpic data of complex [VL^1] were recorded on a Xcalibur, Eos, Gemini diffractometer equipped with a graphite-monochromated Cu Kα radiation (λ = 1.54184). FT-IR spectra of ligands and complexes were recorded as the KBr pellet on the Perkin Elmer Fourier transform (FT-IR) spectrum RX 1 spectrometer. Electronic spectra were recorded on a Perkin Elmer Lambda 35 UV-Vis spectrometer. LC-MS spectra were recorded on a Waters Micromass Q-Tof Micro instrument at SAIF, Panjab University, Chandigarh.

1.3.2.2. Synthesis of tripodal ligands

Synthesis of 3-methyl-5-oxo-1-(p-tolyl)-4,5-dihydro-1H-pyrazole-4-carbaldehyde (1*a*)

A mixture of 9.4 g. (0.05 mol.) of 3-methyl-1-tolyl-2-pyrazolin-5-one and 10 ml. of dry *N,N'*-dimethylformamide was cooled to 0 °C in a ice bath. Then, 5.5 ml (0.06 mol.) of phosphoryl chloride ms added dropwise at such a rate as to maintain the temperature between 5-15 °C. After the addition was complete, the reaction mixture was heated on the steam bath for 1.5 h. The mixture was then poured into 500 ml. of ice-water mixture. The resulting mixture was allowed to stand overnight at room temperature. The yellow solid product was collected by filtration, washed with water and dried to afford 1a. Yield of 8.3 g. (77%) ESI-MS: 216.14 $[M]^+$; ^{1}H NMR (400 MHz $CDCl_3$): δ 2.39 (*s*, 3H), 2.43 (*s*, 3H), 7.25 (*d*, J = 8.4 Hz, 2H), 7.65 (*d*, J = 8.4 Hz, 2H), 8.49 (*s*, 1H), 9.56 (*s*, 1H). ^{13}C NMR (400 MHz $CDCl_3$): δ 184.77, 158.37, 148.80, 136.93, 134.44, 129.68, 120.94, 105.52, 21.02, 12.32. Elem. anal. calcd for $C_{12}H_{12}N_2O_2$: C 66.65, H 5.59, N 12.96; found C 66.68, H 5.64, N 12.96.

Synthesis of 3-methyl-5-oxo-1-phenyl-4,5-dihydro-1H-pyrazole-4-carbaldehyde (1*b*)

Using a similar method to 1a, compound 1b was obtained with a Yield: 8.41 g. (83.3%) ESI-MS: 202.14 $[M]^+$; ^{1}H NMR(400 MHz $CDCl_3$): δ 2.44 (*s*, 3H), 7.28-7.34 (*m*, 1H), 7.45-7.49 (*m*, 2H), 7.79-7.82 (*m*, 2H), 9.07 (*s*, 1H), 9.99 (*s*, 1H). ^{13}C NMR (400 MHz $CDCl_3$): δ 12.38, 105.66, 120.89, 126.97, 129.17, 136.90, 148.99, 158.76,

184.57. Elem. anal. calcd for $C_{11}H_{10}N_2O_2$: C 65.34, H 4.98, N 13.85; found C 65.41, H 5.13, N 13.86.

Synthesis of 1-(5-hydroxy-3-methyl-1-phenyl-1H-pyrazol-4-yl)propan-1-one (2*a*)

Compound **2*a*** was synthesized by the procedure previously reported by us [24,28].

Synthesis of (5-hydroxy-3-methyl-1-(p-tolyl)-1H-pyrazol-4-yl)(phenyl)methanone (2*b*)

Compound **2*b*** was synthesized by the procedure previously reported by us [24,26].

Synthesis of tripodal ligand L^1

Aldehyde 1a (0.648 g, 3 mmol) and 40 ml dry methanol were added to a 3-neck 100 mL round-bottom flask equipped with a magnetic stirrer. The aldehyde was dissolved by heating the solution. A dropping funnel containing diluted Tris(2-aminoethyl)amine (0.142 mL, 1 mmol) with 10 mL of dry MeOH was fitted in to the 3-neck round-bottom flask. Tren solution was added dropwise allowing for complete dispersion of each drop between the additions with constant stirring under N_2 atmosphere. After all tren solution was added, the yellow solution was allowed to stir at reflux temperature for another 6 h. The light yellow compound precipitated was filtered, washed with methanol and dried under vacuum. The product was recrystallized in warm MeCN at RT. Yield 84%. ^{1}H NMR (400 MHz, $CDCl_3$): δ 1.96 (*s*, 3H), 2.33 (s, 3H), 2.89-2.92 (*t*, J = 5.2, 4.8 Hz, 2H), 3.56 (*s*, 2H), 7.15-7.17 (*d*, J = 8.4 Hz, 2H), 7.63-7.66 (*d*, J = 12 Hz, 1H), 7.83-7.85 (*d*, J = 8.4 Hz, 2H), 9.90 (*s*, 1H). ^{13}C NMR (400 MHz, $CDCl_3$): δ 12.28, 20.96, 48.72, 56.57, 100.44, 118.98, 129.22, 133.76, 136.62, 148.05, 152.28, 165.46. Elem. anal. calcd. for $C_{42}H_{48}N_{10}O_3$: C 68.09, H 6.53, N 18.91; found C 68.12, H 6.56, N 18.92. ESI-MS: *m/z* $[M]^+$ 740.39; found 741.41 $[M+H]^+$, 742.46 $[M+2H]^+$, 763.41 $[M+Na]^+$, 779.41 $[M+K]^+$.

Synthesis of tripodal ligand L^2

Tripodal ligand L^2 was synthesized by the procedure similar to L^1. Yield 81%. ^{1}H NMR (400 MHz, $CDCl_3$): δ 1.97 (s, 1H), 2.85-2.88 (*t*, J = 5 Hz, 2H), 3.52 (*s*, 2H), 7.09-7.13 (*m*, 1H), 7.33-7.37 (*m*, 2H), 7.65-7.67 (*d*, J = 10.4 Hz, 1H), 7.96-7.98 (*d*, J =

8 Hz, 2H), 9.88 (*s*, 1H). ^{13}C NMR (400 MHz, $CDCl_3$): δ 12.80, 47.99, 54.72, 99.20, 117.66, 123.57, 129.01, 140.02, 153.91, 165.43. Elem. anal. calcd. for $C_{39}H_{42}N_{10}O_3$: C 67.03, H 6.06, N 20.04; found C 67.08, H 6.09, N 67.08. ESI-MS: m/z $[M]^+$ 698.34; found 699.31 $[M+H]^+$, 700.46 $[M+2H]^+$, 721.42 $[M+Na]^+$, 737.32 $[M+K]^+$.

Synthesis of tripodal ligand L^3

Compound **2** (0.876 g, 3 mmol) and 40 ml dry toluene were added to a 3-neck 100 mL round-bottom flask equipped with a magnetic stirrer. The compound was dissolved by heating the solution. A dropping funnel containing diluted Tris(2-aminoethyl)amine (0.142 mL, 1 mmol) with 10 mL of dry toluene was fitted in to the 3-neck round-bottom flask. Tren solution was added dropwise allowing for complete dispersion of each drop between the additions with constant stirring under N_2 atmosphere. After all tren solution was added, the yellow solution was allowed to stir at reflux temperature for another 6 h. The mixture was coolded and kept over night. The light yellow compound precipitated was filtered, washed with toluene and than methanol and dried under vacuum. The product was recrystallized in warm MeCN at RT. Yield 0.716 (74%). ^{1}H NMR (400 MHz, $CDCl_3$): *δ* 1.14-1.18 (*t*, J = 7.6 Hz, 3H), 2.18 (*s*, 3H), 2.57-2.63 (*q*, J = 7.6 Hz, 2H), 2.96-2.99 (*t*, 2H), 3.63-3.67 (*q*, J = 11.2 Hz, 2H), 7.12-7.16 (*t*, J = 7.6 Hz, 1H), 7.36-7.40 (*t*, 2H), 7.99-8.02 (*dd*, 2H), 11.46-11.49 (*t*, J = 4.8 Hz, 1H). ^{13}C NMR (400 MHz, $CDCl_3$): *δ* 12.28, 16.61, 22.17, 41.78, 54.81, 97.70, 118.97, 124.10, 128.67, 139.27, 146.75, 166.06, 170.46. Elem. anal. calcd. for $C_{45}H_{54}N_{10}O_3$: C 69.03, H 6.95, N 17.89; found C 69.06, H 6.98, N 17.89. LC-MS: *m/z* $[M]^+$ 782.44; found $[M+H]^+$ 783.41, $[M+2H]^+$ 784.5, $[M+Na]^+$ 805.41, $[M+K]^+$ 821.41.

Synthesis of tripodal ligand L^4

Tripodal ligand L^4 was synthesized by the procedure similar to L^3. Yield 0.627 g (76%). ^{1}H NMR (400 MHz, $CDCl_3$): *δ* 1.21 (*s*, 3H), 2.34 (*s*, 3H), 2.57-2.60 (*t*, J = 6 Hz, 2H), 3.18-3.22 (*q*, J = 11.2 Hz, 2H), 7.17-7.20 (*t*, 2H), 7.38-7.40 (*m*, 2H), 7.43-7.53 (*m*, 3H), 7.83-7.85 (*d*, J = 8.4 Hz, 2H), 11.22 (*s*, 1H). ^{13}C NMR (400 MHz, $CDCl_3$): *δ* 15.20, 21.00, 42.29, 53.70, 99.63, 119.38, 125.31, 127.60, 128.24, 128.82, 129.06, 130.24, 131.41, 133.52, 136.71, 147.55, 165.27, 165.54. Elem. anal. calcd. for $C_{60}H_{60}N_{10}O_3$: C 74.36, H 6.24, N 14.45; found C 74.42, H 6.30, N 14.47. LC-MS: *m/z*

$[M]^+$ 968.48; found $[M+H]^+$ 969.51, $[M+2H]^+$ 970.63, $[M+Na]^+$ 991.64, $[M+K]^+$ 1007.65.

1.3.2.3. Synthesis of V(III) complexes of tripodal ligands

Synthesis of complex [V(L^1)]

To a well stirred hot ethanolic solution of tripodal ligand L^1 (0.740 g, 1 mmol), an ethanolic solution of VOSO4·5H2O (0.253 g, 1 mmol) was added drop wise. An ethanolic solution of NaOH (0.20 g in 10 mL) was added drop wise to the reaction mixture till green precipitates of complex were observed (pH = 8-9). The reaction was further stirred on reflux temperature for 1 h. The precipitates were filtered, washed with hot distilled and then ethanol, and dried under a vacuum. The obtained complex was designated as [VL^1]. Yield 421.7 g (53.5%). Elem. anal. calcd. for $C_{42}H_{45}N_{10}O_3V$: C 63.95, 5.75, 17.76; found C 64.26, H 5.72, N 17.46. LC-MS: m/z 788.13 $[M]^+$, 789.41 $[M+H]^+$, 811.44 $[M+Na]^+$, 827.41 $[M+K]^+$.

Synthesis of complex [V(L^2)]

To a well stirred hot ethanolic solution of tripodal ligand L^2 (0.698 g, 1 mmol), an ethanolic solution of vanadyl acetylacetonate (0.256 g, 1 mmol) was added drop wise. An ethanolic solution of NaOH (0.20 g in 10 mL) was added drop wise to the reaction mixture till green precipitates of complex observed (pH = 8-9). The reaction was further stirred on reflux temperature for 1 h. The precipitates were filtered, washed with hot distilled and then ethanol, and dried under a vacuum. The obtained complex was designated as [VL^2]. Yield 0.343 g (46%). Elem anal. calcd. for $C_{39}H_{39}N_{10}O_3V$: C 62.73, 5.26, 18.76; found C 62.53, H 5.58, N 18.18. LC-MS: m/z 746.45 $[M]^+$, 747.42 $[M+H]^+$, 769.48 $[M+Na]^+$, 785.48 $[M+K]^+$.

1.3.2.4. Crystallography

The ligands (L^1 or L^2)were dissolved in acetonitrile and heated till the solution become clear and then it was allowed to crystallize at RT. Light yellow crystals of single crystal X-ray diffraction quality were obtained within a week. The crystals of L^1 and L^2 used for data collection were of dimension 0.3 × 0.2 × 0.2 mm^3 and 0.24 × 0.11 × 0.04 mm^3, respectively. The cell dimensions of L^1 were determined by least-square fit of angular settings of 14834 reflections in the θ range 3.51 to 29.05°. The

intensities were measured by ø and ω scan mode for θ ranges 3.52 to 26.00°. 3811 reflections were treated as observed (I > 2σ(I)). The cell dimensions of L^2 were determined by least-square fit of angular settings of 5476 reflections in the θ range 2.51 to 27.62 °. The intensities were measured by ø and ω scan mode for θ ranges 1.49 to 25.00°. 4853 reflections were treated as observed (I > 2σ(I)).

Single crystal of the complex [VL^1] were grown in N,N'-dimethylformamide (DMF) at 35 °C. Green crystals of [VL^1] were obtained in 15 to 20 days. The crystal used for data collection was of dimensions 0.30 × 0.20 × 0.20 mm^3. The cell dimensions were determined by least-squares fit of angular settings of 4383 reflections in the θ range 4.34 to 71.49 °. The intensities were measured by ø and ω scan mode for θ ranges 3.27 to 64.87 °. 2413 reflections were treated as observed (I > 2σ(I)).

Data were corrected for Lorentz, polarization and absorption factors. The structure was solved by direct methods using *SHELXS97* [29]. All non-hydrogen atoms of the molecule were located in the best E-map. Full-matrix least-squares refinement was carried out using *SHELXL97* [29]. All hydrogen atoms were included as idealized atoms riding on the respective carbon atoms with C-H bond lengths appropriate to the carbon atom hybridization. H atoms are shown as small spheres of arbitrary radii. The geometry of the molecules were calculated using the *WinGX* [30] and *PARST* [31] software.

1.3.2.5. Catalytic reaction

Catalytic oxidation of benzyl alcohol was carried out in a 50 mL round bottom flask fitted with a water circulated condenser using oxovanadium(IV) complexes [$V(L^1)_2$] and [$V(L^2)_2$] of tripodal ligands as a catalyst. In a typical reaction, benzyl alcohol, catalyst and 30% H_2O_2 were intensively stirred at the 90 °C temperature for the whole duration of the reaction. After completion of the reaction, reaction mixture was concentrated on rotary evaporator. Hexane was added to the system, and the organic phase was separated. By this simple procedure, isolation of the carbonyl product in the organic phase was achieved.

1.3.3. Results and Discussion

1.3.3.1. Synthesis and characterization of tripodal ligands (1-4)

Compounds 1*a* and 1*b* were synthesized by the Vilsmeyer formylation of pyrazolone derivatives 3-methyl-1-tolyl-2-pyrazolin-5-one and 3-methyl-1-phenyl-2-pyrazolin-5-one, respectively, using $POCl_3$ and dry DMF. Formylation occurs at C-4 position of the pyrazole ring. Tripodal ligands L^1 and L^2 were synthesized by refluxing a 1:3 ratio of tris(2-aminoethyl)amine and corresponding 4-formyl pyrazolones (1*a* and 1*b*) in dry methanol in N_2. The syntheses of tripodal ligands L^1 and L^2 is depicted in the Scheme 1.3.1. All the compounds were characterized by ^1H & ^{13}C NMR, LC-MS and elemental analyses.

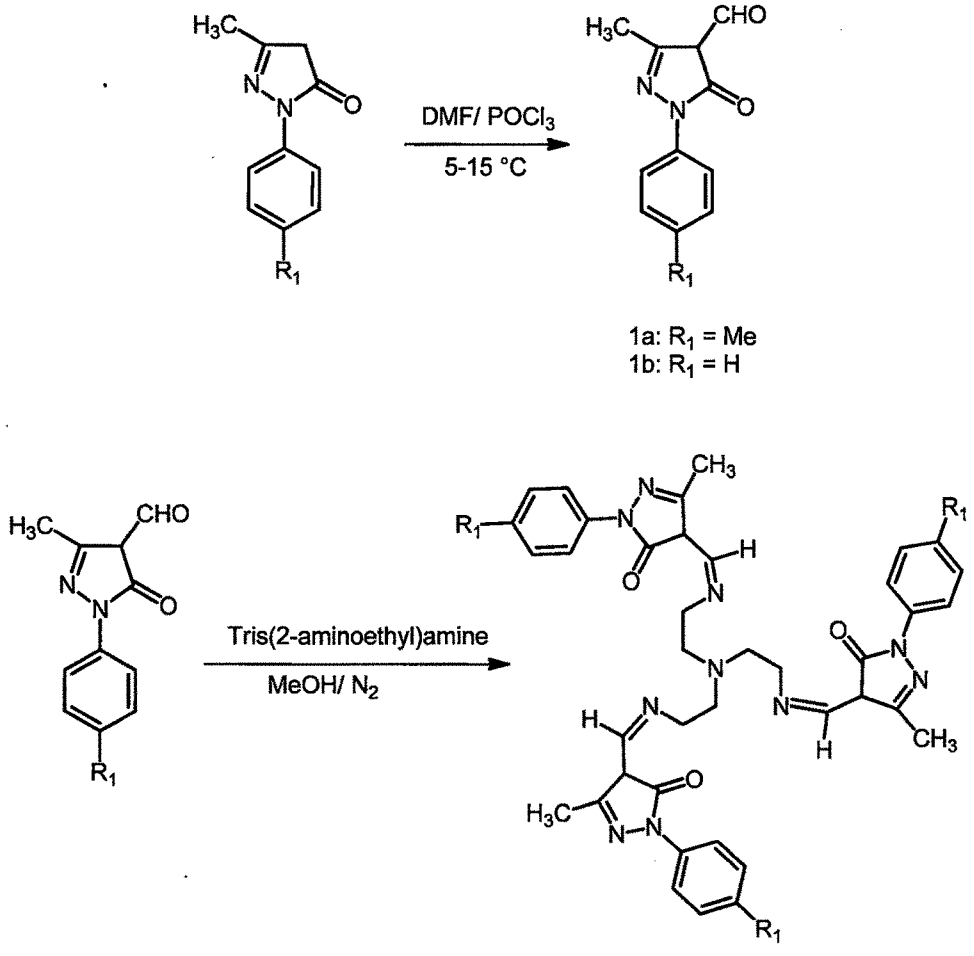

Scheme 1.3.1. Syntheses of tripodal ligands L^1 and L^2.

Tripodal ligands L^3 and L^4 were synthesized by refuxing the compounds 2*a* and 2*b* with tris(2-aminoethyl)amine in dry toluene. Tris(2-aminoethyl)amine and the

corresponding 4-acylpyrazolones were mixed in a 1:3 ratio. After completion, the reaction mixture was kept over night to obtained light yellow crystalline tripodal Schiff base ligands of pyrazolones. Tripodal ligands L^3 and L^4 were also characterized by the various spectroscopic and analytical techniques. The syntheses of ligands L^3 and L^4 is depicted in the Scheme 1.3.2.

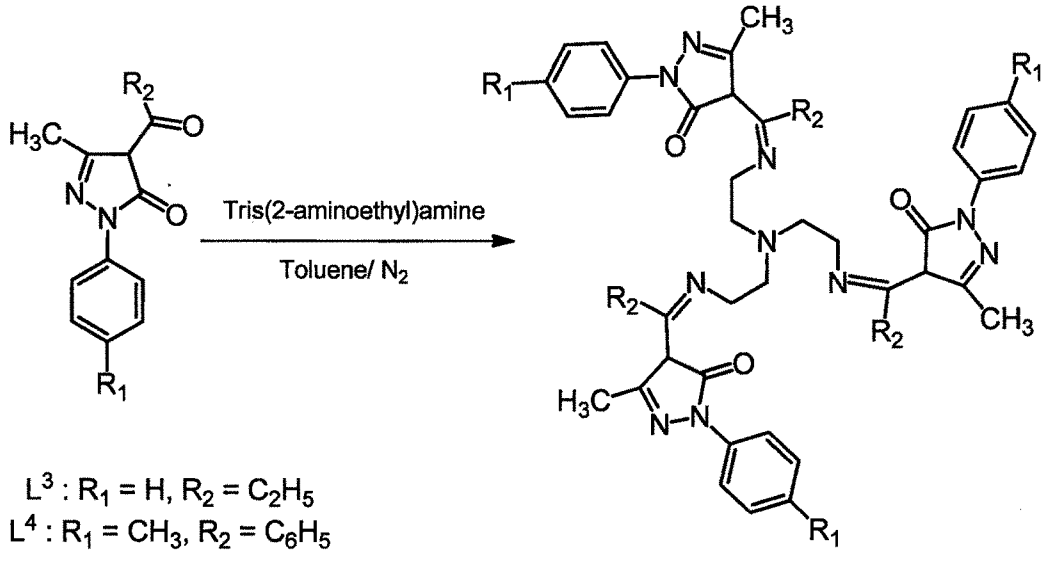

Scheme 1.3.2. Synthesis of the tripodal ligands L^3 and L^4.

NMR spectral characterization of the tripodal ligands (L^1-L^4)

^1H & ^{13}C NMR spectra of all the ligands were in good agreement with the proposed structures of the tripodal ligands. ^1H NMR spectra of the ligand L^1 shows two peaks at 1.96 (3H) and 2.33 (3H) δ, which confirm the presence of two methyl groups of pyrazolone ring, one at the C3 carbon and other one at the phenyl ring attached to N1 nitrogen of pyrazolone ring, respectively. The two peaks at 2.89 (2H) and 3.56 (2H) δ confirm the presence of two -CH_2- groups in the tripodal ligand L^1. The appearance of two doublets at 7.15 (2H) and 7.83 (2H) δ confirm the presence of toluoyl ring at N1 nitrogen of pyrazolone ring. One doublet at 7.63 (1H) δ is due to the presence of one hydrogen atom at the C4 carbon of the pyrazolone ring. The singlet appear at the 9.90 δ is due to the imine proton present in the tripodal ligand L^1. The ^1H NMR spectra of the tripodal ligand L^1 is shown in the Figure 1.3.6. The ^{13}C NMR spectrum show peaks at 12.28 and 20.96 δ, which confirm the presence of two methyl groups in the L^1. The peaks at 48.72 and 56.57 are due to the presence of two -CH_2- carbons. The peak at 100.44 δ is due to the C3 carbon of the pyrazolone ring. ^1H

and ^{13}C spectra are in good agreement with the proposed structure of the of the tripodal ligand L^1. The ^{13}C NMR spectrum of the tripodal ligand is shown in the Figure 1.3.7.

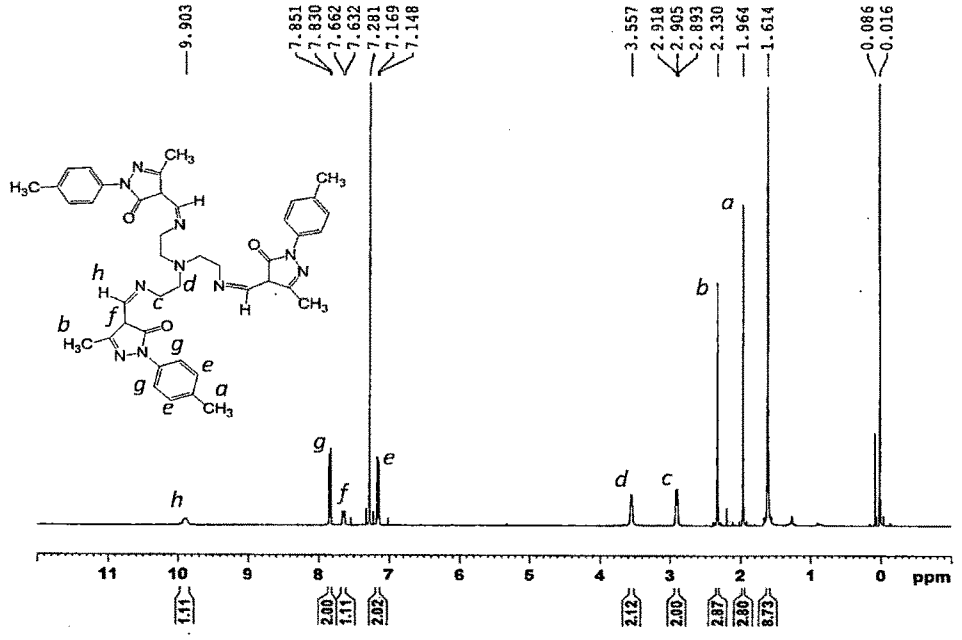

Figure 1.3.6. ^1H NMR spectrum of the tripodal ligand L^1.

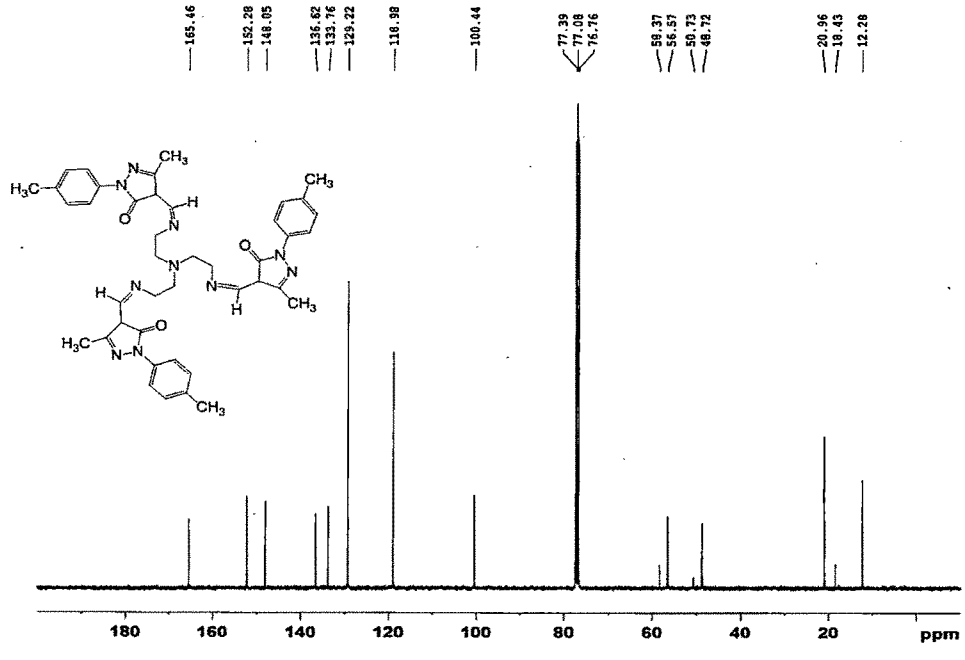

Figure 1.3.7. ^{13}C NMR spectrum of the tripodal ligand L^1.

The ^{1}H NMR spectrum of the ligand L^2 shows a singlet at the 1.97 δ, which confirm the presence of one methyl group at the C3 carbon of pyrazolone ring. The peaks at 2.85 and 3.54 δ are due to the presence of two -CH_2- groups in the tripodal ligand L^2. The appearance of two multiplets at 7.10 (1H) & 7.33 (2H) δ, and one doublet at 7.96 (2H) δ are due to the five protons of the phenyl ring attached to the N1 nitrogen of pyrazolone ring. One doublet at 7.65 (1H) δ is due to the presence of one hydrogen atom at the C4 carbon of the pyrazolone ring. The imine proton present in the tripodal ligand L^2 shows a singlet at the 9.88 δ. The ^{13}C NMR spectrum show peaks at 12. 80, 47.99 and 54.72 δ, which are assigned to the methyl carbon and two -CH_2- carbons present in the ligand L^2. The peaks at 99.20 & 165.43 δ are assigned to the C3 carbon of the pyrazolone ring and imine carbon, respectively. The ^{1}H NMR spectra of the ligand L^3 shows one triplet (1.14 δ, 3H) and one quarteret (2.57 δ, 2H) due to the presence of five protons of CH_3CH_2- group. The singlet appear at 2.18 (1H) δ is due to the presence of one methyl group at the C3 carbon of the pyrazolone ring. The appearance of the three peaks in the aromatic region from 7.12-8.02 δ are due to the five protons of the phenyl ring attached to the N1 nitrogen of the pyrazolone ring. The ^{13}C NMR spectrum shows peaks at 12.28 and 16.61 δ for the two methyl carbons of the ligand L^3. The peaks at 22.17, 41.78 and 54.81 δ are due to the presence of three carbons of three -CH_2- groups. The appearance of the peaks at 97.70 and 170.46 δ are due to the C3 carbon of the pyrazolone ring and imine carbon, respectively. The ^{1}H NMR spectra of the tripodal ligand L^4 shows two singlets at 1.21 (3H) and 2.34 (3H) δ, which confirm the presence of two methyl groups in the ligand. The peaks at 2.57 (2H) and 3.18 (2H) δ are due to the four protons of two -CH_2- groups. The peaks in the aromatic region from 7.17 to 7.85 (9H) δ are due to the presence of one phenyl and one toluoyl ring in the ligand L^4. The singlet for imine proton appear at the 11.22 (1H) δ. The ^{13}C NMR spectrum of the ligand L^4 shows peaks at 15.20 and 21.00 δ for the two methyl carbons. The peaks at 42.29 and 53.70 δ are assigned to the two carbons of two -CH_2- groups. The peaks at 99.63 and 165.54 δ are due to the C3 carbon of the pyrazolone ring and imine carbon, respectively. All the NMR spectra are in good agreement with the proposed structures of tripodal ligands (L^1-L^4).

Mass spectral analysis of the tripodal ligands (L^1-L^4)

LC-MS analyses of all tripodal ligands were carried out and their structures were confirmed by matching the calculated mass of the ligands with the molecular ion

peaks appeared in the spectra. LC-MS of the tripodal ligand L^1 is depicted in the Figure 1.3.8. LC-MS data of all the ligands are presented in the Table 1.3.1.

Table 1.3.1. LC-MS spectral data of tripodal ligands.

Tripodal Ligands	Mass found (calculated mass)
L^1	*m/z*: 741.41 $[M+H]^+$ (740.39 $[M]^+$)
L^2	*m/z*: 699.31 $[M+H]^+$ (698.34 $[M]^+$)
L^3	*m/z*: 783.41 $[M+H]^+$ (782.44 $[M]^+$)
L^4	*m/z*: 969.51 $[M+H]^+$ (968.48 $[M]^+$)

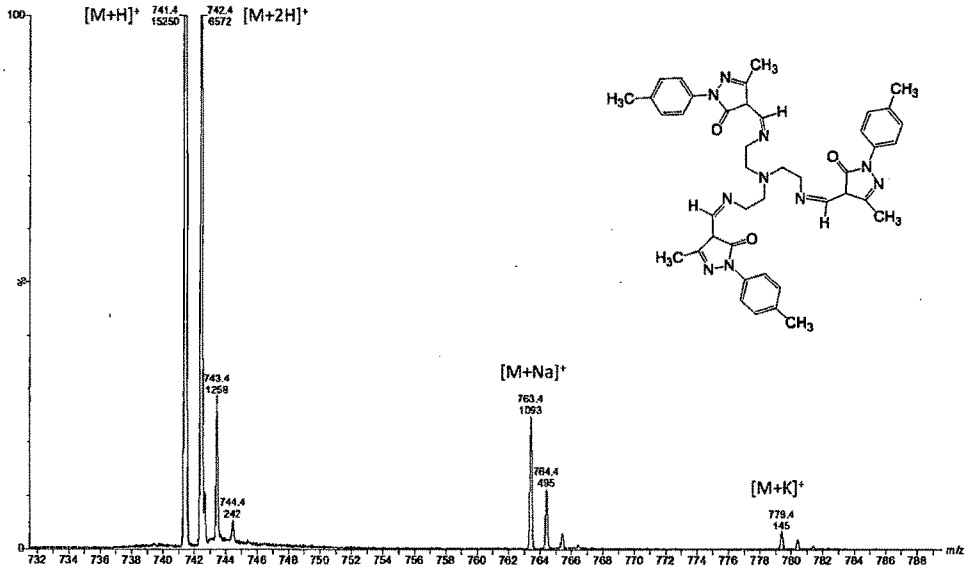

Figure 1.3.8. LC-MS of the tripodal ligand L^1.

Crystal structure

Light yellow block shaped crystals of L^1 suitable for X-ray diffraction analysis were obtained by the slow evaporation of L^1 in acetonitrile. The crystal structure was solved by single crystal XRD in the space group *P*-1 of triclinic system and refined to give the empirical formula $C_{42}H_{48}N_{10}O_3$. X-ray intensity data of 14834 were collected of which 7623 were unique. The light yellow crystals of L^2 suitable for single crystal

XRD were grown in acetonitrile at room temperature. The crystal was solved in the space group *P*-1 of triclinic system and refined to give the empirical formula $C_{39}H_{42}N_{10}O_3$. X-ray intensity data of 6611 were collected of which 5476 were unique. The ORTEP view of the ligands $L^1$and L^2 are depicted in the Figure 1.3.9. The molecular structures reveal that the tripodal ligands exist in an imine-one form in the solid state and forms three intramolecular hydrogen bonds. The crystallographic data for tripodal ligands L^1 and L^2 were summarized in Table 1.3.2.

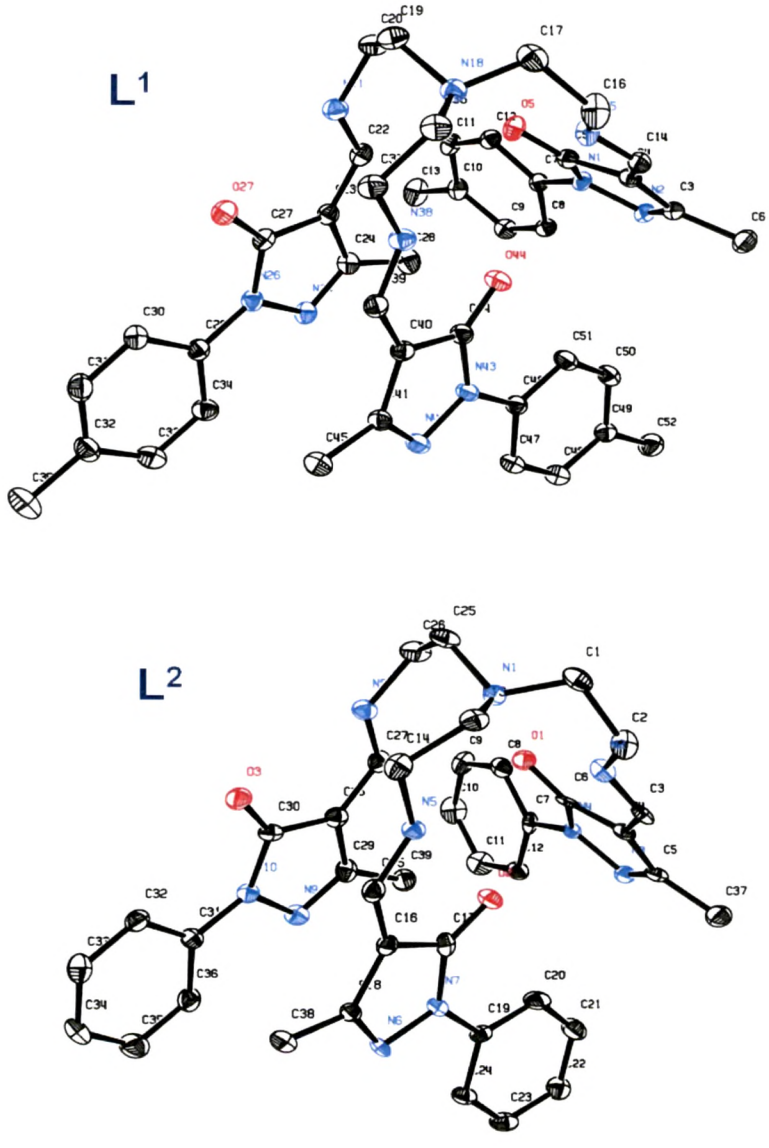

Figure 1.3.9. Molecular structures of tripodal ligands L^1 and L^2. H atoms were omitted for clarity.

Table 1.3.2. Summary of crystallographic data for the ligands L^1 and L^2.

	L^1	L^2
Empirical formula	$C_{42}H_{48}N_{10}O_3$	$C_{39}H_{42}N_{10}O_3$
Crystal system	Triclinic	Triclinic
Space group	*P*-1	*P*-1
a (Å)	10.5266(5)	10.5310(11)
b (Å)	13.6775(7)	12.2330(12)
c (Å)	14.9717(6)	14.8664(15)
α (°)	65.299(4)	113.201(2)
β (°)	89.444(5)	91.722(2)
γ (°)	84.799(5)	92.732(2)
V(Å^3)	1949.35(16)	1755.8(3)
Z	2	2
$\rho_{calcd.}$(g cm^{-3})	1.262	1.316
F(000)	788	734
Index ranges	$-12 \le h \le 12$, $-16 \le k \le 16$, $-17 \le l \le 18$	$-6 \le h \le 12$, $-14 \le k \le 14$, $-17 \le l \le 16$
Radiation	MoKα (λ = 0.71073)	MoKα (λ = 0.71073)
μ(mm^{-1})	0.083	0.087
Reflections collected	14834	6611
Final *R*	0.0595	0.1013
wR	0.1335	0.2651
Goodness-of-fit	1.006	1.147
Residual electron density (eÅ^{-3})	$-0.151 < \Delta\rho < 0.152$	$-0.365 < \Delta\rho < 0.478$
CCDC	869325	994250

Selected bond lengths and bond angles of the tripodal ligands L^1 and L^2 were presented in the Table 1.3.3 and Table 1.3.4.

Table 1.3.3. Selected bond lenths of tripodal ligands L^1 and L^2.

Bond lengths	L^1	L^2
O1-C6	1.245(3)	1.243(6)
O2-C17	1.241(3)	1.234(6)
O3-C30	1.250(3)	1.256(6)
N1-C1	1.454(3)	1.463(6)
N1-C13	1.466(3)	1.469(6)
N1-C25	1.466(3)	1.450(6)
N2-C2	1.454(3)	1.460(7)
N2-C3	1.307(3)	1.323(6)
N3-N4	1.407(2)	1.410(5)
N5-C14	1.450(3)	1.454(7)
N5-C15	1.320(3)	1.328(6)
N6-N7	1.408(3)	1.406(5)
N8-C26	1.453(3)	1.468(7)
N8-C27	1.320(3)	1.315(7)
N9-N10	1.410(3)	1.421(5)
C1-C2	1.496(3)	1.507(8)
C3-C4	1.373(3)	1.386(7)
C13-C14	1.508(4)	1.519(7)
C15-C16	1.374(3)	1.366(7)
C25-C26	1.512(3)	1.515(7)
C27-C28	1.370(3)	1.385(7)
C4-C6	1.439(3)	1.444(7)
C16-C17	1.435(4)	1.452(7)
C28-C30	1.428(4)	1.436(7)

Table 1.3.4. Selected bond angles of tripodal ligands L^1 and L^2.

Bond angles	L^1	L^2
C1-N1-C13	111.4(2)	111.7(4)
C13-N1-C25	112.4(2)	112.6(4)
C25-N1-C1	112.1(2)	113.9(4)
N1-C1-C2	113.5(2)	112.5(4)
N1-C13-C14	111.6(2)	111.2(4)
N1-C25-C26	112.2(2)	113.8(4)
C2-N2-C3	125.1(3)	123.7(4)
C14-N5-C15	123.8(3)	123.3(4)
C26-N8-C27	124.8(3)	122.6(4)
C4-C6-O1	129.4(2)	130.5(4)
C16-C17-O2	129.5(3)	129.0(5)
C28-C30-O3	129.1(3)	128.6(4)
N4-C6-O1	126.6(2)	126.4(4)
N4-C17-O2	126.7(3)	127.2(4)
N10-C30-O3	126.4(3)	126.4(4)
C3-C4-C6	122.4(2)	122.6(4)
C15-C16-C17	124.3(3)	124.4(5)
C27-C28-C30	124.7(2)	125.9(5)
N4-C6-C4	104.0(2)	103.1(4)
N7-C17-C16	103.7(2)	103.8(4)
N10-C30-C28	104.5(2)	104.9(4)

Crystal packing of the tripodal ligands L^1 and L^2 show alternate arrangement of the *lambda*- and *delta*- isomers of the ligands L^1 and L^2 (*see* Figure 1.3.10).

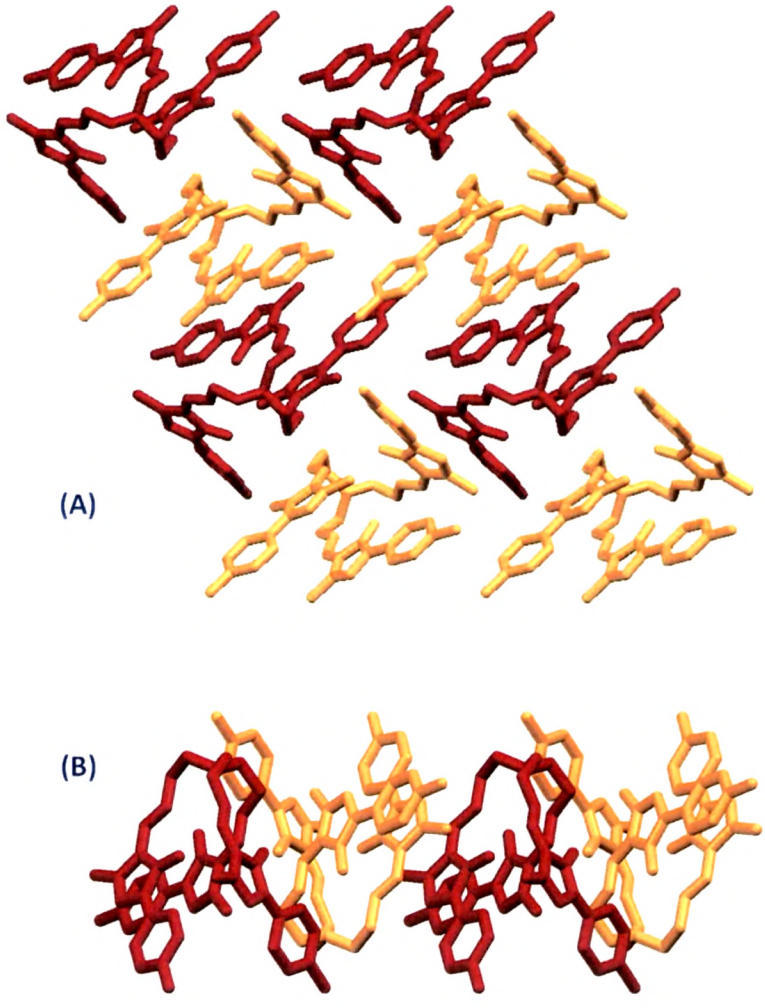

Figure 1.3.10. Crystal packing of the tripodal ligand L^1 (A) view down the *a*-axis and (B) view down the *b*-axis.

1.3.3.2. Synthesis and characterization of vanadium(III) complexes [VL^1] and [VL^2]

Vanadium(III) complexes of tripodal ligands L^1 and L^2 were synthesized by refluxing equimolar amount of tripodal ligand (L^1/ L^2) and $VOSO_4 \cdot 5H_2O$/ $VO(acac)_2$ in the presence of NaOH and ethanol as a solvent. During the reaction ligand losses its proton and oxovanadium(IV) get reduced to vanadium(III), thus afforded green V(III) complexes in 1:1 ratio of ligand to metal (*see* Scheme 1.3.3). This complex is remarkable because of the following: (**1**) this is the first report on the C_3 symmetric

propeller-shaped V(III) complexes of pyrazolones. (**2**) V(III) complexes were synthesized by the *in situ* reduction of VO(IV) into V(III) (**3**) crystal structure of [VL^1] was obtained and revealed that three helical chains interlink one another to form rare triple-stranded helicate.

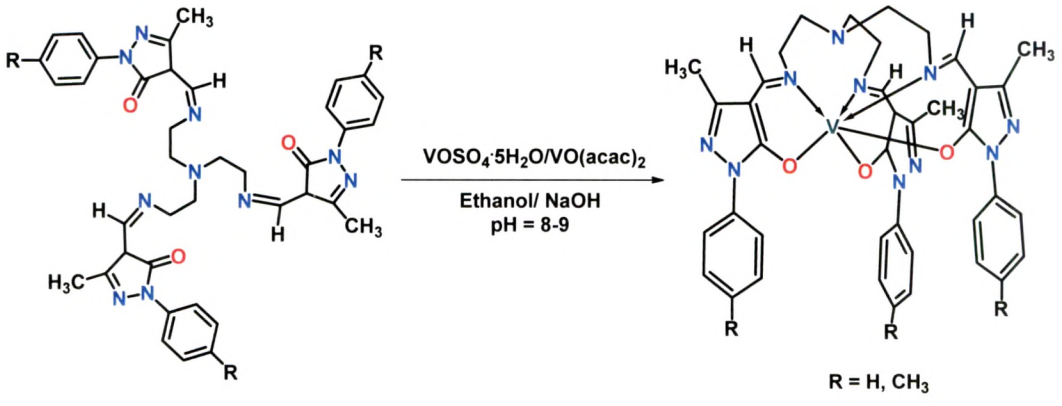

Scheme 1.3.3. Synthetic procedure for [VL^1] and [VL^2].

The complexes are stable to air and moisture, without any kind of decomposition also after several months. The complexes are in soluble in water and other common organic solvents, but soluble in DMF and DMSO. The synthesized V(III) complexes were characterized by various spectroscopic and anlalytical techniques along with the single crystal X-ray analysis. Elemental analyses of C, H and N agreed well with the calculated C, H and N in the complexes [VL^1] and [VL^2]. The purity of the complexes was also checked by the TLC.

LC-MS spectral analysis of the complexes [VL^1] and [VL^2] agreed well with the proposed structures. The mass spectrum of the complex [VL^1] shows molecular ion peak $C_{42}H_{45}N_{10}O_3$ at *m/z* = 788.13 $[M]^+$, which indicate that it is a mononuclear complex having one tripodal ligand L^1 (*see* Figure 1.3.11). The peaks at *m/z* = 789.41, 811.44 and 827.41 were attributed to the $[M+H]^+$, $[M+Na]^+$ and $[M+K]^+$, respectively. Mass fragments also show the peak for the ligand L^1 at *m/z* = 741.52 $[L^1+H]^+$. LC-MS of the complex [VL^2] shows molecular ion peak $C_{39}H_{39}N_{10}O_3$ at *m/z* = 746.45 $[M]^+$, which indicate that it is a mononuclear complex having one tripodal ligand L^2 (*see* Figure 1.3.12). The peaks at *m/z* = 747.42, 769.48 and 785.48 were attributed to the $[M+H]^+$, $[M+Na]^+$ and $[M+K]^+$, respectively. The

peak for the ligand L^2 also appear at *m/z* = 721.58 $[L^1+Na]^+$. Fragmentation of weakly coordinated solvent molecule in LC-MS is not observed.

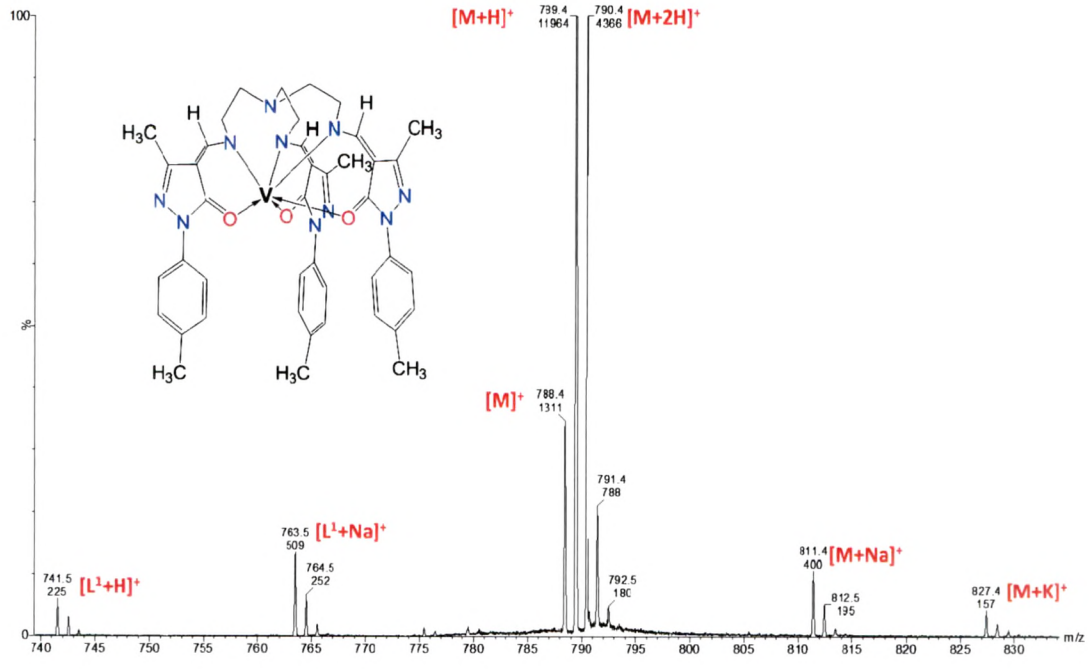

Figure 1.3.11. LC-MS of the complex $[VL^1]$.

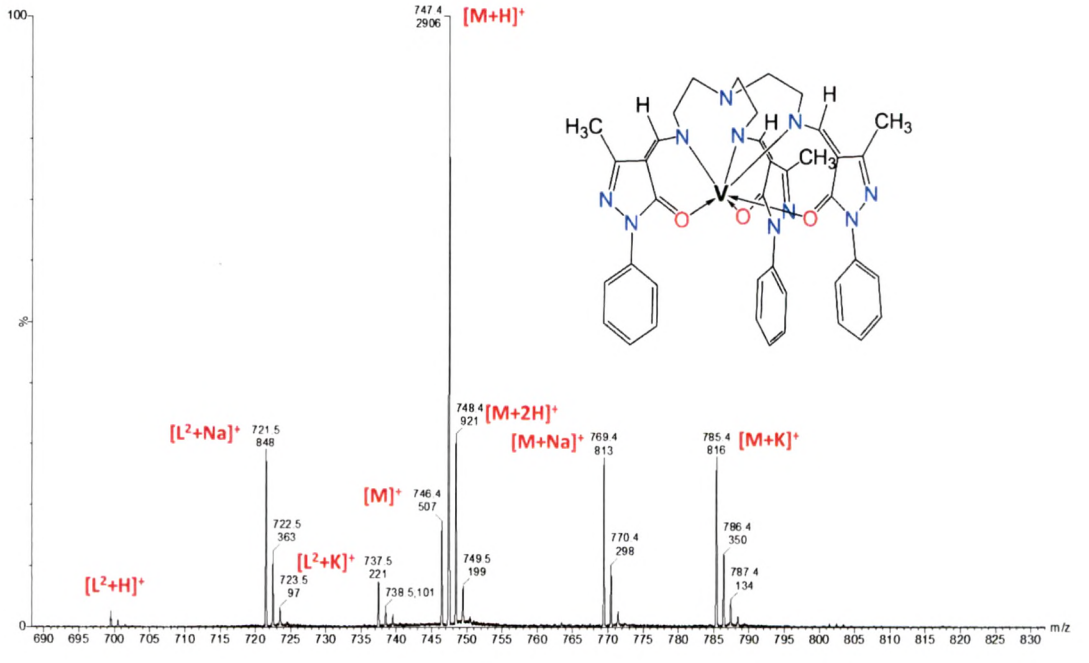

Figure 1.3.12. LC-MS of the complex $[VL^2]$.

Green hexagonal rode shape crystals of [VL^1] suitable for single crystal X-ray diffraction analysis were grown in dimethylformamide (DMF). The complex was dissolved in DMF by heating to get a clear solution then it was allowed to crystallized at 35 °C. Green hexagonal rode shape crystals of complex were obtained in 15-20 days. The molecular structure of the complex [VL^1] was solved by single crystal XRD in space group *P*-3 of the trigonal system with one pyrazolone moiety in asymmetric unit and refined to give the formula [VL^1](Me_3N). Data collection parameters and refinement results of the complex [VL^1] are summarized in Table 1.3.5.

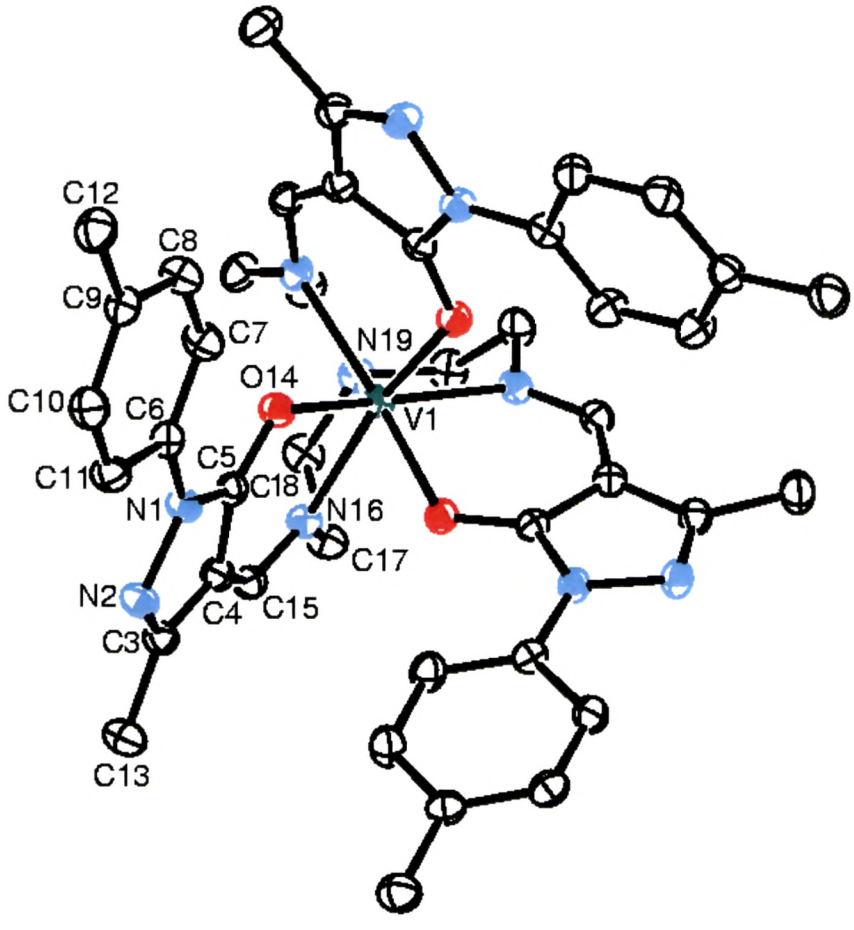

Figure 1.3.13. *ORTEP* view of the complex [VL^1] with displacement ellipsoids drawn at 50% probability level. H atoms and solvent molecule were omitted for clarity.

An ORTEP view of the complex is depicted in the Figure 1.3.13. The ligand L^1 is coordinated with the vanadium as a hexadentate N_3O_3-donar creating an octahedral geometry around the metal ion with the three six-mambered chelate rings. The coordination around the vanadium is distorted from ideal octahedral geometry.

Table 1.3.5. Crystal structure data and structure refinement details for [VL^1].

	[VL^1]
Empirical formula	$C_{42}H_{45}N_{10}O_3V_1.C_3H_9N$
F_w	861.92
Wavelength (Å)	CuKα (λ = 1.54184)
Crystal system	Trigonal
Space group	*P*-3
Crystal colour and size (mm^3)	Green, 0.3 × 0.2 × 0.2
a (Å)	15.5913(4)
b (Å)	15.5913(4)
c (Å)	10.1470(3)
α (°)	90.00
β (°)	90.00
γ (°)	120.00
V ($Å^3$)	2136.16(10)
Z	2
ρ_{calcd} ($g\ cm^{-3}$)	1.340
F(000)	908
2θ range for data collection	$6.54 < 2\theta < 129.74°$
Index ranges	$-16 \leq h \leq 18, -18 \leq k \leq 15, -6 \leq l \leq 11$
Reflections collected/ Unique	4383/ 2413
Final R	0.0456
Goodness-of-fit on F^2	1.048
Final residual electron density ($eÅ^{-3}$)	$-0.388 < \Delta\rho < 0.411$
CCDC	994251

The geometry of the complex is highly symmetric and the bond lengths and bond angles of the molecule in the asymmetric unit are identical in whole molecule. Selected bond lengths in [VL^1] are provided in the Table 1.3.6.

Table 1.3.6. Selected bond lengths in complex [$V(L^1)$].

Bond lengths (Å)	
V(1)-O(14)	2.0631(17)
V(1)-O(14_i)	2.0631(17)
V(1)-O(14_ii)	2.0631(17)
V(1)-N(16)	2.164(2)
V(1)-N(16_i)	2.164(2)
V(1)-N(16_ii)	2.164(2)
N16-C17	1.463(3)
N16-C15	1.291(3)
N1-N2	1.406(3)
C5-O14	1.278(3)
C4-C5	1.402(4)

The bond lengths of V(1)-O(14), V(1)-O(14_i) and V(1)-O(14_ii) are found to be equal 2.0631(17) Å, which have been increased from the previous reported bond lengths (V-O) in vanadium complexes of pyrazolones from 1.969(3)-2.018(2) [23,24,26]. The bond lengths of V(1)-N(16), V(1)-N(16_i) and V(1)-N(16_ii) are found to be equal 2.164(2) Å in the [VL^1]. The bond length of nitrogen-nitrogen (N1-N2) in pyrazolone ring is found similar to the nitrogen-nitrogen bond length (1.408-1.410) in pyrazolone ring of the ligand L^1. The bond length of carbon-oxygen (C5-O14) has been increased after complexation with vanadium from 1.241(3)-1.250(3) to 1.278(3). The carbon-carbon (C4-C5) bond length in pyrazolone ring decreases after complexation with vanadium from 1.428(4)-1.439(3) to 1.402(4), which indicate that after complexation amine-one tautomeric form of ligand L^1 converted into imine-ol

form and C-C single bond converted into C-C double bond. The bond length N16-N17 increased a little after the complexation from 1.450(3)-1.450(3) to 1.463(3), However the bond length N16-C15 get decreased after the complexation from 1.307(3)-1.320(3) to 1.291(3). The change in the bond distances and conversion of double and single bonds after complexes is illustrated in the Figure 1.3.14.

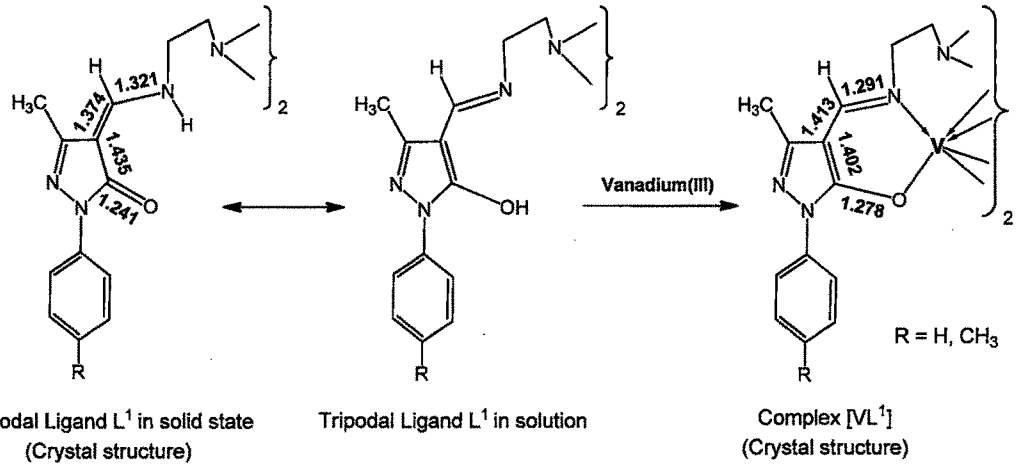

Figure 1.3.14. bond distances of L^1, before and after complexation.

Selected bond angles of the complex $[VL^1]$ are provided in the Table 1.3.7. The bite angles O(14)-V(1)-N(16), O(14_i)-V(1)-N(16_i) and O(14_ii)-V(1)-N(16_ii) are found to be 84.86(7)°. The bond angles C(19)-N(18)-C(19_i), C(19_i)-N(18)-C(19_ii) and C(19_ii)-N(18)-C(19) are found to be decreased from 111.4(2)-112.4(2)° to 110.15(16)° after complexation of L^1 with vanadium. After complexation of L^1 with vanadium the bond angle N19-C17-C18 decreased from 111.6(2)-113.5(2)° to 108.2(2)°. The bond angle C15-C16-C17 has also been decreased from 124.8(3)-125.1(3)° to 116.5(2)°. The bond angle C4-C5-O14 (129.6(2)°) did not change after complexation and found similar to the bond angle in L^1. However, the bond angle N1-C5-O14 decreased after the complexation with vanadium from 126.4(3)-126.7(3)° to 124.7(2)°. The bond angle C4-C5-N1 in the pyrazolone ring decreases after the complexation from 103.7(2)-104.5(2)° to 105.7(2)°.

Table 1.3.7. Selected bond angles in complex $[V(L^1)]$.

Bond angles (°)	
O(14)-V(1)-N(16)	84.91 (7)
O(14_i)-V(1)-N(16_i)	84.91 (7)
O(14_ii)-V(1)-N(16_ii)	84.91 (7)
O(14)-V(1)-N(16_i)	78.15 (8)
O(14)-V(1)-N(16_ii)	159.02 (8)
O(14_i)-V(1)-N(16)	78.15 (8)
O(14_i)-V(1)-N(16_ii)	159.02 (8)
O(14_ii)-V(1)-N(16)	159.02 (8)
O(14_ii)-V(1)-N(16_i)	78.15 (8)
N(16)-V(1)-N(16_i)	109.52 (6)
N(16)-V(1)-N(16_ii)	109.52 (6)
N(16_i)-V(1)-N(16_ii)	109.52 (6)
O(14)-V(1)-O(14_i)	83.26 (8)
O(14)-V(1)-O(14_ii)	83.26 (8)
O(14_i)-V(1)-O(14_ii)	83.26 (8)
C(19)-N(18)-C(19_i)	110.15(16)
C(19_i)-N(18)-C(19_ii)	110.15(16)
C(19_ii)-N(18)-C(19)	110.15(16)
N19-C17-C18	108.2(2)
C15-C16-C17	116.5(2)
C4-C5-O14	129.6(2)
N1-C5-O14	124.7(2)
C4-C5-N1	105.7(2)

The crystal structure suggests that the structure of [VL^1] approximates to C_3 symmetry with the axis passing through the tertiary N atom and the central V^{3+} ion. Usually, in the C_3 symmetric mononuclear complexes vanadium is four or five coordinated, while in this case vanadium is six coordinated [16-21]. The ligand coordinated to central metal atom to give a mononuclear complex [VL^1], resembling a three-bladed propeller (*see* Figure 1.3.15), in which each blade is derived from a pyrazolone moiety and each blade is piled to the next blade in either clockwise or counter clockwise direction by 32.38° to the C_3 axis to form helical chains.

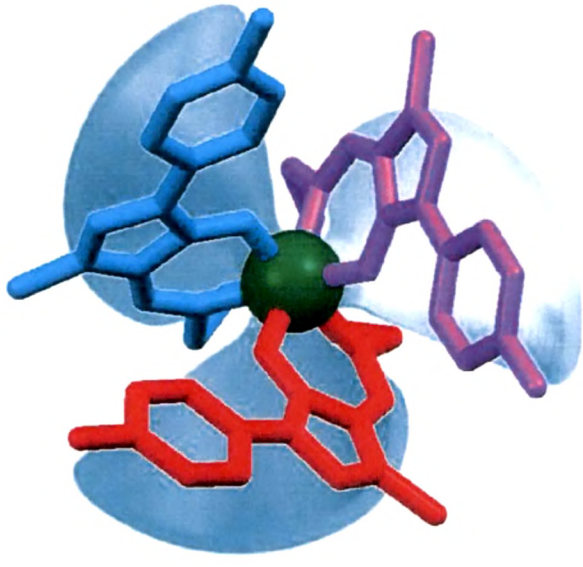

Figure 1.3.15. Vanadium(III) complex [VL^1] resembling a three-bladed propeller.

The C_3 symmetric *lambda* (∧) and *delta* (Δ) isomers of [VL^1] are depicted in the Figure 1.3.16. It is interesting that three such helical chains intertwine one another to result in a rare triple-stranded helicate. The helical assemblies form an achiral compound, a racemic mixture of alternating clock and anticlockwise spinning helices has been found.

The mirror image relation of right and left handed triple-stranded helical motifs composed of achiral building blocks in [VL^1] are depicted in the Figure 1.3.17.

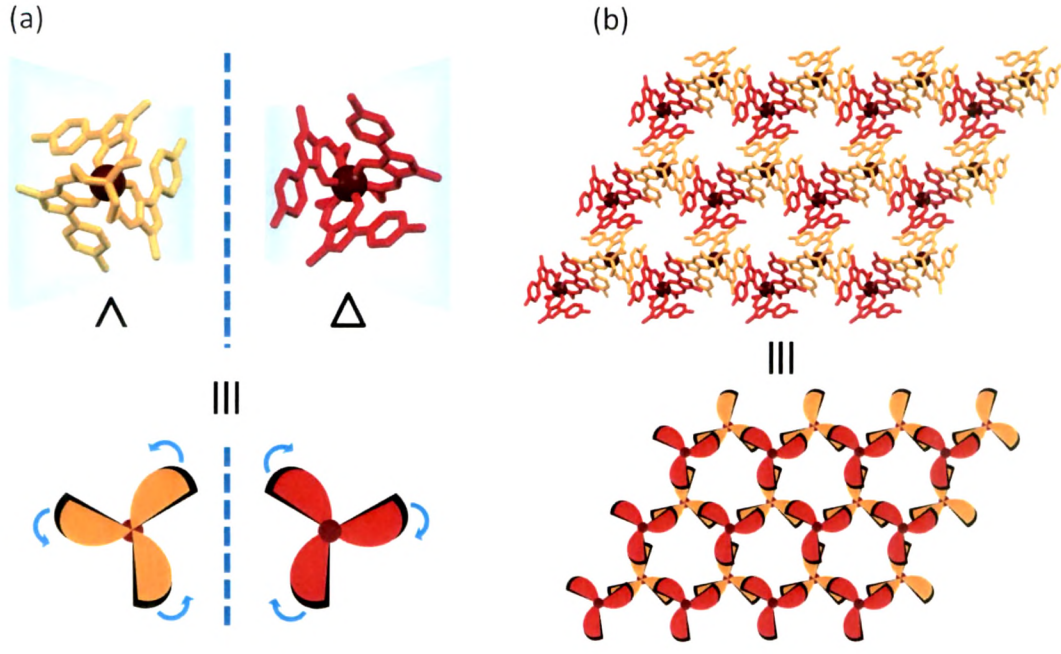

Figure 1.3.16. (a) Crystal structure and cartoon depiction of propeller shaped C_3 symmetric *lambda*- and *delta*- isomers of vanadium complex observed in [VL^1]; (b) packing diagram down *c*-axis depicts the alternate arrangement of *lambda*- and *delta*- isomers which is attributable to the racemic (achiral) nature of the compound.

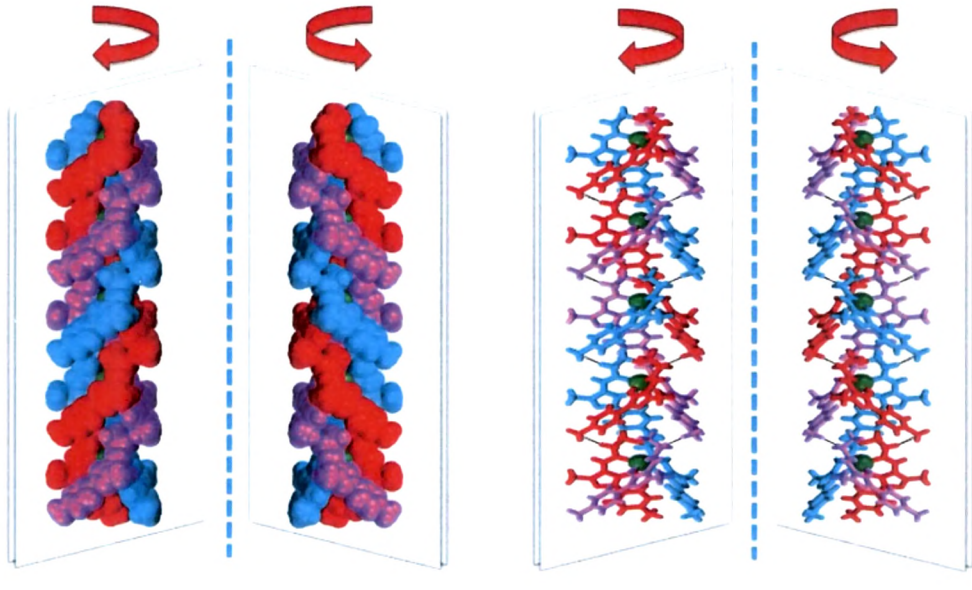

Figure 1.3.17. Mirror image relation of right and left handed triple-stranded helix composed of achiral building blocks in [VL^1].

Crystal structural analysis indicates no significant intermolecular interactions among three strands except van der Waals interactions [32]; however, there exist supramolecular interactions between the adjacent helices. As depicted in Figure 1.3.18, every single strand of the triple helix forms weak C-H···π interaction (Hydrogen-to-centroid distance 3.594 Å) with a neighboring strand belonging to the adjacent triple helix. This causes closely interdigitating packing and hence directs the handedness of the neighboring triple helices. The right-handed and left-handed triple helices are aligned alternately by such C-H···π interactions to result in 2D racemic layers.

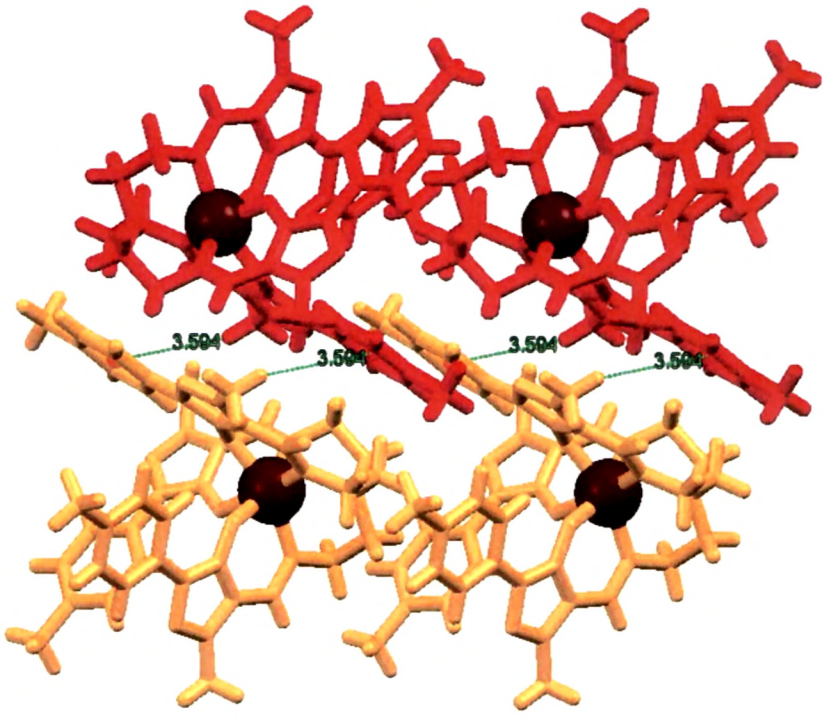

Figure 1.3.18. C-H···π interactions between the single strands belonging to the adjacent triple-stranded helices

FT-IR spectra of the complexes [VL^1] and [VL^2] show strong absorption bands between the range 1493 to 1651 cm^{-1}, due to the stretching mode υ(C=O), υ(C=C) and υ(C=N) of the pyrazolone ligand. The absorption bands 2920 & 2859 cm^{-1} of [VL^1] and 2925 & 2857 cm^{-1} of [VL^2] are assigned to the υ(CH) stretching of $-CH_3$. The absorption bands at 3056 cm^{-1} are assigned to the aromatic υ(CH) stretching. The strong band usually observed for υ(V=O) in the range 880 to 1000 cm^{-1} is not found in the FT-IR spectra of both the complexes, which indicate that

oxovanadium(IV) group has been converted in the V(III) and oxido group has been removed after complexation with the tripodal ligands L^1 and L^2. The strong absorption bands at 513 and 450 cm^{-1} in [VL^1] and [VL^2] are assigned to the υ(V-N) and υ(V-N), respectively. FT-IR spectra of the complexes [VL^1] and [VL^2] are shown in the Figure 1.3.19.

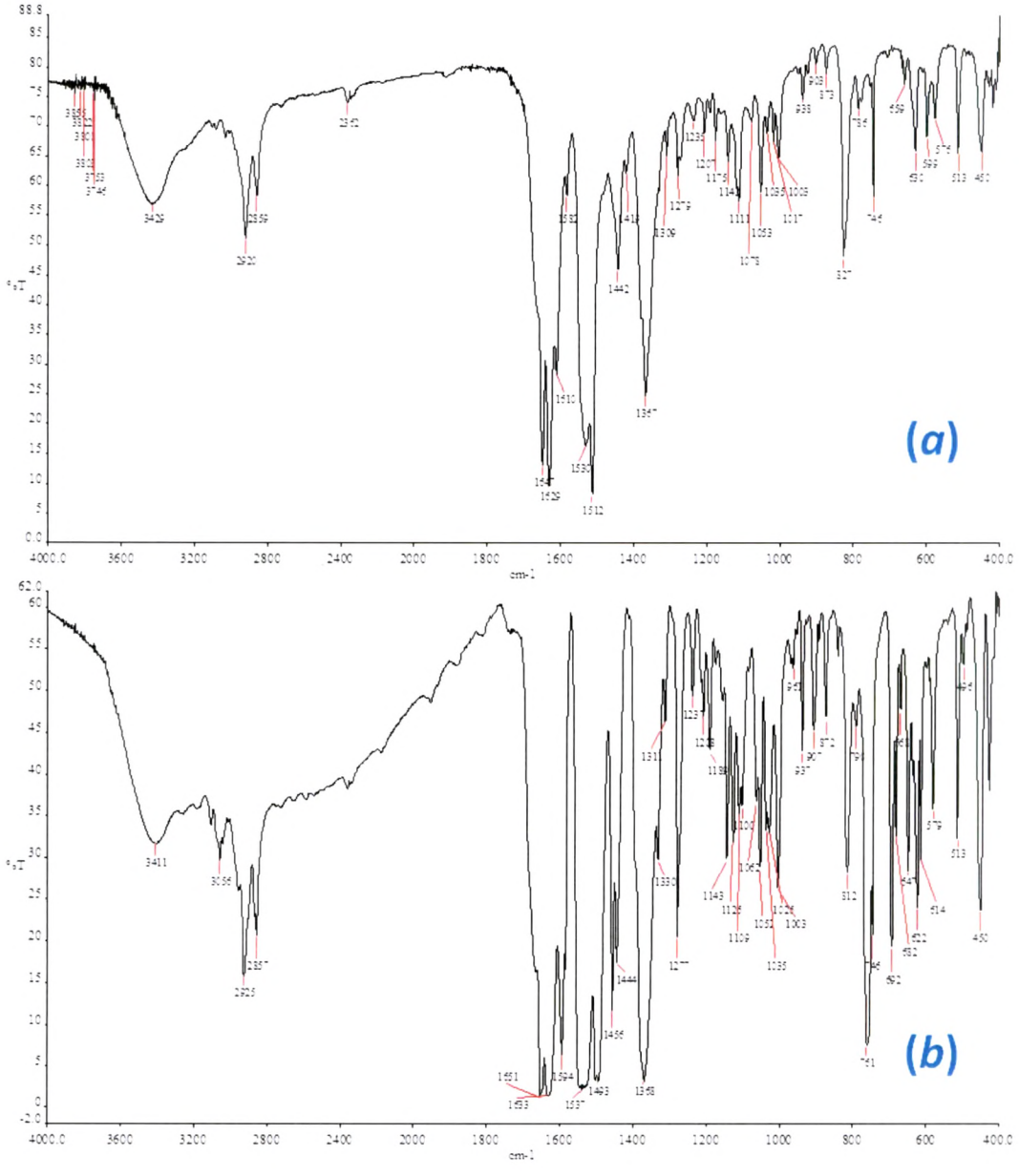

Figure 1.3.19. FT-IR spectra of the complexes (*a*) [VL^1] and (*b*) [VL^2].

A 3 mmol solution of [VL^1] was prepared in DMF and its electronic spectrum was recorded using a UV-Vis spectrophotometer. The vanadium(III) complex [VL^1] shows four absorption bands in electronic spectrum (*see* Figure 1.3.20). The lower

energy and less intense bands bands appear at 592 nm, 670 nm and 760 nm, which are due to the $d \rightarrow d$ transitions in the complex. Three $d \rightarrow d$ transition bands are the indication of the presence of vanadium in +3 oxidation state [14*a*]. The absorption band appear at 473 nm is due to the ligand to metal charge transfer (LMCT).

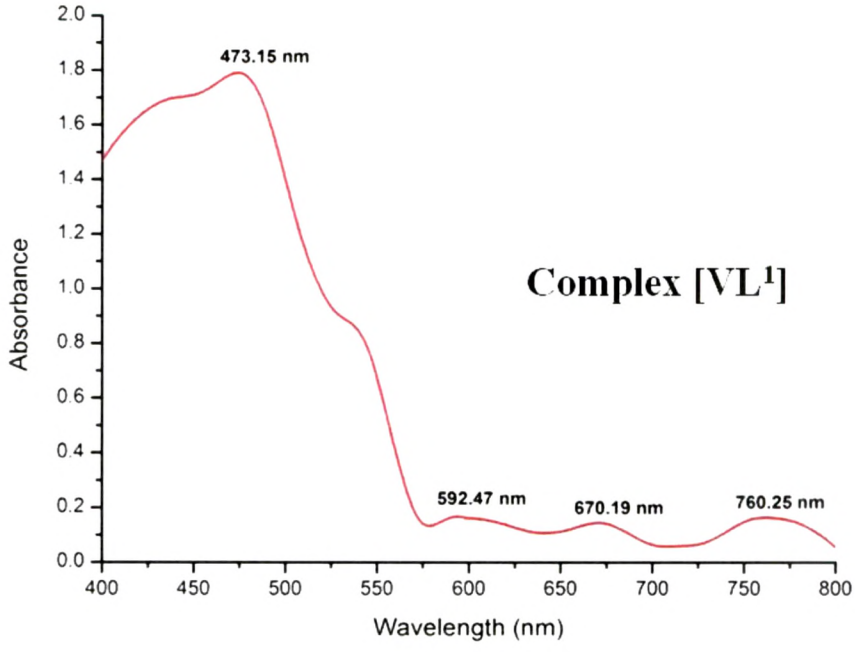

Figure 1.3.20. Electronic spectrum of the complex [VL^1] in DMF.

To study the oxidation state of vanadium in the synthesized complexes of tripodal ligands magnetic susceptibilities were measured using PAR 155 vibrating sample magnetometer. Magnetic susceptibility measurements showed that both the complexes are paramagnetic with the effective magnetic moment (μ_{eff}) 3.12 BM and 2.94 BM for the [VL^1] and [VL^2], respectively, which corresponds to the +3 oxidation state of vanadium ($3d^2$) in these complexes.

1.3.3.3. Oxidation of benzyl alcohol

Oxidation of benzyl alcohol was carried out by vanadium(III) complexes of tripodal ligands using H_2O_2 as an oxidant. The oxidation reaction were carried out in solvent free condition and the reaction conditions adopted from the part 1 of the chapter 1. Thus, the optimum condition for the maximum % conversion as well as selectivity for the oxidation of benzyl alcohol to benzaldehyde is reaction temperature (90 °C), benzyl alcohol (10 mmol), 30% H_2O_2 (30 mmol), catalyst amount (0.045

mmol) and reaction time (24 h) The progress of the reaction was monitored by GC-MS analysis and products formed in the reactions were matched with those reported in the literature.

Table 1.3.8. Catalytic activity of vanadium(III) complexes towards the oxidation of benzyl alcohol.

Complex	Substrate	Product	%Conversion of benzyl alcohol	%Selectivity of benzaldehyde	TON
$[VL^1]$	Benzyl alcohol	Benzaldehyde	82	87	178
$[VL^2]$	Benzyl alcohol	Benzaldehyde	89	81	189

As per the data presented in the Table 1.3.8 we could observe that complex $[VL^2]$ shows better conversion (89%) of benzyl alcohol in comparision to the complex $[VL^1]$. However, complex $[VL^1]$ shows good selectivity (87%) for the benzaldehyde in comparision to the complex $[VL^2]$.

1.3.4. Conclusions

In summary, four new tripodal ligands of 4-formyl and 4-acyl derivatives of pyrazolone were synthesized and characterized by various spectroscopic techniques along with the crystal structyure XRD. The single crystal X-ray show that the tripodal ligands exist in the amine-one form in the solid state. Two new vanadium(III) complexes using tripodal ligands of pyrazolones (L^1 & L^2) were synthesized and their structures were experimentally confirmed. The single-crystal XRD structure of the complex $[VL^1]$ reveals that it is a C_3 symmetric propeller shaped mononuclear complex which forms triple-stranded helical chains in which each blade is stack with the next blade in either clockwise or counter clockwise direction. The crystal packing of the complex shows the alternate arrangement of *lambda-* and *delta-* isomers which is attributable to the racemic (achiral) nature of the complex. Supramolecular interactions such as C-H$\cdots\pi$ interactions between the single strands belonging to the

adjacent triple-stranded helices causes closely interdigitating packing and hence directs the handedness of the neighboring triple helices. Vanadium(III) complexes of tripodal ligands pyrazolones were used as homogeneous catalysts for the solvent free oxidation of benzyl alcohol. The complexes were found to be successful in the oxidation of benzyl alcohol to benzaldehyde under mild reaction conditions.

1.3.5. References

[1] (*a*) E. C. Constable, in *Comprehensive Supramolecular Chemistry*, (Ed: J. -M. Lehn) Pergamon: Oxford, U.K., **1996**, *Vol. 9*, p 213; (*b*) S. Leininger, B. Olenyuk, P. J. Stang, *Chem. Rev.*, **2000**, *100*, 853-907.

[2] J. -M. Lehn, *Supramolecular Chemistry- Concepts and Perspectives*, VCH: Weinheim, Germany, **1995**.

[3] (*a*) J. -M. Lehn, *Chem. Eur. J.*, **2000**, *6*, 2097-2102; (*b*) J. -M. Lehn, *Science*, **2002**, *295*, 2400-2403.

[4] (*a*) M. Albrecht, *Angew. Chem., Int. Ed.*, **2005**, *44*, 6448-6451; (*b*) A. K. Speck, M. Meixner, D. Fong, P. R. McCullough, D. E. Moser, T. Ueta, *Astron. J.*, **2002**, *123*, 346-361.

[5] (*a*) H. H. Park, T. H. Noh, Y. B. Shim, O. S. Jung, *Chem. Commun.*, **2013**, *49*, 4000-4002; (*b*) Y. F. Guan, Z. Y. Li, M. F. Ni, C. Lin, J. Jiang, Y. Li, L. Wang, *Cryst. Growth Des.*, **2011**, *11*, 2684-2689. (*c*) R. Oda, I. Huc, M. Schmutz, S. J. Candau, F. C. MacKintosh, *Nature*, **1999**, *399*, 566-569.

[6] N. Sewald, H.-D. Jakubke, *Peptides: Chemistry and Biology*, Wiley-VCH: Weinheim, Germany, **2002**.

[7] (*a*) E. Yashima, K. Maeda, H. Iida, Y. Furusho, K. Nagai, *Chem. Rev.*, **2009**, *109*, 6102-6211. (*b*) M. A. B. Block, C. Kaiser, A. Khan, S. Hecht, *Top. Curr. Chem.*, **2005**, *245*, 89-150. (*c*) O. V. Gutov, *Cryst. Growth Des.*, **2013**, *13*, 3953-3957.

[8] G. D. Pantos, P. Pengo, K. M. J. Sanders, *Angew. Chem., Int. Ed.*, **2007**, *46*, 194-197.

[9] (*a*) K. H. Par, T. H. Noh, Y.-B. Shim, O.-S. Jung, *Chem. Comm.*, **2013**, *49*, 4000-4002. (*b*) R. Krämer, J.-M. Lehn, A. Marquis-Rigault, *Proc. Natl. Acad. Sci. U.S.A.*, **1993**, *90*, 5394-5398.

[10] X. Huang, C. Li, S. Jiang, X. Wang, B. Zhang, M. Liu, *J. Am. Chem. Soc.*, **2004**, *126*, 1322-1323.

[11] (*a*) K. Kataoka, M. Yanagi, T. Katagiri, *Cryst. Eng. Comm.*, **2011**, *13*, 6342-6344. (*b*) J. L. Atwood, J. W. Steed, *Organic Nanostructures*, Wiley-VCH: Weinheim, Germany, **2008**. (*c*) J. N. Moorthy, R. Natarajan, G. Savitha, P. Venugopalan, *Cryst. Growth Des.*, **2006**, *6*, 919-924.

[12] (*a*) A. Roth, D. Koth, M. Gottschaldt, W. Plass, *Cryst. Growth Des.*, **2006**, 6, 2655-2657; (*b*) P. Cucos, M. Pascu, R. Sessoli, N. Avarvari, F. Pointillart, M. Andruh, *Inorg. Chem.*, **2006**, *45*, 7035-7037; (*c*) W. -G. Lu, J. -Z, Gu, L. Jiang, M. -Y. Tan, T. -B. Lu, *Cryst. Growth Des.*, **2008**, *8*, 192-199; (*d*) T. Riis-Johannessen, G. Bernardinelli, Y. Filinchuk, S. Clifford, N. D. Favera, C. Piguet, *Inorg. Chem.*, **2009**, *48*, 5512–5525; (*e*) Z. Zhang, D. Dolphin, *Chem. Commun.*, **2009**, 6931–6933; (*f*) Y. Morita, Y. Yakiyama, S. Nakazawa, T. Murata, T. Ise, D. Hashizume, D. Shiomi, K. Sato, M. Kitagawa, K. Nakasuji, T. Takui, *J. Am. Chem. Soc.*, **2010**, *132*, 6944–6946; (*g*) K. K. Bisht, E. Suresh, *Inorg. Chem.*, **2012**, *51*, 9577-9579; (*h*) K. K. Bisht, E. Suresh, *Cryst. Growth Des.* **2013**, *13*, 664-670; (*i*) K. K. Bisht, E. Suresh, *J. Am. Chem. Soc.*, **2013**, *135*, 15690-15693.

[13] (*a*) P. L. Caradoc-Davies, L. R. Hanton, *Chem. Commun.*, **2001**, 1098-1099; (*b*) C. Janiak, *Dalton Trans.*, **2003**, 2781-2804; (*c*) B. Kesanli, W. Lin, *Coord. Chem. Rev.*, **2003**, *246*, 305-326; (*d*) L. Han, M. Hong, *Inorg. Chem. Commun.*, **2005**, *8*, 406-419; (*e*) C. P. Pradeep, P. S. Zacharias, S. K. Das, *Eur. J. Inorg. Chem.*, **2005**, 3405-3408; (*f*) H. -R. Wen, C. -F. Wang, Y. -Z. Li, J. -L. Zuo, Y. Song, X. -Z. You, *Inorg. Chem.* **2006**, *45*, 7032-7034.

[14] (*a*) L. F. V. Boas, J. C. Pessoa, *Comprehensive Coordination Chemistry: The Synthesis, Reaction, Properties & Applications of Coordination Compounds* (Eds: G. Wilkinson, R. D. Gillard, J. A. McCleverty) Pergamon: Oxford, **1987**, *Vol. 3*. (*b*) T. Hirao, Coord. *Chem. Rev.*, **2003**, *237*, 271-279; (*c*) K. Kustin, J. C. Pessoa, D. C. Crans, *Vanadium: The Versatile Metal*, ACS Symposium Series, ACS: Washington, DC, **2007**.

[15] (*a*) P. Frank, E. J. Carlson, R. M. K. Carlson, B. Hedman, K. O. Hodgson, *J. Inorg. Biochem.*, **2008**, *102*, 809–823; (*b*) D. Rehder, *Bioinorganic Vanadium Chemistry*, John Wiley & Sons, Chichester, **2008**; (*c*) D. C. Crans, J. J. Smee, E. Gaidamauskas, L. Yang, *Chem. Rev.*, **2004**, *104*, 849–902; (*d*)

H. Michibata, N. Yamaguchi, T. Uyama, T. Ueki, *Coord. Chem. Rev.*, **2003**, *237*, 41-51; (*e*) K. Kanamori, *Coord. Chem. Rev.*, **2003**, *237*, 147-161.

[16] S. Barman, S. Patil, J. Desper, C. M. Aikens, C. J. Levy, *Eur. J. Inorg. Chem.*, **2013**, 5708–5717.

[17] Z. Chi, L. Zhu, X. Lu, H. Yu, B. Liu, *Z. Anorg. Allg. Chem.*, **2012**, *638*, 1523–1530.

[18] M. Albrecht, I. Janser, H. Houjou, R. Fröhlich, *Chem. Eur. J.*, **2004**, *10*, 2839-2850.

[19] S. C. Davies, D. L. Hughes, Z. Zanas, L. Jerzykiewicz, R. L. Richards, J. R. Sanders, P. Sobota, *Chem. Commun.*, **1997**, 1261-1262.

[20] R. R. Schrock, *Acc. Chem. Res.*, **1997**, *30*, 9-16.

[21] M. Mba, M. Pontini, S. Lovat, C. Zonta, G. Bernardinelli, P. E. Kündlg, G. Licini, *Inorg. Chem.*, **2008**, *47*, 8616-8618.

[22] (*a*) F. Marchetti, C. Pettinari, R. Pettinari, *Coord. Chem. Rev.*, **2005**, *249*, 2909-2945; (*b*) R. N. Jadeja, J. R. Shah, *Polyhedron*, **2007**, *26*, 1677-1685; (*c*) P. N. Remya, C. H. Suresh, M. L. P. Reddy, *Polyhedron*, **2007**, *26*, 5016-5022; (*d*) B. T. Thakar, R. S. Barvalia, *Spectrochim. Acta Part A*, **2011**, *84*, 51-61.

[23] F. Marchetti, C. Pettinari, C. D. Nicola, R. Pettinari, A. Crispini, M. Crucianelli, A. D. Giuseppe, *Appl. Catal. A: Gen.*, **2010**, *378*, 211-233.

[24] S. Parihar, S. Pathan, R. N. Jadeja, A. Patel, V. K. Gupta, *Inorg. Chem.*, **2012**, *51*, 1152-1161.

[25] A. D. Giuseppe, C. D. Nicola, R. Pettinari, I. Ferino, D. Meloni, M. Passacantando, M.Crucianelli, *Catal. Sci. Technol.*, **2013**, *3*, 1972-1984.

[26] S. Parihar, R. N. Jadeja, V. K. Gupta, *RSC Adv.*, **2014**, *4*, 10295–10302.

[27] W. L. F. Armarego, C. L. L. Chai, *Purification of Laboratory Chemicals*, 5th *ed.*, Butterworth-Heinemann, Elsevier Science (USA), **2003**.

[28] K. M. Vyas, V. K. Shah, R. N. Jadeja, *J. Coord. Chem.*, **2011**, *64*, 1069-1081.

[29] G. M. Sheldrick, *SHELX97*, University of Göttingen: Göttingen, Germany **1997**.

[30] L. J. Farrugia, *J. Appl. Cryst.*, **1999**, *32*, 837-838.

[31] M. Nardelli, *J. Appl. Cryst.*, **1995**, *28*, 659.

[32] Y. Cui, H. L. Ngo, W. Lin, *Chem. Commun.*, **2003**, 1388-1389.

In: Advances in Chemistry Research. Volume 22
Editor: James C. Taylor

ISBN: 978-1-63-117-572-5

Chapter 9

CATALYSIS USING OXOVANADIUM(IV) COMPLEXES OF 4-ACYLPYRAZOLONE LIGAND

Sanjay Parihar and R. N. Jadeja*
Department of Chemistry, Faculty of Science,
The Maharaja Sayajirao University of Baroda, Vadodara 390 002, Gujarat, India

ABSTRACT

The interest in the coordination chemistry and catalytic activity of oxovanadium(IV) complexes of 4-acylpyrazolones has increased greatly in recent years. However, at the beginning of this time, only a minor amount of research was being done on catalysis using these complexes. This chapter includes discussion on the geometries and catalytic activities of the oxovanadium(IV) complexes of 4-acylpyrazolone. The single crystal XRD proven to be a powerful technique for the study of coordination geometry of oxovanadium(IV) complexes with 4-acylpyrazolone ligands. The single-crystal XRD analysis of the complexes reveals that the ligands coordinate with a vanadium atom to create an octahedral geometry and two *O, O*-chelating acylpyrazolonate ligands constitute two six-member rings with the vanadium. These complexes can exist in *syn*, *anti* and *twisted* coordination geometries. The catalytic activities of these complexes have been studied for the oxidation of styrene and benzylic alcohols. The complexes were immobilized over a solid support (ZrO_2/ SBA-15) and used as heterogeneous catalyst for the selective oxidation of styrene to benzaldehyde using H_2O_2 as an oxidant. The use of these complexes as homogeneous catalyst for the oxidation of styrene has also been reported. The oxidation of benzyl alcohol and a wide array of electronically diverse substituted benzyl alcohols were carried out using these complexes as homogeneous catalysts with H_2O_2. The results elucidate that the oxovanadium(IV) complexes of 4-acylpyrazolone ligands are efficient heterogeneous as well as homogeneous catalysts for the selective oxidation of styrene and benzylic alcohols to their corresponding benzaldehydes.

* Corresponding author: Email: rajendra_jadeja@yahoo.com.